
Masters Theses

Student Theses and Dissertations

Spring 2018

Thermal curing efficiency of geopolymer mortars

Simon Peter Sargon

Follow this and additional works at: https://scholarsmine.mst.edu/masters_theses



Part of the [Civil Engineering Commons](#)

Department:

Recommended Citation

Sargon, Simon Peter, "Thermal curing efficiency of geopolymer mortars" (2018). *Masters Theses*. 8063.
https://scholarsmine.mst.edu/masters_theses/8063

This thesis is brought to you by Scholars' Mine, a service of the Missouri S&T Library and Learning Resources. This work is protected by U. S. Copyright Law. Unauthorized use including reproduction for redistribution requires the permission of the copyright holder. For more information, please contact scholarsmine@mst.edu.

THERMAL CURING EFFICIENCY OF GEOPOLYMER MORTARS

by

SIMON PETER SARGON

A THESIS

Presented to the Graduate Faculty of the

MISSOURI UNIVERSITY OF SCIENCE AND TECHNOLOGY

In Partial Fulfillment of the Requirements for the Degree

MASTER OF SCIENCE IN CIVIL ENGINEERING

2018

Approved by

Mohamed A. ElGawady, Advisor

John J. Myers

Grace Yan

© 2017

SIMON PETER SARGON

All Rights Reserved

PUBLICATION THESIS OPTION

This thesis consists of the following two articles which have been submitted for publication, or will be submitted for publication as follows:

Paper I: Pages 6 - 50 are intended for submission to the Journal of Construction and Building Materials

Paper II: Pages 51 - 91 are intended for submission to the Journal of Construction and Building Materials

ABSTRACT

Missouri is the fourth largest coal consumer in the U.S. with coal-fired power plants generate 81.3% of the electricity in the state which generate about 2.7 million tons of coal combustion residuals (CCRs) annually. The CCR, including fly ash, disposal issue is not limited to Missouri, rather it is a national issue with CCRs being the second largest waste stream in the U.S. Ninety million tons of fly ash are stored in landfills and ash ponds annually. Hence, using this waste product effectively is necessary. One of the emerging applications of fly ash is to use it as binder in geopolymer concrete. While geopolymer concrete possess attractive characteristics, there remain many questions to be answered before it can be widely adopted in the construction industry.

Five geopolymer concrete mixtures with fly ash sourced from five power plants were investigated during the study. The physical and chemical properties of the fly ash were characterized using X-ray fluorescence, SEM, particle size distribution, and surface area. Different mixtures having different alkaline and silicate molarities were tested. The fresh properties of the concrete were determined. The compressive strengths of different specimens cured at five different temperatures of 30, 40, 55, 70, and 85 °C for 4, 8, 16, 24, and 48 hours were determined. The compressive strength results indicate that the calcium content and ratio of silica to alumina played a pivotal role in the optimum curing conditions for geopolymer concrete. Energy efficiency of these mixtures were analyzed to determine the most energy-effective curing regime. Relatively higher calcium fly ashes performed most efficiently at ambient curing conditions while lower calcium fly ashes were performed much better at 70 °C for 24 hours.

ACKNOWLEDGMENTS

I am so grateful and proud to have such an amazing advisor like Dr. Mohamed ElGawady, he is an outstanding professor and excellent researcher. I thank him for all that he taught me and for the encouragement and support he has provided through my work. I would like to thank all my family members and friends who were a great support.

Special thanks to my advisory committee members, Dr. John J. Myers, and Dr. Grace Yan for their time to review this document.

My great thanks to my wonderful team members Eslam Gomaa and Ahmed Gheni.

My sincere appreciation to John Bullock, Greg Leckrone, Gary Abbott, Jason Cox, Michael Lusher, and Brian Swift for their technical assistance.

TABLE OF CONTENTS

	Page
PUBLICATION THESIS OPTION	iii
ABSTRACT	iv
ACKNOWLEDGMENTS	v
LIST OF ILLUSTRATIONS	x
LIST OF TABLES	xii
 SECTION	
1. INTRODUCTION.....	1
1.1. BACKGROUND.....	1
1.2. OBJECTIVE AND SCOPE OF WORK	1
1.3. THESIS OUTLINE.....	2
2. LITERATURE REVIEW.....	3
2.1. MATERIAL PROPERTIES	3
2.1.1. Background	3
2.1.2. Binder.....	3
2.1.3. Alkali Activators.....	4
2.1.4. Curing Effect	5
 PAPER	
I. OPTIMIZATION OF THERMAL CURING OF CLASS C FLY ASH-BASED GEOPOLYMER MORTARS.....	6
ABSTRACT.....	6
1. INTRODUCTION	7
2. MATERIAL PROPERTIES	10

2.1. FLY ASH CHEMICAL COMPOSITION	10
2.1.1. Scanning Electron Microscopy and Energy Dispersive X-ray Spectroscopy (SEM/EDS) Analysis	14
2.2. ALKALI ACTIVATORS.....	14
2.3. FINE AGGREGATE (SAND).....	15
3. EXPERIMENTAL PROGRAM	15
3.1. MIX PROPORTIONS	15
3.2. MIXING PROCEDURE	16
3.3. MORTAR PLACING AND CURING PROCEDURE.....	17
3.4. SETTING TIME AND FLOW	19
3.5. COMPRESSIVE STRENGTH	19
3.6. X-RAY DIFFRACTION (XRD) ANALYSIS.....	19
4. RESULTS AND DISCUSSION	20
4.1. SCANNING ELECTRON MICROSCOPY/ENERGY DISPERSIVE X-RAY SPECTROSCOPY (SEM/EDS) ANALYSES.....	20
4.2. SETTING TIME AND FLOW.....	24
4.3. COMPRESSIVE STRENGTH OF THERMALLY CURED GEOPOLYMER.....	28
4.4. COMPRESSIVE STRENGTH OF AMBIENT CURED GEOPOLYMER...33	
4.5. ENERGY CONSUMPTION	35
4.6. X-RAY DIFFRACTION (XRD) ANALYSIS.....	39
5. CONCLUSION	42
REFERENCES	44

II. IMPROVING THE FREEZE THAW DURABILITY OF CLASS C FLY ASH-BASED GEOPOLYMER MORTARS USING COMPATIBLE ADDITIVES	51
ABSTRACT	51
1. INTRODUCTION	52
2. MATERIAL PROPERTIES	56
2.1. FLY ASH CHEMICAL COMPOSITION	56
2.2. ALKALI ACTIVATORS.....	59
2.3. FINE AGGREGATE (SAND).....	60
2.4. RECYCLED RUBBER.....	60
2.5. ADMIXTURES.....	61
3. EXPERIMENTAL PROGRAM	62
3.1. MIX PROPORTIONS	62
3.2. MIXING PROCEDURE	63
3.3. WORKABILITY.....	63
3.4. CURING PROCEDURE.....	63
3.5. FREEZE-THAW CHAMBER	64
4. RESULTS AND DISCUSSION	65
4.1. SUPERPLASTICIZER EFFECTS.....	65
4.2. AIR ENTRAINMENT.....	70
4.2.1. Air Entraining Admixtures.....	70
4.2.2. Rubber.....	76
5. CONCLUSION	83
REFERENCES	85

ACKNOWLEDGEMENTS	91
SECTION	
3. SUMMARY, CONCLUSIONS AND RECOMMENDATIONS	92
3.1. SUMMARY OF RESEARCH WORK	92
3.2. CONCLUSIONS	92
3.3. RECOMMENDATIONS	94
BIBLIOGRAPHY	96
VITA.....	103

LIST OF ILLUSTRATIONS

PAPER I	Page
Figure 1. CaO-SiO ₂ -Al ₂ O ₃ ternary diagram	11
Figure 2. Particles size distribution of fly ashes	13
Figure 3. Surface area of fly ashes	13
Figure 4. Thermocouple Set-up	18
Figure 5. Environmental chamber temperature for one week	18
Figure 6. SEM Images for fly ash particles	21
Figure 7. C36-2.65 EDS Image	23
Figure 8. C28-2.20 EDS Image	23
Figure 9. C25-2.35 EDS Image	23
Figure 10. C24-2.30 EDS Image	24
Figure 11. C21-2.20 EDS Image	24
Figure 12. Setting times of fly ash mixes	27
Figure 13. Flowability of fly ash mixes	27
Figure 14. Compressive strength of different mixes at different temperatures and durations.....	32
Figure 15. 7 Day Testing at 30°C and Missouri Summer conditions	34
Figure 16. Compressive Strength related to energy consumption.....	36
Figure 17. Compressive strength results on fly ash pastes	39
Figure 18. XRD analysis	41
 PAPER II	
Figure 1. CaO-SiO ₂ -Al ₂ O ₃ Ternary Phase Diagram.....	57
Figure 2. Element analysis using the energy dispersive spectroscopy (EDS) for fly ash C21.....	58
Figure 3. Element analysis using the energy dispersive spectroscopy (EDS) for fly ash C36.....	59
Figure 4. Scanning electron microscopy (SEM) images of fly ash (a) Labadie (C36), and (b) Sikestone (C21)	59
Figure 5. Particle size distribution of C21, C36, Cement, and Rubber.....	61

Figure 6. Oven curing procedure.....	64
Figure 7. Effect of reducing water on workability.....	65
Figure 8. Effects of SP on workability.....	67
Figure 9. Effects of freeze-thaw on compressive strength of M21 mixture with and without using SP.....	67
Figure 10. Effects of freeze and thaw cycles on M36 with and without SP.....	68
Figure 11. Visual representation of specimens, Before Freeze thaw (left), After 26 Cycles Freeze Thaw (right)	68
Figure 12. Air Entrainment Workability.....	70
Figure 13. % Air entrainment of AEA.....	71
Figure 14. Initial compressive strength-AEA Additive.....	72
Figure 15. M21 AEA Freeze Thaw Compressive Strength.....	73
Figure 16. M36 AEA Freeze Thaw Compressive Strength.....	73
Figure 17. Visual representation of AEA specimens, Before Freeze thaw (left), After 26 Cycles Freeze Thaw (right)	73
Figure 18. Rubber Replacement Workability.....	77
Figure 19. Effect of using rubber on the compressive strength before and after freeze- thaw cycles.....	78
Figure 20. M21 Rubber Freeze Thaw Compressive strength.....	79
Figure 21. M36 Rubber Freeze Thaw Compressive strength.....	79
Figure 22. Visual representation of Rubber specimens, Before Freeze thaw (left), After 26 Cycles Freeze Thaw (right)	80

LIST OF TABLES

PAPER I	Page
Table 1. Chemical composition of fly ash determined using XRF	12
Table 2. Physical properties of fly ashes	12
Table 3. Mix designs	16
Table 4. Sodium/FA ratios	16
Table 5. Energy Consumption	35
PAPER II	
Table 1. X-Ray Fluorescence Chemical Analysis.....	56
Table 2. Physical properties of Rubber.....	60
Table 3. Mix Designs.....	62
Table 4. Admixture Mix Designs.....	62

1. INTRODUCTION

1.1. BACKGROUND

Dependence on coal power plants is predicted to increase over the next 20 years contrary to popular reports [1]. One of the few by-products of this energy dependence is fly ash. However, fly ash has been found to be a detrimental material to the atmosphere for the environment and the health of living beings. Therefore, it has been collected and stored in landfills and ponds to circumvent these effects. This short-sighted approach has been helpful but is not viable in long term energy dependence of the society. Fly ash has been depended upon in partial replacement of cementitious materials in the construction industry. However, relatively new technology investigates the use of 100% replacement of ordinary Portland cement (OPC) with fly ash [2]. The use of this concept has, however, been subjected to criticism due to studies indicating very slow strength gain or extensive energy subjugation to obtain relative strengths to OPC.

1.2. OBJECTIVE AND SCOPE OF WORK

This study investigates the optimum curing conditions required to obtain comparable strengths to OPC. The extensive approach for this study includes five sources of class C fly ash, tested at five curing conditions 30, 40, 55, 70, and 85°C at five curing times 4, 8, 16, 24, 48 hours. Relatively higher calcium fly ashes were tested at Missouri climatic conditions, varying the temperature ranges between 22°C at night, and 36°C during the day. Extensively studying these conditions could lead to the substantial cost savings and circumvent reservations of slow strength gain in 100% replacement of cement.

1.3. THESIS AND OUTLINE

This thesis includes three sections. The first section discusses a brief introduction into the concept and the need for the study investigated. The next section includes the paper describing the details in the optimization of thermal curing of class C fly ash-based geopolymer mortars, including the variable curing conditions, temperatures, mixtures, and sources.

The third section summarizes and concludes the study, proposing possible implementations of the results found.

2. LITERATURE REVIEW

The purpose of this section is to review the previous work on geopolymers with emphasis on the material properties, strength gain, and its curing procedures

2.1. MATERIAL PROPERTIES

2.1.1. Background. Missouri is the fourth largest coal consumer in the U.S. [3]. Coal-fired power plants generate 6,679 thousand MWh or 81.3% of the electricity in the State of Missouri which generate about 2.7 million tons of coal combustion residuals (CCRs) annually. The CCR disposal issue is not limited to Missouri, rather it is a national issue with CCRs being the second largest waste stream in the U.S. One-hundred and forty million tons of fly ash, byproduct of coal combustion, is generated annually in the U.S. Only 50 million tons is reused and the remaining fly ash is stored in landfills for dry storage and ponds, where water is added to stabilize the fly ash [1]. Embankment collapses in these ponds may lead to destruction of nearby areas and leaching of heavy metal into soil [4]. Despite the effort to reduce the contribution of coal to energy production due to environmental concerns, there will be a relatively unchanged amount of electrical power generating from coal in the next few decades due to several socioeconomic factors [1]. Hence, using this waste product effectively is necessary. One of the emerging applications of fly ash is to use it as binder in geopolymer concrete. Geopolymer concrete possess attractive characteristics such as sustainability [5], lower shrinkage [6], better fire and acid resistance, durability [7], lower creep [8], and better resistance to sulphuric acid attack [9].

2.1.2. Binder. The binder in geopolymer concrete consists of an alumina-silicate rich material such as fly ash and alkali activators. Fly ash is a combination of coal

impurities and flue gases and hence there is strong variability in the physical and chemical properties of fly ash. Increasing the surface area of fly ash by grinding, resulted in higher strength [10]. However, grinding fly ash increases the production cost. Similarly, the particle size distribution of fly ash affects the performance of geopolymer concrete [11]. Fly ash chemical compositions, which depends on the coal burning temperatures and process as well as the coal source, type, and storage conditions, play a crucial role in the performance of geopolymer [12]. For example, increasing the ratio of SiO_2 to Al_2O_3 in the fly ash resulted in longer setting time and higher compressive strength [13, 14].

2.1.3. Alkali Activators. The performance of geopolymer concrete is affected by the properties of the alkaline activator. Sodium hydroxide is preferred over other alkaline solutions due to its lower cost and the higher solubility of the Si and Al from the solid alumina-silicate material in the existence of NaOH [15]. A molarity of 10M of the sodium hydroxide resulted in a good balance between strength and workability of geopolymer [2, 16]. Furthermore, it is common practice to mix sodium hydroxide with sodium silicate producing the aqueous alkaline where the existence of soluble silicate is important as it provides the species required to initiate the oligomers formation and polycondensation of silicate and/or alumina-silicate. The high ratio of SiO_2 -to- Na_2O allows the polycondensation to initiate from the early stage of mixing geopolymer concrete [17]. Hence, this will increase the mechanical properties of the geopolymers [18]. There is no consensus on the optimum ratio of Hydroxide to Silicate. Optimum ratios of 1.0 or higher was proposed [2, 10, 19, 20]. It should be noted that sodium silicate is generally more expensive than sodium hydroxide and hence optimizing the

ratio of sodium hydroxide to sodium silicate is crucial for economic production of geopolymer concrete

2.1.4. Curing Effect. Curing is another influential parameter for the strength of geopolymer concrete. Depending on the chemical composition of fly ash, different curing regime maybe required. Class F fly ash requires high temperature curing while Class C fly ash can be cured at ambient or high temperature [2, 10, 21].

Proliferation of strength in geopolymers have been found to have very slow strength gain or require excessive temperatures [10]. Temperatures of 70°C or 85°C are the most popularly used to improve the strength mechanisms in the mortars [21].

PAPER

I. OPTIMIZATION OF THERMAL CURING OF CLASS C FLY ASH-BASED GEOPOLYMER MORTARS

Simon Peter Sargon^a, and Mohamed A. ElGawady^b

^aCivil, Architectural and Environmental Engineering, Missouri University of Science and Technology.

^bAssociate Professor and Benavides Faculty Scholar; Civil, Architectural and Environmental Engineering, Missouri University of Science and Technology, corresponding author.

HIGHLIGHTS

- Setting times and workability of various fly ash sources were investigated for multiple mix proportions.
- The findings provide the optimum curing regimes for five sources of fly ashes with optimized mixing procedures.
- The energy consumption for each testing period was investigated to determine efficient curing conditions

ABSTRACT

The replacement of cement with high alumino-silicate materials to form geopolymers, is pertinent to improve society and reduce the effects of harmful by-products like fly ash. The implementation of these products are hindered due to their slow strength gain and high cost for curing that is associated with geopolymers. This comprehensive study addresses this issue by using five sources of fly ashes, in three mixture proportions, at five curing temperatures 4, 8, 16, 24, and 48 hours, at five

temperatures of 30, 40, 55, 70, 85°C. The energy usage of these curing conditions were investigated to reduce the cost and improve efficiency.

Keywords

Geopolymer; Mortar; Class C Fly ash; Curing; Compressive strength; Energy efficiency

1. INTRODUCTION

Missouri is the fourth largest coal consumer in the U.S. [3]. Coal-fired power plants generate 6,679 thousand MWh or 81.3% of the electricity in the State of Missouri which generate about 2.7 million tons of coal combustion residuals (CCRs) annually. The CCR disposal issue is not limited to Missouri, rather it is a national issue with CCRs being the second largest waste stream in the U.S. One-hundred and forty million tons of fly ash, byproduct of coal combustion, is generated annually in the U.S. Only 50 million tons is reused and the remaining fly ash is stored in landfills for dry storage and ponds, where water is added to stabilize the fly ash [1]. Embankment collapses in these ponds may lead to destruction of nearby areas and leaching of heavy metal into soil [4]. Despite the effort to reduce the contribution of coal to energy production due to environmental concerns, there will be a relatively unchanged amount of electrical power generating from coal in the next few decades due to several socioeconomic factors [1]. Hence, using this waste product effectively is necessary. One of the emerging applications of fly ash is to use it as binder in geopolymer concrete. Geopolymer concrete possess attractive characteristics such as sustainability [5], lower shrinkage [6], better fire and acid resistance, durability [7], lower creep [8], and better resistance to sulphuric acid attack [9].

The binder in geopolymer concrete consists of an alumina-silicate rich material such as fly ash and alkali activators. Fly ash is a combination of coal impurities and flue gases and hence there is strong variability in the physical and chemical properties of fly ash. Increasing the surface area of fly ash by grinding, resulted in higher strength [10]. However, grinding fly ash increases the production cost. Similarly, the particle size distribution of fly ash affects the performance of geopolymer concrete [11]. Fly ash chemical compositions, which depends on the coal burning temperatures and process as well as the coal source, type, and storage conditions, play a crucial role in the performance of geopolymer [12]. For example, increasing the ratio of SiO_2 to Al_2O_3 in the fly ash resulted in longer setting time and higher compressive strength [13, 14].

The performance of geopolymer concrete is affected by the properties of the alkaline activator. Sodium hydroxide is preferred over other alkaline solutions due to its lower cost and the higher solubility of the Si and Al from the solid alumina-silicate material in the existence of NaOH [15]. A molarity of 10M of the sodium hydroxide resulted in a good balance between strength and workability of geopolymer [2, 16]. Furthermore, it is common practice to mix sodium hydroxide with sodium silicate producing the aqueous alkaline where the existence of soluble silicate is important as it provides the species required to initiate the oligomers formation and polycondensation of silicate and/or alumina-silicate. The high ratio of SiO_2 -to- Na_2O allows the polycondensation to initiate from the early stage of mixing geopolymer concrete [17]. Hence, this will increase the mechanical properties of the geopolymers [18]. There is no consensus on the optimum ratio of Hydroxide to Silicate. Optimum ratios of 1.0 or higher was proposed [2, 10, 19, 20]. It should be noted that sodium silicate is generally more expensive than sodium hydroxide

and hence optimizing the ratio of sodium hydroxide to sodium silicate is crucial for economic production of geopolymer concrete.

Another factor that affects the performance of geopolymer concrete is the mixing process. A mixing time of 10 minutes at high speeds of approximately 300rpm, resulted in high strength and porosity over normal mixing of 130rpm [22, 23]. High speed mixing resulted in uniform mixing of raw materials which is important for initial dissolution of the fly ash [24]. Furthermore, increasing the mixing speed, improved the workability of the materials [13].

Curing is another influential parameter for the strength of geopolymer concrete. Depending on the chemical composition of fly ash, different curing regime maybe required. Class F fly ash requires high temperature curing while Class C fly ash can be cured at ambient or high temperature [2, 10, 21].

The Midwest region of the U.S. has abundant resources for class C fly ash [25], using fly ash in geopolymer production will address a serious environmental issue. Producing geopolymer concrete for different structural applications will require determining the optimum-curing regime. However, there are scarce studies investigating the optimum temperature and curing time for Class C fly ash geopolymer mortar. This study presents the results of a comprehensive experimental study investigates the performance of geopolymer mortar mixtures with Class C fly ash sourced from five different power plants in Missouri. Three different mixtures were prepared using each type of fly ash. Then, the 15 mixtures were cured at five different temperatures for five different durations. Furthermore, curing at a synthetic Missouri summer day was investigated as

well. This will help in determining which temperature will ultimately be more cost effective.

2. MATERIAL PROPERTIES

2.1. FLY ASH CHEMICAL COMPOSITION

Fly ash samples were obtained from five different coal power plants in Missouri, United States (U.S.) (Table 1). The nomenclatures of the fly ashes start with the letter “C” for a Class C fly ash followed by the calcium content percentage, the ratio of silica-to-alumina as it plays an important role in the geopolymerization mechanism. For example, C36-2.65 is a fly ash having a calcium content of 36% (sourced from Labadie power plant per Table 1) and silica-to-alumina ratio of 2.65. The nomenclature of a given fly ash is used for mortar and paste mixtures made out of that fly ash with the letter C at the beginning was changed to M for mortar and P for paste mixtures, respectively.

X-ray fluorescence (XRF) analyses were performed, using a ThermoScientific ARLTM Quantx spectrometer, to determine the chemical compositions of each fly ash. The spectrometer was first calibrated using the results of analyzing 25 different certified standard reference materials obtained from the U.S. Geological Survey, National Institute of Standards and Technology, and Geological Survey of Japan. The spectrometer was operated under four separate conditions to optimize sensitivity for different elements. These conditions were: (1) 4 kV with vacuum and no filter to measure Na₂O, MgO, Al₂O₃, SiO₂, and P₂O₅; (2) 8 kV with vacuum and cellulose filter to measure K₂O and CaO; (3) 12 kV in air with Al filter to measure TiO₂ and MnO; and (4) 16 kV in air with a thin Pd filter to measure Fe₂O₃. Loss on ignition was determined by burning fly ash samples at 700 °C for two hours.

A sample was prepared of each fly ash by placing approximately 5 grams of loose powder mixed with 1 ml of Elvacite binder into 30 mm diameter aluminum cups [26]. The powder samples were pressed into flat disks using a steel die and a pressure of 56,000 psi. The results of the XRF (Table 1) showed that all five samples are classified as Class C fly ash per ASTM C618 [27] with calcium contents ranging from 21.2% to 36.9%. All sourced fly ashes are also rich in silica and alumina with silica-to-alumina ratios ranging from 2.20 to 2.65. Furthermore, the ternary phase diagram of the CaO-SiO₂-Al₂O₃ of each type of fly ash is shown in Figure 1. These elements were selected for the ternary phase diagram as the performance of the activated fly ash strongly depends on these oxides.

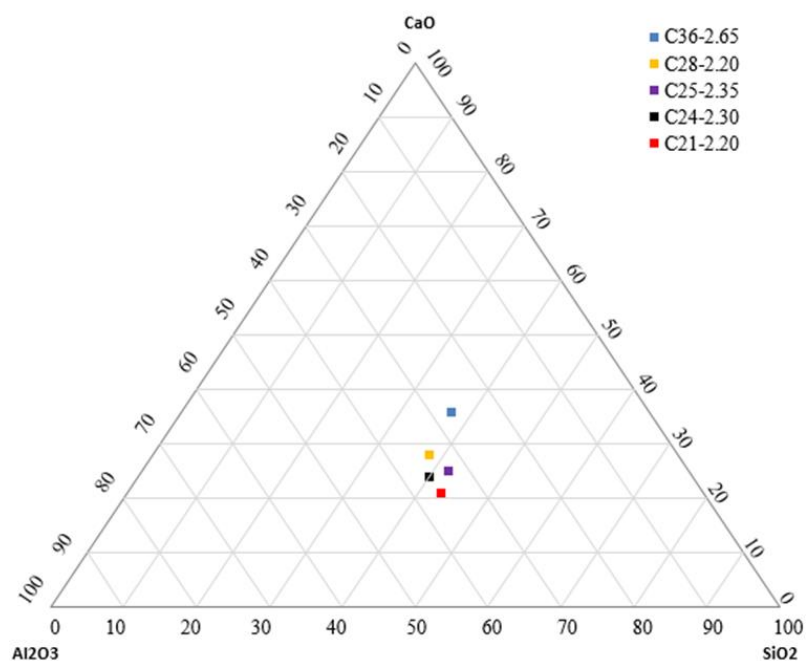


Figure 1. CaO-SiO₂-Al₂O₃ ternary diagram.

Table 1. Chemical composition of fly ash determined using XRF.

Fly Ash Nomenclature	Na₂O (%)	MgO (%)	Al₂O₃ (%)	SiO₂ (%)	P₂O₅ (%)	K₂O (%)	CaO (%)	TiO₂ (%)	MnO (%)	Fe₂O₃ (%)	LOI (%)
C36-2.65	1.62	4.80	13.9	36.8	0.70	0.62	36.9	0.87	0.03	3.52	0.50
C28-2.20	1.85	8.00	17.4	37.9	0.71	0.39	28.7	1.17	0.04	3.67	0.82
C25-2.35	1.58	4.74	17.9	42.2	0.89	0.56	25.8	1.44	0.04	4.73	0.12
C24-2.30	1.17	9.39	17.5	40.4	0.79	0.48	24.1	1.40	0.02	4.72	0.62
C21-2.20	2.87	4.29	20.1	43.9	0.51	0.70	21.2	1.36	0.05	4.96	0.40

LOI: Loss on ignition.

Table 2 summarizes the physical properties of the used fly ash. The specific gravity of the different fly ash types ranged from 2.70 to 2.97.

Table 2. Physical properties of Fly ashes.

Test		Fly Ash				
		C36-2.65	C28-2.20	C25-2.35	C24-2.30	C21-2.20
Particle size distribution	D10 μm	4.5	3.53	2.73	2.66	2.523
	D50 μm	14.75	14.87	16.25	16.13	12.81
	D90 μm	54.35	58.57	69.32	73.16	77.34
Specific gravity		2.9705	2.8912	2.7022	2.8912	2.8166
Surface area (BET) m^2/kg		2560	3925	1446	2858	2921

The surface area of the different fly ash types (Figure 3) ranged from 1446 to 3124 m^2/kg with C25-2.35 has the highest and C28-2.20 has the lowest surface areas, respectively.

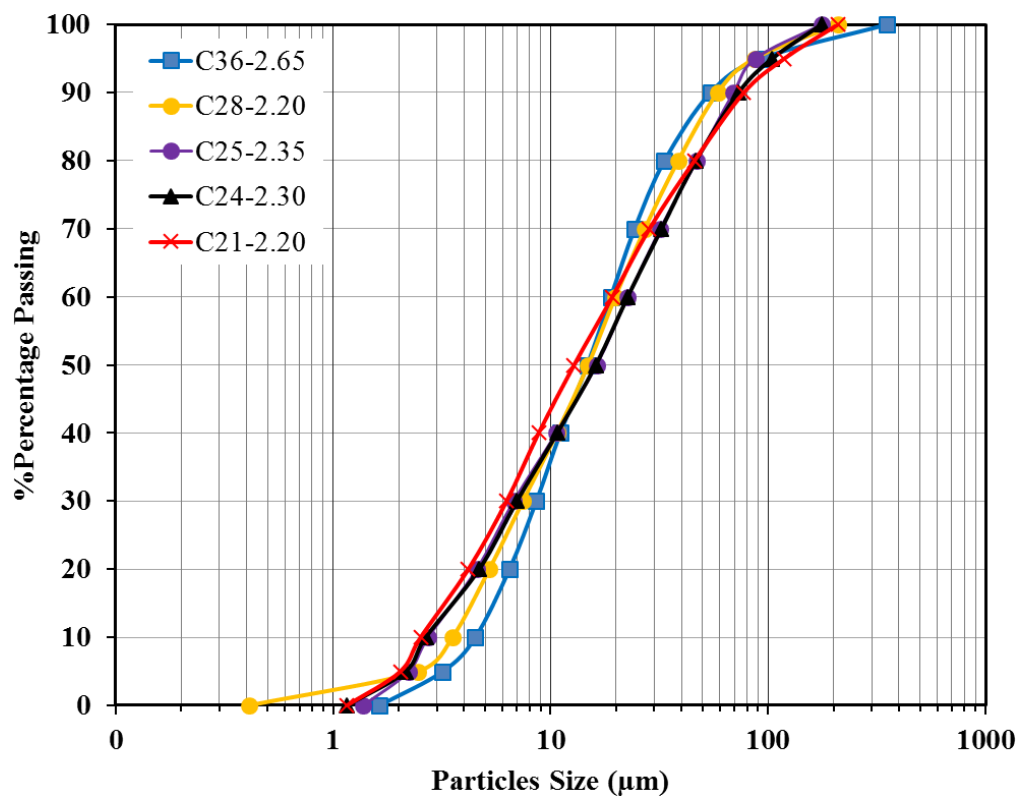


Figure 2. Particles size distribution of fly ashes.

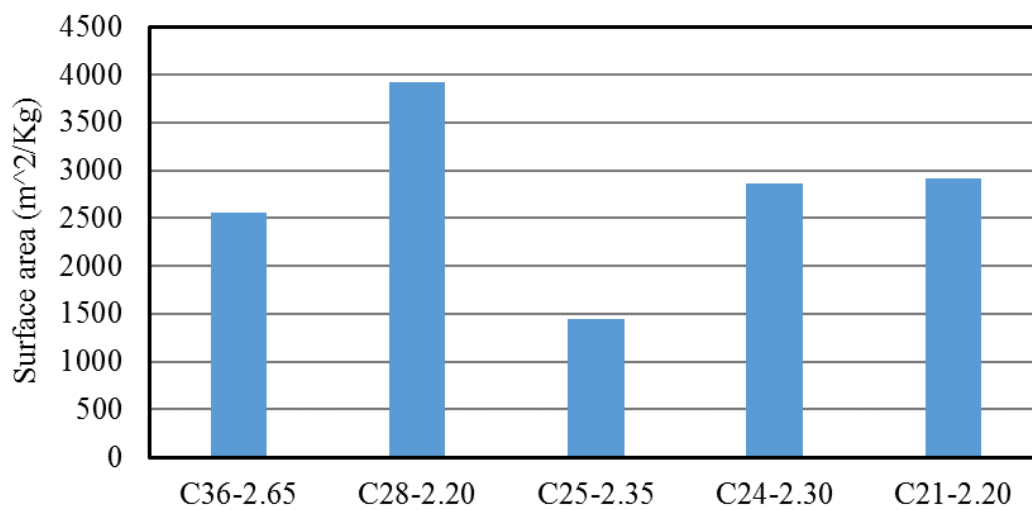


Figure 3. Surface area of fly ashes.

2.1.1. Scanning Electron Microscopy and Energy Dispersive X-Ray Spectroscopy (SEM/EDS) Analysis. A Hitachi S-4700 Field Emission Scanning Electron Microscope was used to perform SEM and EDS analyses. Each sample was prepared by coning and quartering. The sample was then mounted using a carbon paper since carbon has low emissions in X-ray detection and it does not interfere with the EDS results. During the process of the SEM-EDS, X-rays bump off the closest electron to the nucleus of an element. The signature energy released by an electron attempting to move closer to the nucleus of an atom to replace the displaced electron is recorded and used to determine that element.

The results were prepared using two magnifications, 3000K and 250K, which is relative to the machine used. This was done to get a holistic average of a larger area at 250K and comparing the data at a much smaller magnification. Scan speeds were adjusted to obtain clearer data at both magnifications. The results obtained from SEM/EDS can be related to oxide elements from X-ray Fluorescence.

2.2. ALKALI ACTIVATORS

Sodium hydroxides (NaOH) and type D sodium silicate (Na_2SiO_3) were used as the reagents during the course of this research. Sodium hydroxide was supplied in solid pellet form and prepared to a molarity of 10M [2, 16, 23], a few hours prior to mortar mixing to allow for dissipation of heat emitted from the solid pellets reaction with water. The type D sodium silicate had a solid sodium silicate of 44.1% by weight from the manufacturer. Hence, it included 14.7% Na, 29.4% SiO_2 , and 55.9% H_2O .

2.3. FINE AGGREGATE (SAND)

Missouri river sand with specific gravity 2.6 in surface saturated dry (SSD) condition was used as fine aggregate and prepared per ASTM C778 [28].

3. EXPERIMENTAL PROGRAM

3.1. MIX PROPORTIONS

More than thirty trial mixtures investigating the effects of mixing procedures and time, water content, alkaline-to-fly ash ratio, silicate-to-hydroxide ratio, material of mortar molds used which affected the heat transfer during the thermal curing, and rest periods were prepared to optimize the strength and workability. Based on the extensive trial mixtures, three different mixtures were selected as reference mixtures and prepared out of each of the five fly ash types, i.e., 15 mixtures were prepared during the course of this research.

All three mixtures have sand-to-binder (fly ash) ratio of 2.75 for all mixtures (Table 3). The first mixture, LA, had relatively low alkaline-to-fly ash ratio of 0.275 with water-to-fly ash ratio of 0.380. The silicate modulus, i.e., sodium silicate-to-sodium hydroxide ratio in the alkali activator was 1.0. The second mixture, HA, had relatively high alkaline-to-fly ash ratio of 0.300 while keeping the water-to-fly ash ratio the same as mix 1. Both LA and HA mixtures had a sodium silicate-to-sodium hydroxide ratio of 1.0. The third mixture, HS, the sodium silicate-to-sodium hydroxide ratio was increased to 2.0 since increasing the silicate content increase the dissolution rate of alkali activators [19].

However, the high viscosity of the silicate reduced the mixture workability and extra water was added to improve the workability of mixture HS.

Table 3. Mix designs.

MixNo.	LA	HA	HS
Alkaline/Fly ash Ratio	0.275	0.300	0.275
Water/Fly ash Ratio	0.380	0.380	0.400
Silicate/Hydroxide Ratio	1.000	1.000	2.000
Sodium Hydroxide (Kg/m ³)	75	81	50
Sodium Silicate (Kg/m ³)	75	81	100
Water (Kg/m ³)	114	106	128
Sand (Kg/m ³)	1485	1485	1485
Fly ash (Kg/m ³)	540	540	540

The Na₂O of the alkali activator to the fly ash ratio in the different mixtures are shown in Table 4.

Table 4. Sodium/FA Ratios.

Mix	Sodium (Na₂O) Ratio	Sodium (Na₂O) by weight
LA	4.90	29.25 Kg/m ³
HA	5.30	31.90 Kg/m ³
HS	4.45	26.85g/m ³

3.2. MIXING PROCEDURE

A Hobart mixer with three mixing speeds was used to prepare the different mortar mixtures. Sand and fly ash were added and mixed together for 30 seconds at 130 rpm. Water was then added gradually over a period of 60 seconds at the same speed. Sodium hydroxide was mixed with the sodium silicate solution; then, the alkaline solution was

gradually added over a period of 300 seconds and the speed of the mixture increased to 300 rpm. Increasing the mixing speed beyond 300 rpm led to spreading the mixture out of the mixing bowl. After finishing adding the alkaline solution, mixing was continued for another 300 seconds.

3.3. MORTAR PLACING AND CURING PROCEDURE

After mixing, the fresh mortar mixtures were placed into 50 mm metal cube molds according to ASTM C109. Brass molds were used in this study due to their high thermal conductivity at elevated temperatures. The specimens were allowed to have a rest time of 2 hours at an ambient temperature of $22^{\circ}\text{C} \pm 2^{\circ}\text{C}$, to achieve an optimum strength [2]. After the rest period, the molds were placed in oven bags to avoid moisture evaporation and place in an oven [23]. The temperature was controlled using thermocouples that were placed at different locations of the oven.

The mortar specimens were cured at different temperatures of 30°C , 40°C , 55°C , 70°C and 85°C for periods of 4, 8, 16, 24, and 48 hours, except for 30°C , which was considered to be an ambient temperature. Therefore, specimens cured at 30°C were cured for 16, 24, 48, 96, and 168 hours. Furthermore, a typical Missouri summer day was imitated using an environmental chamber. The temperature ranged from 22°C representing night time and 36°C representing the morning (Figure 5) [29].

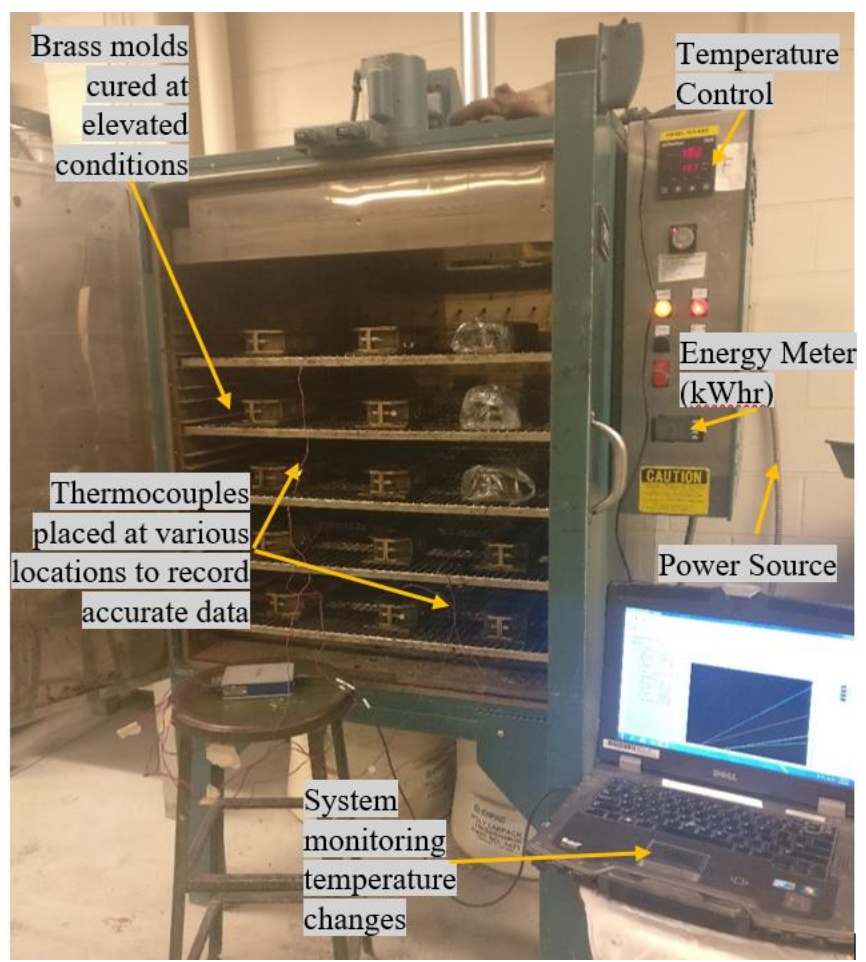


Figure 4. Thermocouple Set-up.

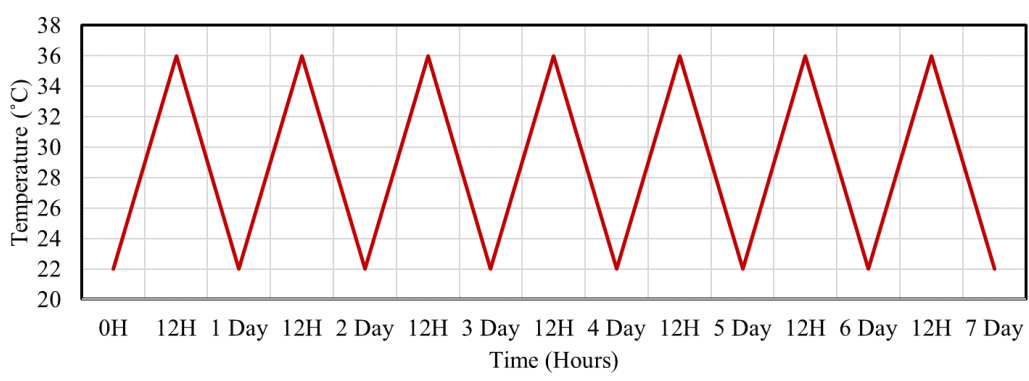


Figure 5. Environmental chamber temperature for one week.

3.4. SETTING TIME AND FLOW

The setting time and flow of each mixture were tested according to ASTM C191 [30] using Vicat apparatus and ASTM C1437 [31] using the flow table, respectively. An average of three results of each test mixture is reported in this manuscript.

3.5. COMPRESSIVE STRENGTH

After curing each 50mm cube specimen for the required duration at the required temperature, the compressive strength for that specimen was determined. Each cube was tested using a Tinius Olsen loading machine directly after taking the cubes out of the oven without any rest period. The acceptable variance and elimination criteria for compressive strength results were followed as per ASTM C109 [32].

3.6. X-RAY DIFFRACTION (XRD) ANALYSIS

A PANalytical X'Pert diffractometer utilizing a Cu K-alpha source and a PIXcel detector were used to investigate fly ash paste mixtures. Paste was selected in lieu of mortar mixtures to exclude the effect of the quartz in the sand. Fly ash composes of crystalline and amorphous substances. XRD can accurately detect the crystalline compounds, as the diffraction patterns of crystalline phases are sharp peaks. Amorphous materials are detectable but result in scattered peaks over a larger distribution curve since they do not possess a repetitive structure of atoms. The samples were prepared by crushing the alkali-activated pastes and passing through a 75 μ m, number 200 sieve. The scan rate of these scattered X-rays was approximately 3 degree/min. XRD analysis was useful in determining the hydration versus geopolymerization mechanisms.

For mixtures rich in calcium content, i.e., P36-2.65 and P28-2.20, the XRD analyses were carried out on the mixtures after 7 days of ambient curing while for other mixtures the XRD analyses were carried out after 1 day of elevated temperature curing. Fly ashes P36-2.65, and P28-2.20 had the highest calcium content, so the ambient curing was preferred for them to identify the hydration products. However, the other fly ashes P24-2.30, P25-2.35, and P21-2.20 had the lowest calcium content among the five fly ashes, meaning that the geopolymerization products were more dominant than the hydration products. Geopolymerization reactions were accelerated at elevated temperatures and can be identified after one day of elevated curing. The hydration process was tested at age of 7 days of ambient curing to allow for the pastes to form the compounds from which it acquires the strength.

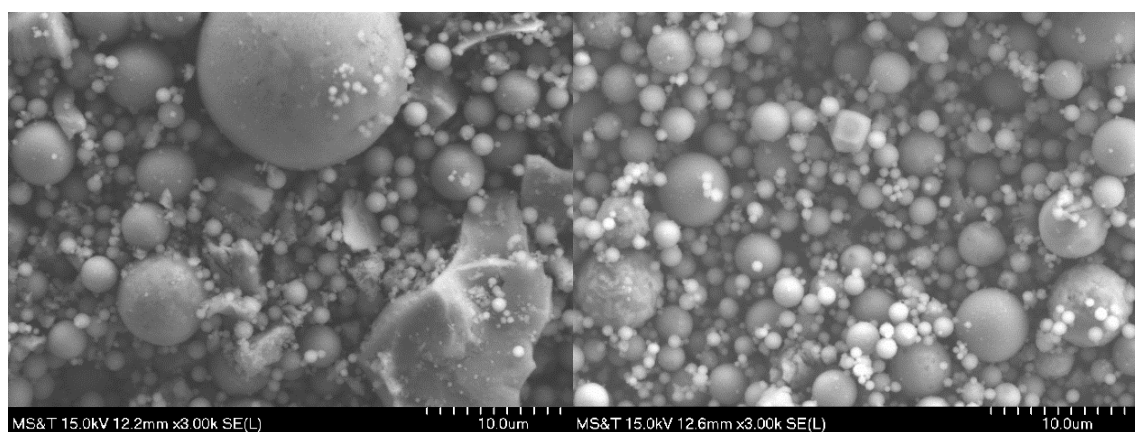
4. RESULTS AND DISCUSSION

4.1. SCANNING ELECTRON MICROSCOPY/ENERGY DISPERSIVE X-RAY SPECTROSCOPY (SEM/EDS) ANALYSES

The figures are not a quantitative indication of elements present in the fly ash samples. This is because fly ash is not a controlled substance and would have small changes in chemical composition [12]. SEM can only analyze a small fraction of an area sample, XRF provides a more holistic chemical analysis of the data and therefore more useful for that perspective. Raw fly ash powders, directly obtained from the different sources were used for the analysis. They are therefore referred to as “C36-2.65”, “C28-2.20”, “C24-2.30”, “C25-2.35”, and “C21-2.20”. SEM was used to study the structure of the fly ash particles as seen in the images and give us an indication of similar chemical results as seen in XRF. The fly ash particles are seen to have a spherical shape as this is a characteristic of the material. SEM results indicate that C36-2.65 and C25-2.35 had considerably larger

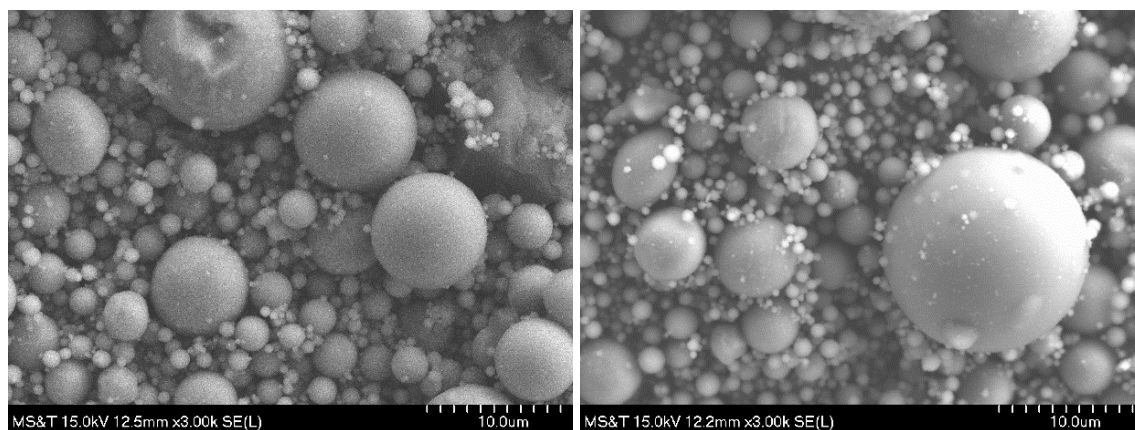
fly ash particles. Fly ash C28-2.20, C24-2.30, and C21-2.20 had considerably smaller particles at a 3000K magnification.

Fly ash and slag particle morphologies obtained using scanning electron microscopy is shown in Figure 6 (a) and (b) respectively. Fly ash has smooth spherical particles whereas slag is composed of angular particles of varying sizes.



(a) C36-2.65

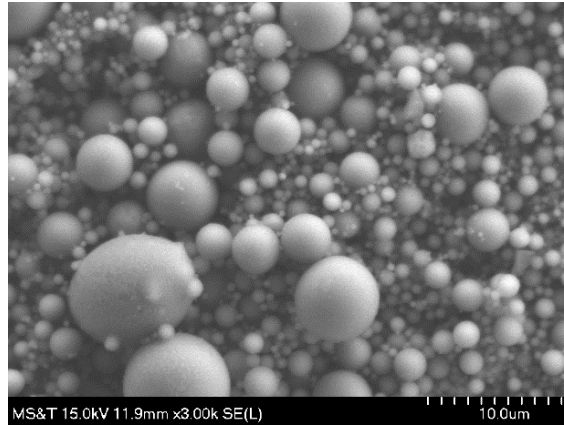
(b) C28-8.0



(c) C24-9.3

(d) C25-4.7

Figure 6. SEM Images for fly ash particles.



(e) C21-4.2

Figure 6. SEM Images for fly ash particles. (Cont.)

The EDS results obtained from SEM is acquired on a much smaller scale and therefore cannot be relied upon as a holistic result for the whole batch of fly ash even after cone and quatering. The EDS results indicate that results of elements found through X-ray Diffraction are confirmed. The intensity of the energy recorded indicate the increased amounts of these elements being present. Fly ash C36-2.65 and C28-2.20 have a very high peak of Calcium which indicates better performance at ambient curing to obtain strength. The increased peak of Silica and Alumina in F1-36-2.65 indicates that it could also perform very well at increased curing temperatures.

Fly ash C24-2.30, C25-2.35, and C21-2.20 had a much lower recording of Calcium but also had higher peaks of Silica and Alumina. This would help with the propensity of these fly ashes in forming NASH crystals at higher temperatures of curing. The detected Carbon content is a known quantity that is used to create a background surface for the fly ash powders. This detected carbon can therefore be ignored in the anlysis.

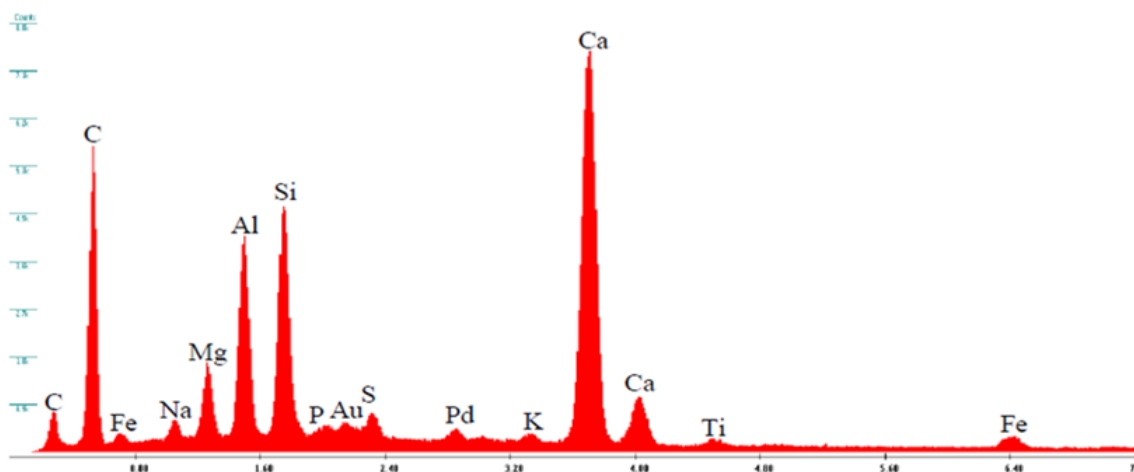


Figure 7. C36-2.65 EDS Image.

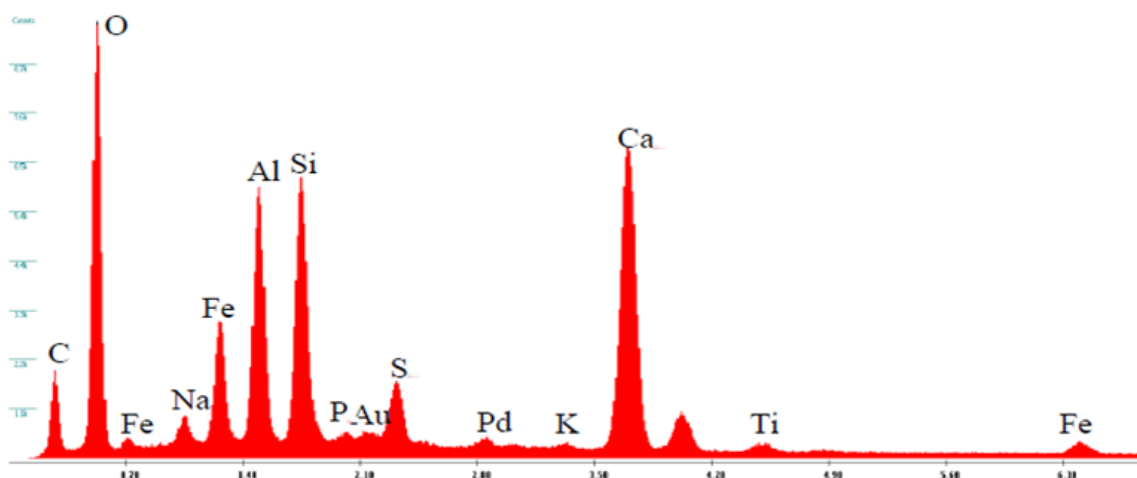


Figure 8. C28-2.20 EDS Image.

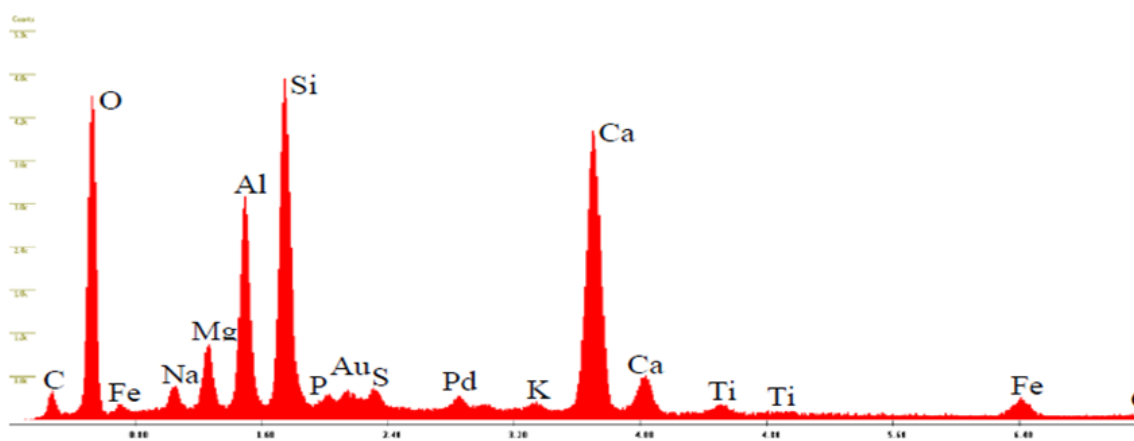


Figure 9. C25-2.35 EDS Image.

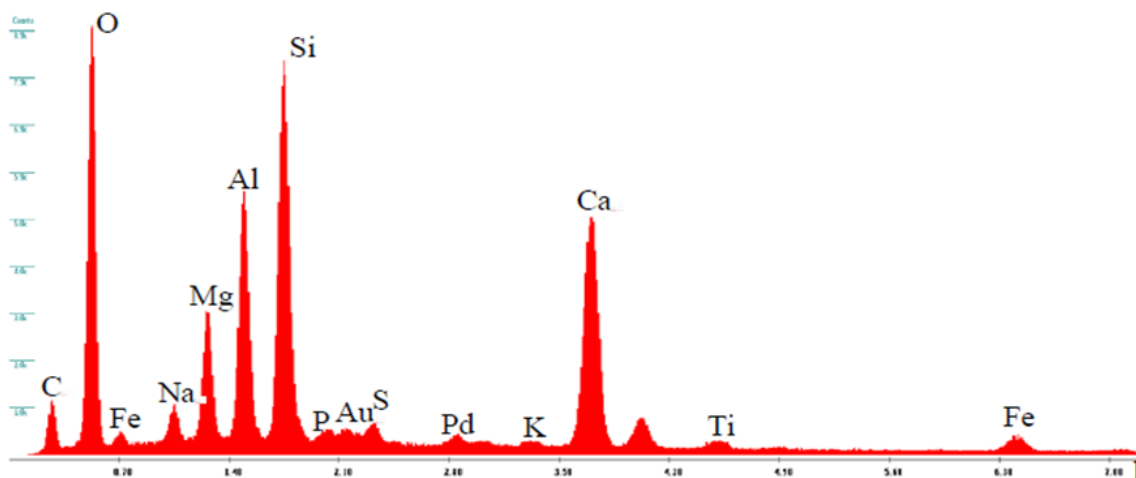


Figure 10. C24-2.30 EDS Image.

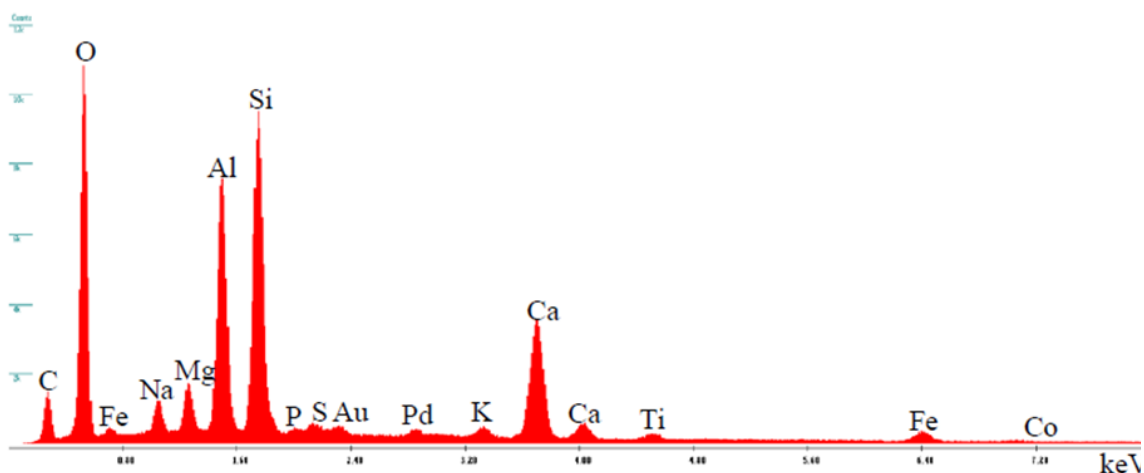


Figure 11. C21-2.20 EDS Image.

4.2. SETTING TIME AND FLOW

All the mixtures displayed initial setting times ranging from 75 minutes to 350 minutes and final setting times ranged from 100 minutes to 390 minutes (Figure 12). While there is no ASTM standard for determining an acceptance criteria for the setting times of mortar, the ASTM C191 [30] requires an initial and final setting times greater than 45 minutes and less than 375 minutes for *paste* mixtures, respectively. Hence, all mixtures satisfied the ASTM C191 [30] requirement for initial setting times. Furthermore, all mixtures except M25-2.35 mixed using the high sodium silicate (HS) satisfied the ASTM

C191 [30] requirements. For the HS M25-2.35, it displayed a final setting time of 390 minutes.

For silicate modulus of 1, most oxygen sites on the silicate tetrahedrons are occupied by either hydrogen or sodium ions. Thus, in this case fewer amounts of negatively charged oxygen sites are available for dissolved calcium ions, and as a result, the initial setting time is further increased.

For the solution of the lowest modulus ($n = 0.99$) larger silicate aggregates are completely absent, and the solution consists to a large extent only of smaller structural units like Q0 and Q1. At this water glass composition, the pH is close to 14 and the total amount of sodium ions in the solution are high. However as mentioned above, previous studies 7,29 have shown that when the peak position of the main peak is located around 985 cm^{-1} , most oxygen sites on the silicate tetrahedrons are occupied by either hydrogen or sodium ions. Thus, in this case fewer amounts of negatively charged oxygen sites are available for dissolved calcium ions, and as a result, the initial setting time is further increased.

According to the ^{29}Si spectra, the solution with modulus $n = 3.35$ is dominated by larger silicate aggregates, which suggests that a large amount of the sodium ions in the material are incorporated, or buried, in the silicate structures. As a consequence, only a few sites of negatively charged oxygens on the silica aggregates should be available for interaction with, for instance, dissolved ions in the surrounding. As the modulus n is decreased, larger silicate structural units break up and become smaller and thereby also a larger fraction of oxygen sites are found on the corners of the silicate aggregates.

Generally, doubling the amount of silicate in the HS mixtures compared to LA mixtures while keeping the total alkaline-to-fly ash ratio the same, decreased the initial setting time by approximately 30% for all fly ash sources except M25-2.35 and M24-2.30 where increasing the sodium silicate increased the setting time. Increasing the alkaline content by approximately 10% from mixtures LA to HA, reduced the initial setting time by approximately 10% due to the increased alkaline content activating the geopolymer compounds.

Investigating Figure 12 reveals that the effect of increasing the modulus of silicate on setting times is more pronounced than that of increasing alkalinity of the activator while keeping low modulus of the silicate. It is widely accepted that a higher concentration of SiO_4 increases the reaction rate [Chang et al. 2003].

From the graph it can be seen that the ratio of SiO_2 to Al_2O_3 had a consistent behavior on the overall lower setting times of the fly ashes up to 28% of Calcium content in the fly ash. The higher calcium content of 36% was determined to be the decisive factor in changing this trend in setting time.

The flowability results (Figure 13) are consistent with the initial setting time of the respective mixtures. The flow results indicate that increasing the silicate in the ratio of alkali activators reduces the workability of the geopolymer mixtures by an average of 30%. This is attributed to the viscosity of the sodium silicate. Similarly, increasing the alkaline activators by 10% reduced workability by an average of 15%. Generally, increasing the sodium silicate to sodium hydroxide ratio resulted in a lower workability and shorter setting time.

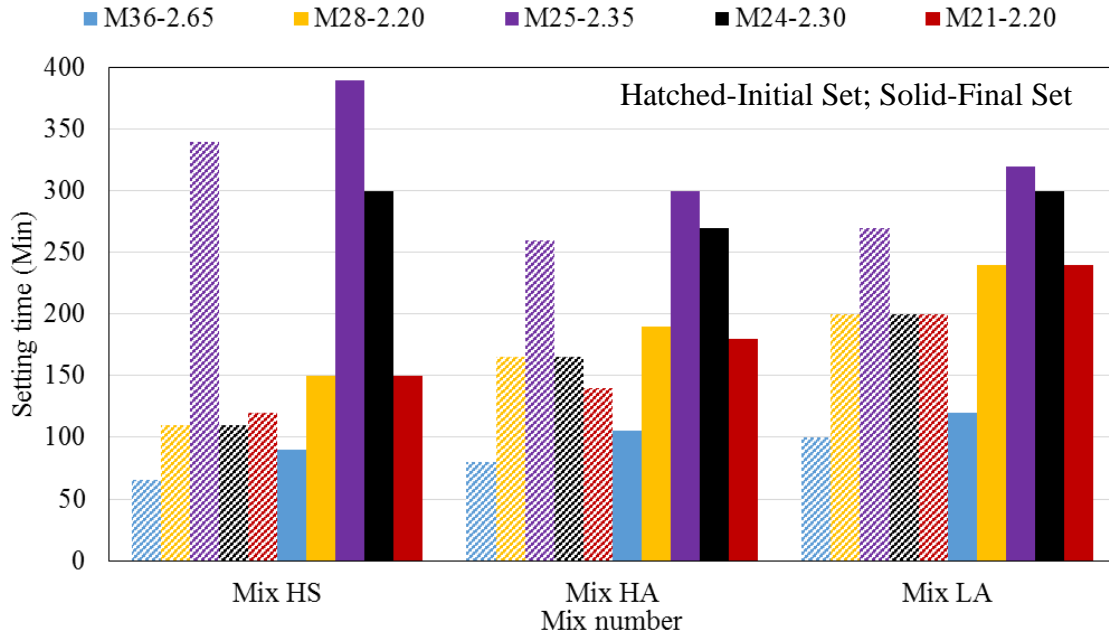


Figure 12. Setting times of fly ash mixes.

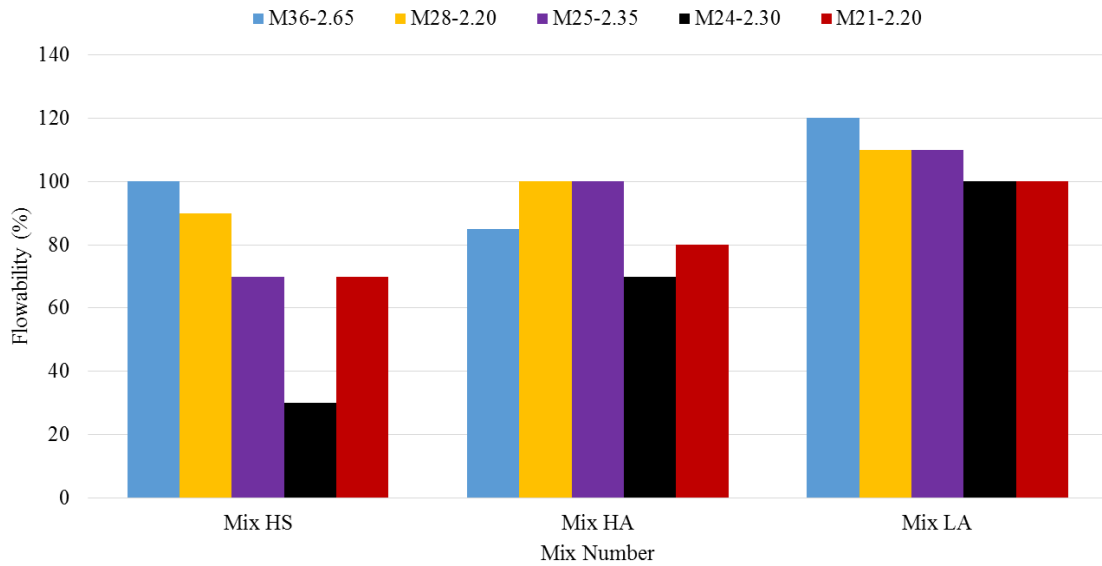


Figure 13. Flowability of fly ash mixes.

The lower workability of the high sodium silicate to sodium hydroxide ratio mixtures was a result of the high viscosity of the sodium silicate solution [33]. Increasing the sodium silicate to sodium hydroxide ratio from 1.0 to 2.0, increases the amount the soluble silica in the solution. Higher soluble silica in the system, improves the geopolymerization process and causes a shorter time to dissolve and leach the fly ash species [13, 34]. Also, it can be seen that with increasing the alkali activators to the fly ash ratio from 0.275 to 0.300 with keeping the water content constant, mix LA to mix LA, reduced the workability and the setting time as well. Adding higher amount of alkali solutions in the system accelerated the dissolution and leaching of the alumina and silica species from the source (fly ash) which caused a reduction in the workability and the setting time of the mixture.

While there are no ASTM limits for the flowability, a 60% flowability was found to be favorable in placing the mortar in the molds.

4.3. COMPRESSIVE STRENGTH OF THERMALLY CURED GEOPOLYMER

Figure 15 shows the compressive strength of each mixture after being cured for different periods at different temperatures. As shown in the figure, there is an optimum curing temperature and duration to produce the highest compressive strength for a given mixture. The compressive strengths for mixtures LA presented in the left column in Figure 15, which had lower alkaline contents and a silicate-to-hydroxide ratio of one, showed that the highest compressive strength for the high calcium mixtures are generally lower than those of mixtures having lower calcium content. For example, mixture M21-2.20 displayed a peak strength of 51 MPa (7350 psi) after curing of 16 hours at 70°C while mixture M36 displayed a peak strength of 41 MPa (5926 psi) after curing of 48 hours at 40°C. For all

sourced fly ash but C25-2.35 decreasing the calcium content increased the region where relatively high compressive strength can be achieved. Furthermore, decreasing the calcium content shifted the required temperature to achieve relatively higher strength toward higher thermal curing temperatures. It should be noted that C25-2.35 had significantly lower surface area compared to all other fly ashes (Figure 3).

For example, for M36-2.65 mixtures which had the highest calcium content, curing at 35 - 60°C for 24 to 48 hours produced the highest compressive strengths ranging from 37 to 44 MPa (5700 to 6400 psi) (Figure 15). For M28-8.0 mixtures, curing at 30 - 55°C for 16 - 48 hours produced the highest compressive strengths ranging from 34 to 47 MPa (5000 to 6900 psi). For M25-2.35 mixtures which had 31% lower calcium content than M36-2.65, curing at 55 - 85°C for 24 - 48 hours produced the highest compressive strengths ranging from 34 to 45 MPa (5000 to 6600 psi). For M24-2.30 mixtures which had 33% lower calcium content than M36-2.65, curing at 55 - 85°C for 24 - 48 hours produced the highest compressive strengths ranging from 34 to 46 MPa (5000 to 6700 psi). For M21-2.20 mixtures which had 42% lower calcium content than M36-2.65, curing at 55 - 85°C for 8-24 hours produced the highest compressive strengths ranging from 31 to 50 MPa (4500 to 7300 psi). These strengths were also replicated by curing at 55 °C for 48 hours.

The calcium content in the fly ash affects the geopolymerization process in the following three different aspects. 1) It can form $\text{Ca}(\text{OH})_2$ and precipitates. The formation of $\text{Ca}(\text{OH})_2$ will remove the OH^- ions which in turn reduce the pH of the alkaline solution and hence reduce the dissolution rate of the silicon and aluminum [35, 36]. 2) The free calcium ions reacted with the silica and alumina forming C-S-H gel. 3) The free calcium can replace a cation in the geopolymeric gel [19]. Increasing the curing temperature reduce the solubility

of Ca in geopolymer concrete. For example, increasing the temperature from 23C to 75C reduced the leached calcium by 50% [19]. Reducing the solubility of calcium allowed more geopolymerization to take place and hence fly ash with lower calcium content to display higher compressive strength and vice versa.

The compressive strengths for mixtures HA presented in the middle column in Figure 15, which had a higher alkaline content and a silicate-to-hydroxide ratio of one, showed higher strengths compared to the corresponding LA mixtures. Increasing the alkaline solution allowed higher strengths to be reached at relatively lower curing temperature and/or shorter curing times. Furthermore, the effects of increasing the alkaline was more prominent in the cases of fly ash with lower calcium content. This can be explained as follows. Increasing the surface hydroxylation which is proportional to the bulk concentration of hydroxide ions $[OH^-]$ increase the dissolution rates of Si and Si-Al. Furthermore, increasing the alkaline content significantly increases the leaching rate of Ca that are available in fly ash [37]. In the case of low calcium content, low level of calcium ions are dissolved and hence the monomers and oligomeric of the silicate and aluminate will form the geopolymer. Increasing the alkaline content in fly ashes having high calcium content led to formation and precipitation of $Ca(OH)_2$ which reducing the alkalinity of the solution and hence hinder the geopolymerization process resulting in less increase in the strength at early age and high temperatures.

The results for the HS mixtures, where the sodium silicate is doubled while keeping the total alkaline activator the same as the LA mixtures, are presented in the right column of Figure 15. For fly ash having high calcium content, the compressive strengths of the HS mixtures are generally higher than those of the corresponding LA mixtures. For example,

the peak strength of M36-2.65-Mix HS is 48 Mpa (7000 psi) reached after 16 to 48 hours of curing at 60 to 85°C while the peak strength for the corresponding LA mixture is 41 Mpa (6000 psi) and reached after 48 hours of curing at 35 to 55°C.

For fly ash having low calcium content, the compressive strengths of the HS mixtures are generally smaller than those of the corresponding LA mixtures. For example, the peak strength of M21-2.2-Mix HS is 38 Mpa (5500 psi) reached after 48 hours of curing at 70°C while the peak strength for the corresponding LA mixture is 48 Mpa (7000 psi) and reached after 16 to 48 hours of curing at 55 to 70°C. This reduction in strength occurred for two interrelated reasons. 1) Mixtures LA had lower sodium silicate and hence a higher pH than mixtures HS. This higher pH led to higher dissolution of the fly ash and high geopolymer gel formation specially at high temperatures. 2) The difference in the extended chain conformation and its degree of polymerization in the two mixtures affect the geopolymerization formation with LA mixtures having more favorable silicate conformations. Eighteen silicate conformations such as monomers, dimers, trimmers, large rings, chains and cyclic trimmers, and large rings generally coexist in silicate aqueous solution depending on the sodium silicate modulus [38]. Sodium silicate with modulus of one similar to that used in LA mixtures is typically richer in depolymerized lower-order species such as monomer and dimer which accelerate fly ash dissolution by reducing the reprecipitation of aluminosilicate gel particles onto the fly ash surfaces as well as initiate the polycondensation of geopolymer gel. Furthermore, sodium silicate with modulus of two similar to that used in HS mixtures is typically richer in more condensed and larger rings silicate species with few low-order uncondensed silicate monomers which reduce the speed of fly ash dissolution.

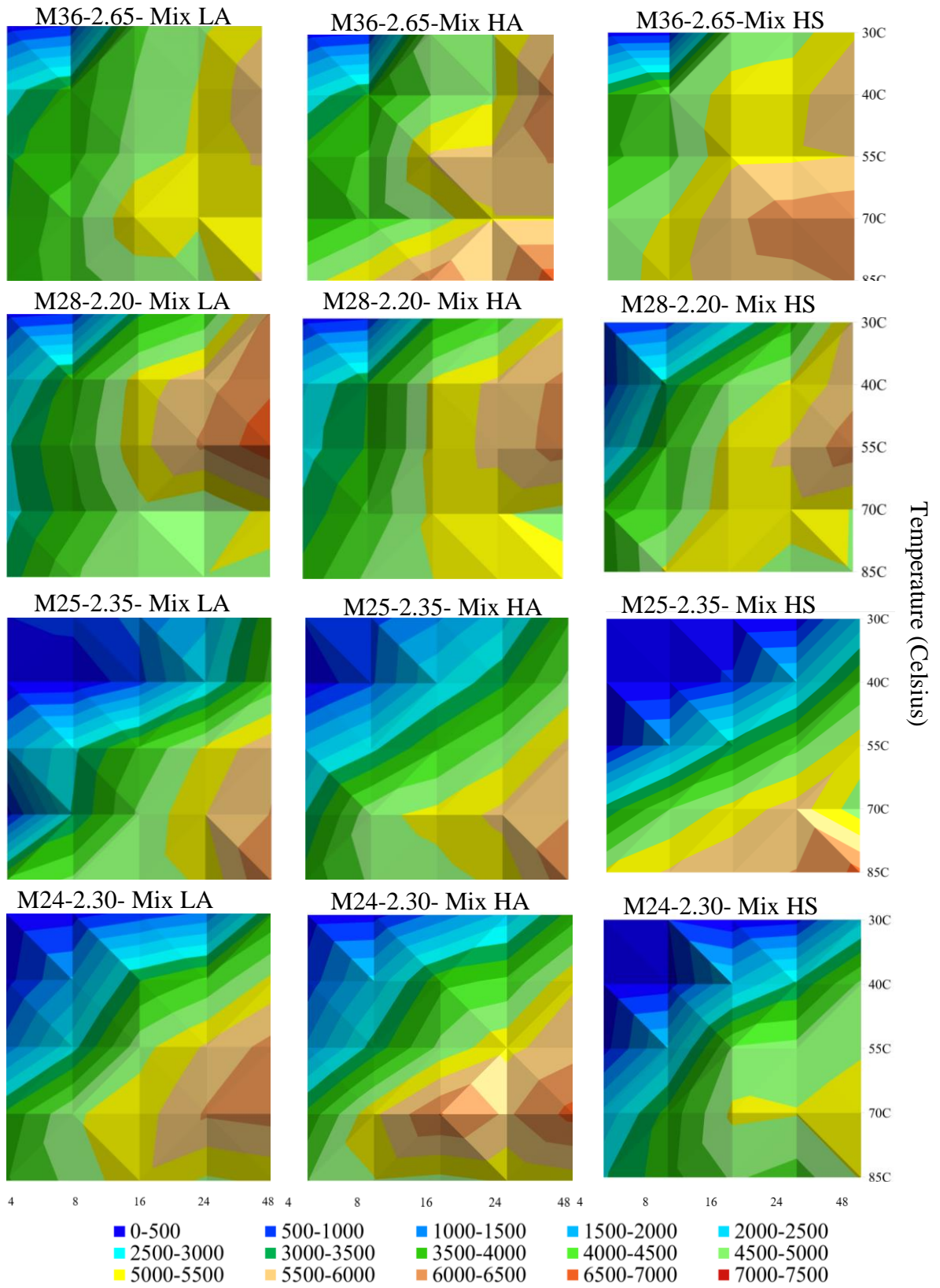


Figure 14. Compressive strength of different mixes at different temperatures and durations.

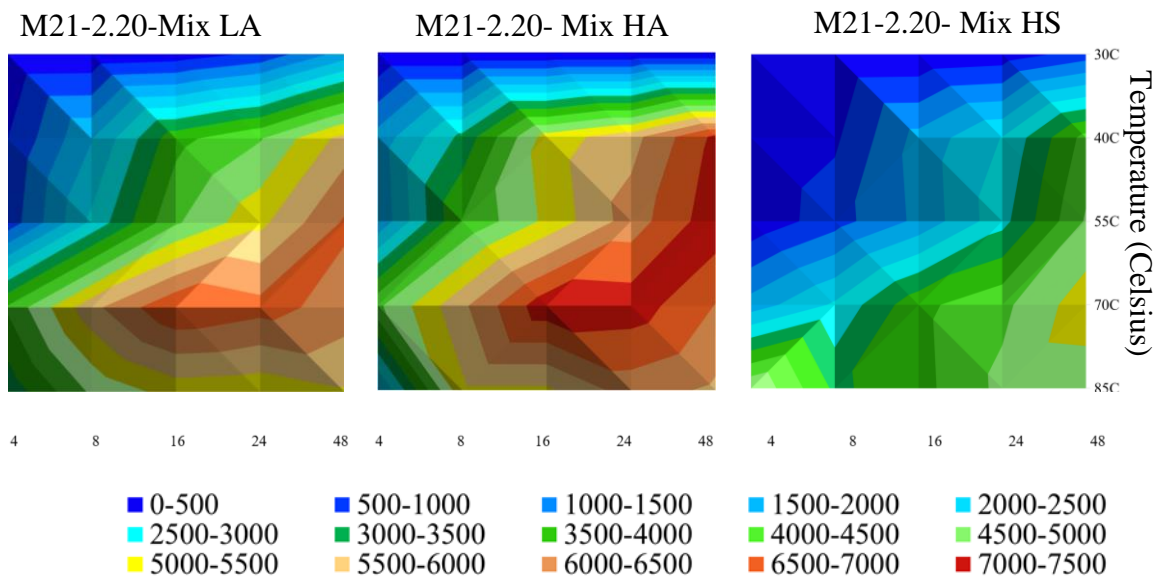


Figure 14. Compressive strength of different mixes at different temperatures and durations.
(Cont.)

4.4 COMPRESSIVE STRENGTH OF AMBIENT CURED GEOPOLYMER

Figure 16 is the representation of compressive strength results of a 12 hour variation to imitate Missouri summer conditions and a controlled consistent 30°C results for the three mix designs taken over a period of seven days. Comparatively higher calcium fly ashes, M36-2.65 and M28-2.20, were used to study the imitation of a typical Missouri summer. The results indicate that the seven day curing period for a controlled environment of 30°C had similar strengths to varying the temperatures conditions gradually, after 7 days. Furthermore, the mixes with higher calcium content, M36-2.65 and M28-2.20, also showed considerably more strength over a longer curing period. This is attributed to the formation of CASH crystals that depend on its hydration mechanisms to obtain strength. The lowest calcium fly ash, M21-2.30, consistently showed the lowest strengths over the 7 days of curing. The remaining two fly ashes, M25-2.35 and M24-30, showed comparable strengths at these lower temperature conditions. This similarity was improved by increasing the

alkaline activator content, as well as increasing the silicate to allow for greater dissolution of the hydroxide compounds.

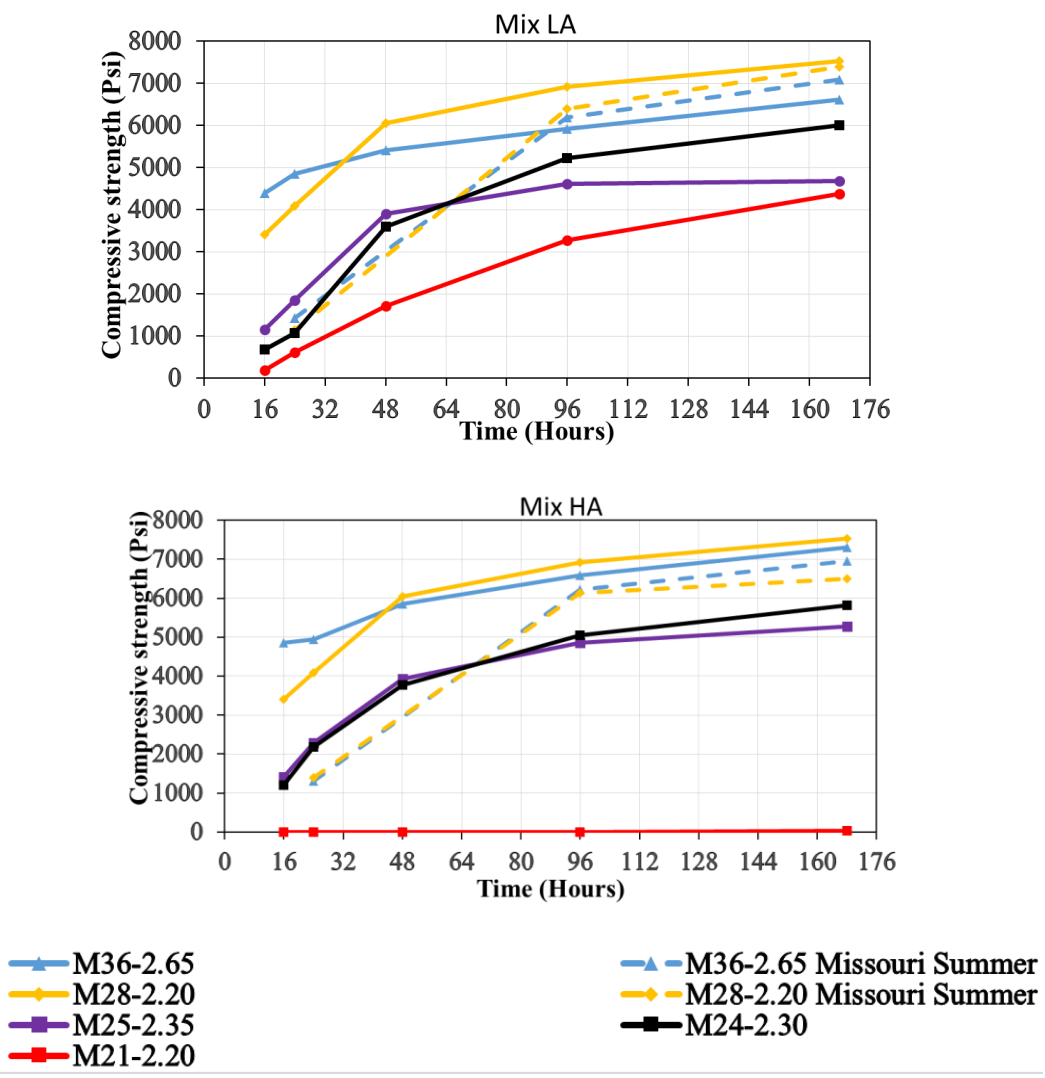


Figure 15. 7 Day Testing at 30°C and Missouri Summer conditions.

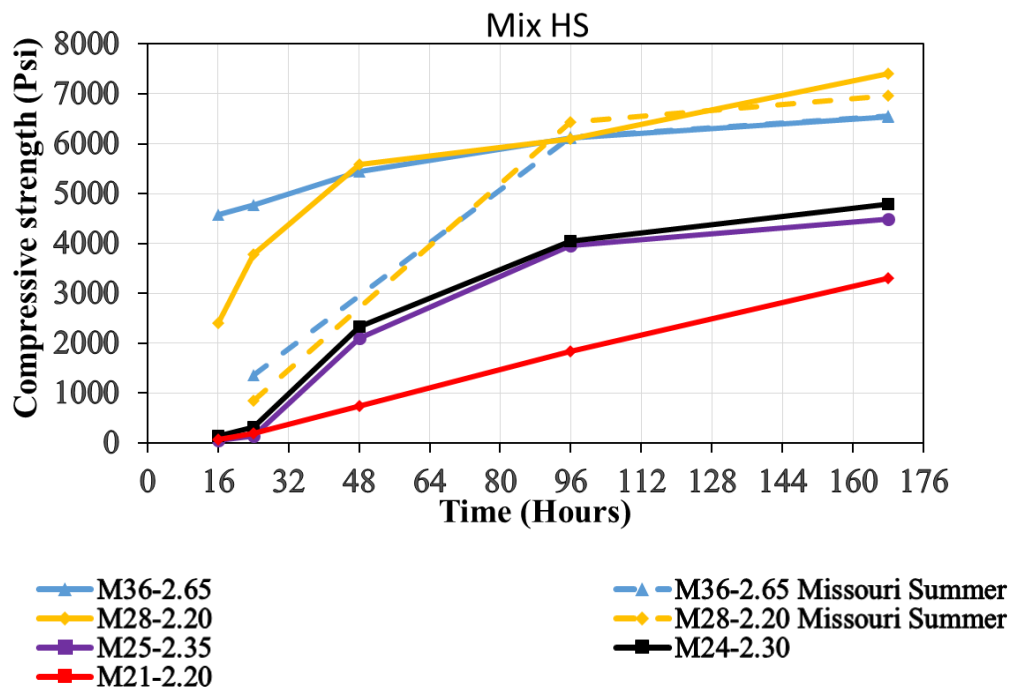


Figure 15. 7 Day Testing at 30°C and Missouri Summer conditions. (Cont.)

4.5. ENERGY CONSUMPTION

The energy values consumed during the curing of each mixture at different temperature and duration were recorded using a 270 kiloWatt voltmeter. The recorded data can be used to find the most energy efficient curing regime for a given strength and geopolymer mixture. Table 3 shows the energy consumption per temperature and duration.

Table 5. Energy Consumption. (kWhr)

Temp	4hrs	8hrs	16hrs	24hrs	48hrs
30 °C	2	4	8	12	24
40 °C	3	6	12	18	36
55 °C	6	12	24	36	72
70 °C	7	14	28	42	84
85 °C	10	20	40	60	120

As discovered from a preliminary study (Figure 14) in a typical Missouri summer, data for 30°C oven curing may be relied upon for practical field applications during a summer month. Therefore, this temperature can be considered as zero energy consumption, which is denoted on the y-axis for 7 day compressive strengths. Based on the Table 5 and Figure 16, we can deduce the most efficient energy consumption for each mortar mix of the fly ashes. Comparing the limitations for of the relatively higher calcium fly ashes, C36-2.65 and C28-2.20, it was more efficient to cure the specimens at ambient conditions than to obtain comparable strengths at elevated conditions. Higher compressive strengths were possible at just 30kWhrs of energy than curing for 7 days in the case of both, C25-2.35 and C24-2.30. C21-2.20 showed the same characteristics as C25-2.35 and C24-2.30, too a much higher scale. Close to ambient conditions at lower energy consumptions, consistently showed poorer results for comparatively lower calcium content fly ashes. Fly ash C36-2.65 and C28-2.20 was found to be the most energy efficient, for all three fly ash mixes as its lower limitations for strength were consistently higher than the other three fly ashes. However, upon increasing the imparted energy, the upper limitations for the other three fly ashes increased higher than that of C36-2.65 and C28-2.20.

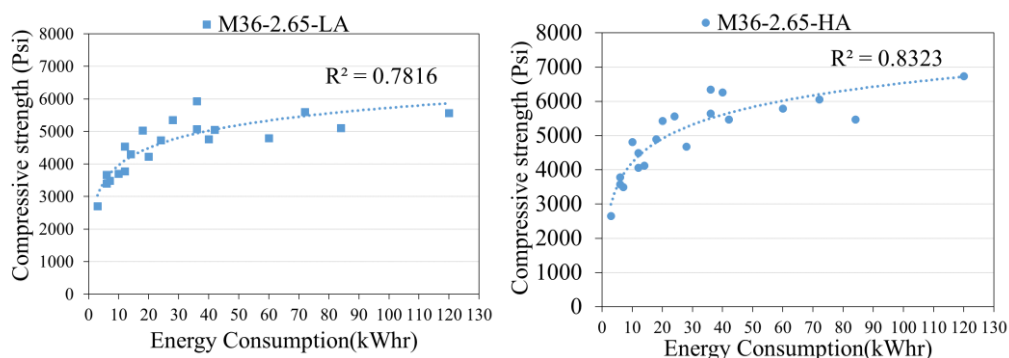


Figure 16. Compressive Strength related to energy consumption.

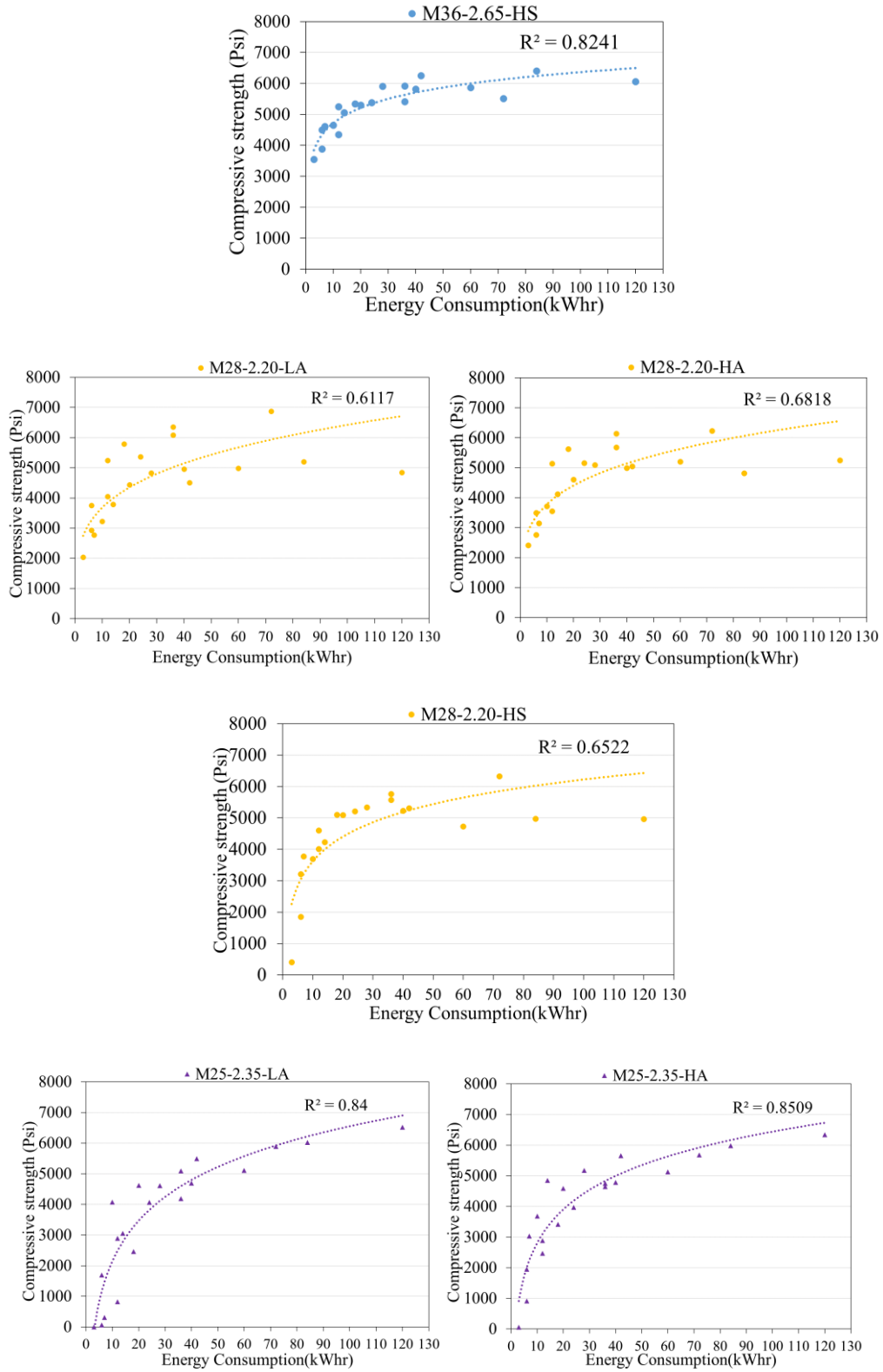


Figure 16. Compressive Strength related to energy consumption. (Cont.)

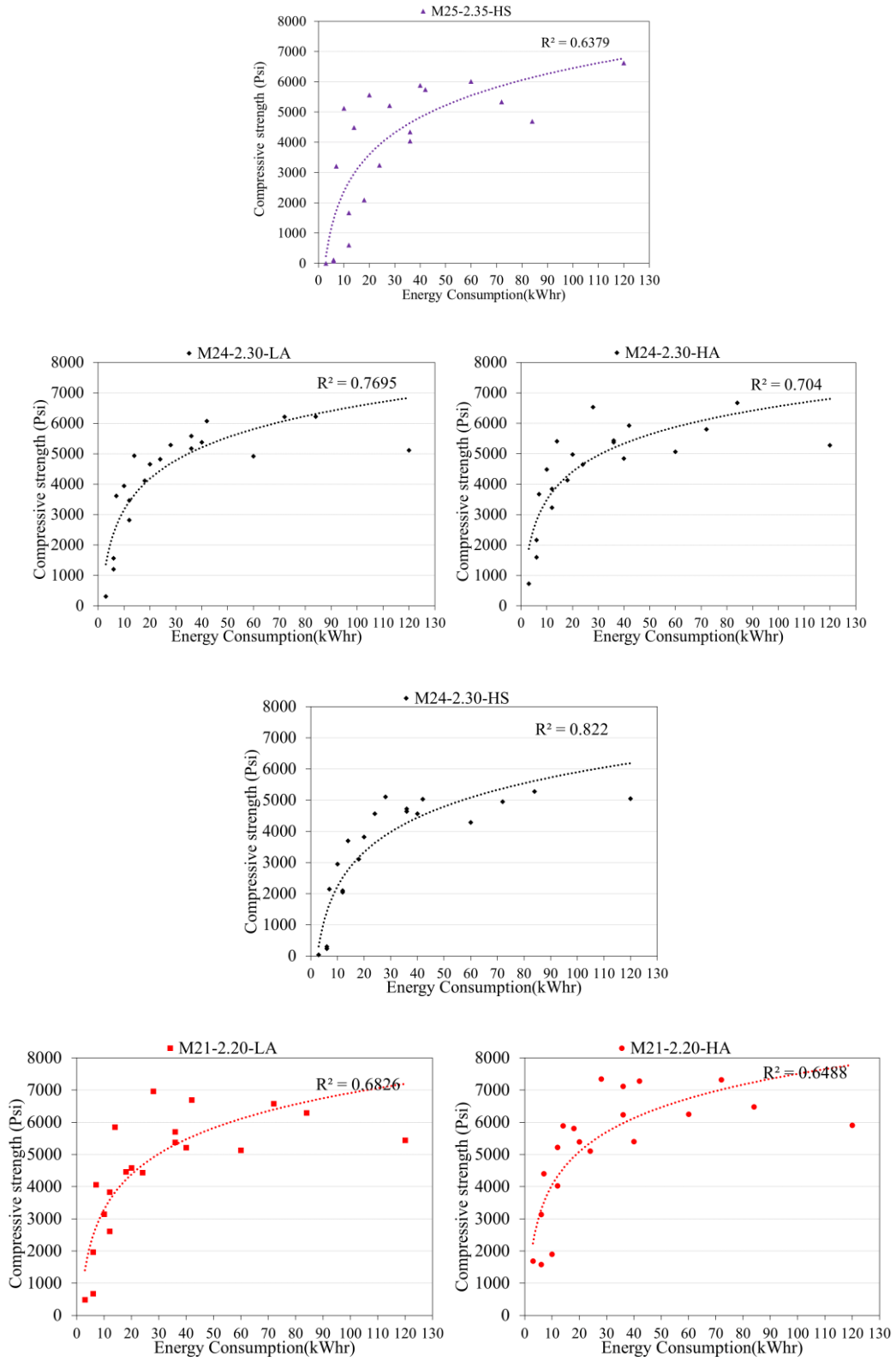


Figure 16. Compressive Strength related to energy consumption. (Cont.)

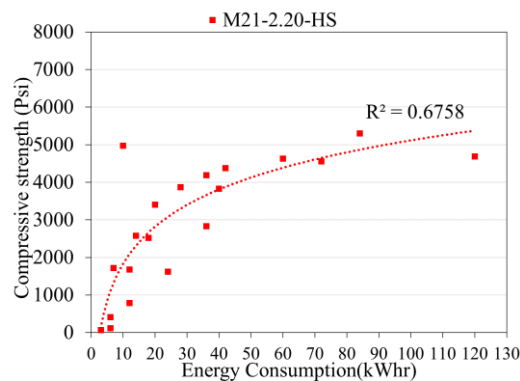


Figure 16. Compressive Strength related to energy consumption. (Cont.)

4.6. X-RAY DIFFRACTION (XRD) ANALYSIS

Figure 17 shows the compressive strength results of the fly ash pastes that were then crushed and grinded to perform the XRD analysis. It was observed that the higher calcium pastes, P36-2.65 and P28-2.20, had the highest strengths at ambient curing conditions due to the present hydration mechanisms. The comparatively lower calcium fly ash performed relatively poorly at these same conditions. The strength for these fly ashes were improved significantly at an elevated curing of 70°C over 24 hours.

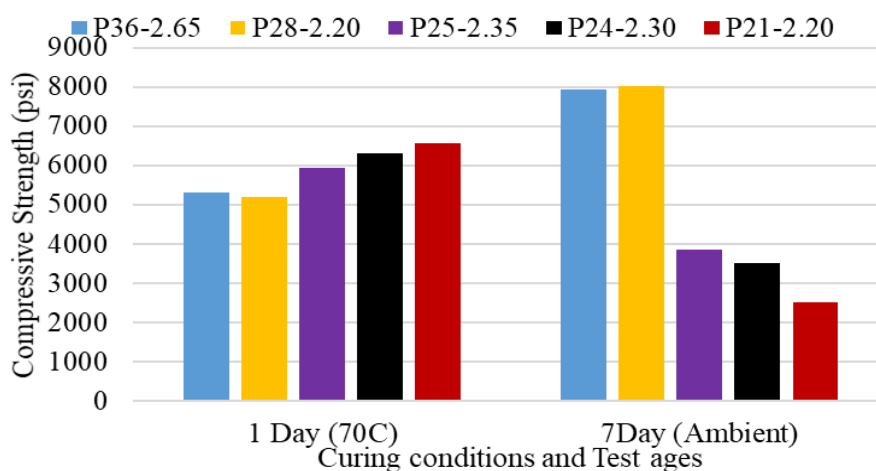


Figure 17. Compressive strength of the fly ash pastes.

Based on these observations, the pastes were run for the respective optimum curing conditions. Figure 18 shows the XRD results of the five samples, which were tested as fly ash pastes and therefore referred to as “P”. In the XRD analysis results, peaks of quartz (SiO₂) in the crystalline phase can be observed in all fly ashes. In addition, in P36-2.65, P28-2.20, P24-2.30, and P25-2.35, peaks of magnesium oxide were observed due to the high magnesium content in the raw fly ashes powders. In the paste that were prepared using P36-2.65, with the highest calcium content, more hydration products were observed comparatively than with P24-2.30, P25-2.35, and P21-2.20.

Where calcium aluminate silicate hydrate (Heulandite) (A; CaAl₂Si₇O₁₈·7H₂O), calcium silicate oxide (H; Ca₃SiO₅), and Cebollite (C; Ca₅Al₂(OH)₄Si₃O₁₂) were detected in P36-2.65 particularly. However, the other three fly ashes P24-2.30, P25-2.35, and P21-2.20 had the hydration and geopolymerization products such as, sodium calcium silicate (K; Na₂Ca₃Si₂O₈), and calcium sodium aluminum silicon oxide (N; Ca₇O₂Na_{1.73}(Al_{15.5}Si_{0.5}O₁₈)). P28-2.20 had a calcium content that was lower than P36-2.65 and higher than P24-2.30, P25-2.35, and P21-2.20, the detected phases were A and C. So, the C were observed only in P36-2.65 and P28-2.20 due to the hydration process and K and N were observed due to the geopolymerization process that were developed at the elevated heat curing only.

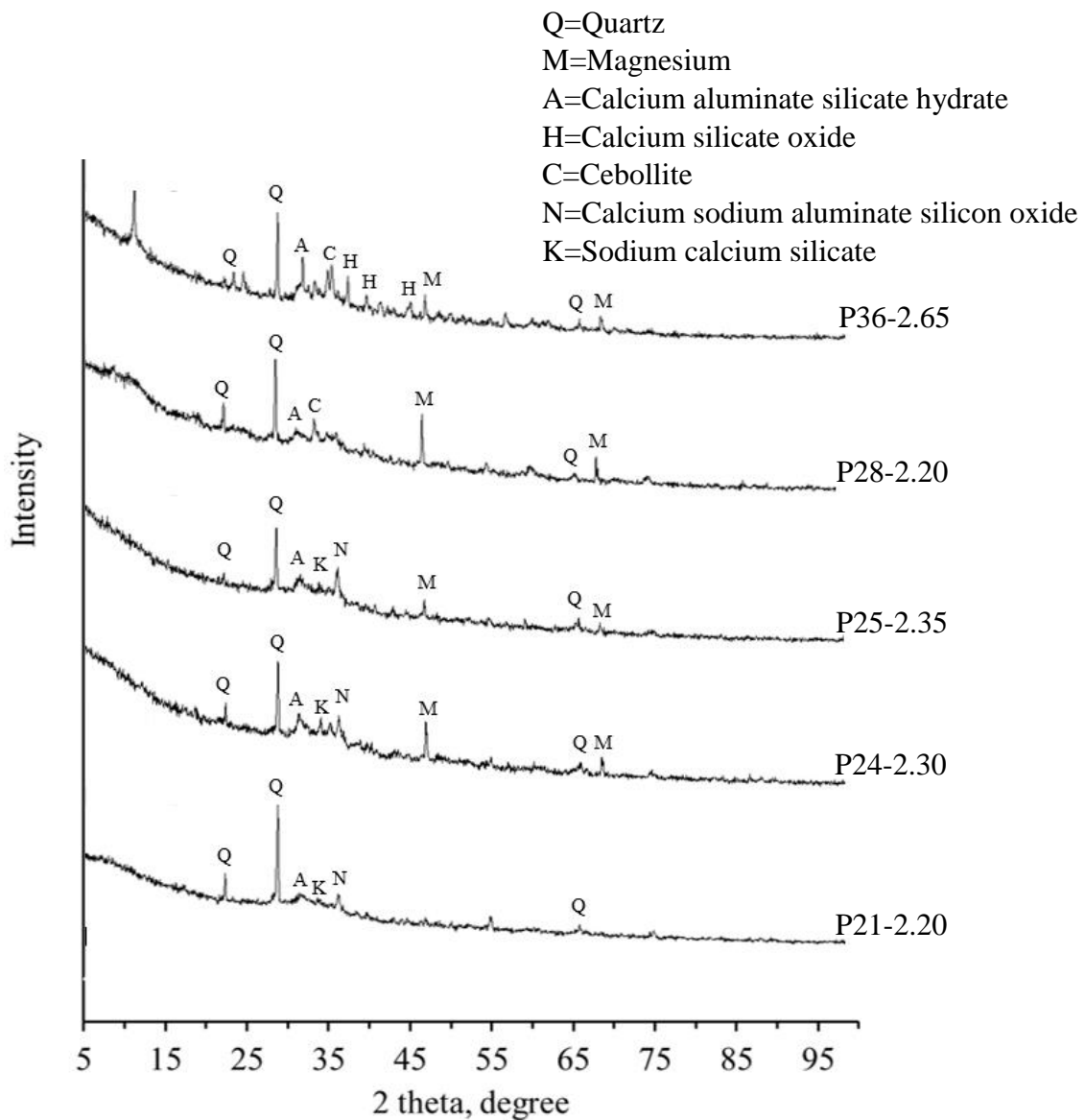


Figure 18. XRD analysis.

X-ray diffraction results from the prepared fly ash pastes confirm the presence of strong hydration mechanisms present in fly ash P36-2.65 and P28-2.20. Fly ash pastes P24-2.30, P25-2.35, and P21-2.20 showed more prominent NASH products in various combinations and structures of the fly ashes of the alkali activated pastes samples.

5. CONCLUSION

Testing fly ashes from different sources at various time intervals and temperatures helped determine the optimum ratios of chemicals, curing times, and curing temperatures for a particular chemical composition. This optimization can be attributed to energy efficiency or time necessary to achieve strength based on the particular needs in practical implementations. Five fly ashes were sourced from five different coal power plants in Missouri and studied at five different curing temperatures at five intervals of time. This will optimize chemical ratios and curing conditions for different fly ash chemical contents, and save time and money. The fly ashes were tested for X-ray Fluorescence (XRF), SEM-EDS, and X-ray Diffraction (XRD) to understand the various elements and subsequent compounds formed in the respective hydration and geopolymerization mechanisms. Setting time was determined to be governed by the calcium content of the fly ash and workability was governed by the amount of viscous silicate and water added.

1. Preliminary strength results found a negligible difference in strength between consistently exposing the specimens in a controlled environment of 30 °C and an imitated regime of elevated curing of a typical Missouri summer week. Therefore, results of 30 °C can be relied upon to imitate a Missouri summer. There was considerable strength gain over lower temperatures for all the fly ashes. Fly ash M36-2.65 and M28-2.20, which had higher calcium contents, showed improved performances at lower temperatures indicating prominent hydration mechanisms, similar to cement.

2. Fly ash M24-2.30 had a higher amount of silica and alumina but was still consistently out-performed in strength due to its lower calcium content at ambient

conditions and higher calcium content at elevated conditions. The optimized mixing procedure was found to be at an elevated temperature of 70 Celsius for 24 hours.

3. Fly ash M25-2.35, and M21-2.20 were found to be closely relatable in performance at the various curing regimes and chemical conditions. M21-2.20 outperformed all the other fly ashes at higher temperatures due to its lower Si/Al ratio and preferable calcium content to be unhindered at these elevated conditions.

REFERENCES

1. Association, A.R.T.B., *Production and Use of Coal Combustion Products in the United States*. American Coal Ash Association, June 2015.
2. Chindaprasirt, P., T. Chareerat, and V. Sirivivatnanon, *Workability and strength of coarse high calcium fly ash geopolymer*. *Cement and Concrete Composites*, 2007. 29(3): p. 224-229.
3. Administration, U.S.E.I. *Missouri State Profile and Energy Estimates*. 2015.
4. Agency, U.S.E.P. *National Primary Drinking Water Regulations*. 2017.
5. Blissett, R.S. and N.A. Rowson, *A review of the multi-component utilisation of coal fly ash*. *Fuel*, 2012. 97(Supplement C): p. 1-23.
6. Hardjito, D., *On the Development of Fly Ash-Based Geopolymer Concrete*. ACI Materials, 2004.
7. Kong, D.L.Y. and J.G. Sanjayan, *Effect of elevated temperatures on geopolymer paste, mortar and concrete*. *Cement and Concrete Research*, 2010. 40(2): p. 334-339.
8. Wallah, S.E., *Creep Behaviour of Fly Ash-Based Geopolymer Concrete*. *Civil Engineering Dimension*, September 2010.
9. Thokchom, S., *Resistance of Fly Ash Based Geopolymer Mortars in Sulphuric Acid*. *ARPN Journal of Engineering and Applied Sciences* February 2009.
10. Somna, K., et al., *NaOH-activated ground fly ash geopolymer cured at ambient temperature*. *Fuel*, 2011. 90(6): p. 2118-2124.
11. Jian Ping Zhu, Q.L.G., Dong Xu Li, Cun Jun Li, *Influence of Particle Size Distribution of Fly Ash on Compressive Strength and Durability of Portland Cement Concrete*. *Materials Science Forum*, June 2011.
12. Vassilev, S.V., *Methods for Characterization of Composition of Fly Ashes from Coal-Fired Power Stations: A Critical Overview*. Central Laboratory of Mineralogy and Crystallography, March 9, 2005.
13. Chindaprasirt, P., et al., *Effect of SiO₂ and Al₂O₃ on the setting and hardening of high calcium fly ash-based geopolymer systems*. *Journal of Materials Science*, 2012. 47(12): p. 4876-4883.

14. Silva, P.D., K. Sagoe-Crenstil, and V. Sirivivatnanon, *Kinetics of geopolymerization: Role of Al₂O₃ and SiO₂*. Cement and Concrete Research, 2007. 37(4): p. 512-518.
15. van Jaarsveld, J.G.S. and J.S.J. van Deventer, *Effect of the Alkali Metal Activator on the Properties of Fly Ash-Based Geopolymers*. Industrial & Engineering Chemistry Research, 1999. 38(10): p. 3932-3941.
16. Rattanasak, U. and P. Chindaprasirt, *Influence of NaOH solution on the synthesis of fly ash geopolymer*. Minerals Engineering, 2009. 22(12): p. 1073-1078.
17. Dimitrios Panias, I.P.G., Theodora Perraki, *Effect of synthesis parameters on the mechanical properties of fly ash-based geopolymers*. Metallurgy and Materials Technology, December 2006.
18. Criado, M., A. Palomo, and A. Fernández-Jiménez, *Alkali activation of fly ashes. Part I: Effect of curing conditions on the carbonation of the reaction products*. Fuel, 2005. 84(16): p. 2048-2054.
19. Guo, X., H. Shi, and W.A. Dick, *Compressive strength and microstructural characteristics of class C fly ash geopolymer*. Cement and Concrete Composites, 2010. 32(2): p. 142-147.
20. Abdullah, M.M.A., et al., *The Relationship of NaOH Molarity, Na₂SiO₃/NaOH Ratio, Fly Ash/Alkaline Activator Ratio, and Curing Temperature to the Strength of Fly Ash-Based Geopolymer*. Advanced Materials Research, 2011. 328-330: p. 1475-1482.
21. Pan, Z., J.G. Sanjayan, and B.V. Rangan, *An investigation of the mechanisms for strength gain or loss of geopolymer mortar after exposure to elevated temperature*. Journal of Materials Science, 2009. 44(7): p. 1873-1880.
22. Chindaprasirt, P., P. De Silva, and S. Hanjitsuwan, *Effect of High-Speed Mixing on Properties of High Calcium Fly Ash Geopolymer Paste*. Arabian Journal for Science and Engineering, 2014. 39(8): p. 6001-6007.
23. Gomaa, E., et al., *Fresh properties and compressive strength of high calcium alkali activated fly ash mortar*. Journal of King Saud University - Engineering Sciences, 2017. 29(4): p. 356-364.
24. Lowke, D., *Effect of Mixing Energy on Fresh Properties of SCC*. March 2005.
25. Conrad, K.L., *Geochemical Database of Feed Coal and Coal Combustion Products (CCPs) from Five Power Plants in the United States*. United States Geological Survey, November, 2011.

26. Manual, X.A., *X-Ray Radiation Safety-Manual for Operator Training*. 2010.
27. ASTM, *Standard Specification for Coal Fly Ash and Raw or Calcined Natural Pozzolan for Use in Concrete*. 2015, ASTM International.
28. International, A., *C778 - 17 Standard Specification for Standard Sand*. ASTM, 2017.
29. Hammer, G.R., *Climate of Missouri*. National Oceanic and Atmosphere Administration, 01/31/2006.
30. C191-13, A.S., *Standard Test Methods for Time of Setting of Hydraulic Cement by Vicat Needle*. ASTM International, 2013.
31. 15, A.S.C., *Standard Test Method for Flow of Hydraulic Cement Mortar*. ASTM International, 2015.
32. C109/C109M-16a, A.S., *Standard Test Method for Compressive Strength of Hydraulic Cement Mortars (Using 2-in. or [50-mm] Cube Specimens)*. ASTM International, 2016.
33. Provis, J.L. and S.A. Bernal, *Geopolymers and Related Alkali-Activated Materials*. Annual Review of Materials Research, 2014. 44: p. 299-327.
34. Siyal, A.A., et al., *Effects of Parameters on the Setting Time of Fly Ash Based Geopolymers Using Taguchi Method*. Procedia Engineering, 2016. 148: p. 302-307.
35. Yip, C.K., et al., *Effect of calcium silicate sources on geopolymerisation*. Cement and Concrete Research, 2008. 38(4): p. 554-564.
36. van Deventer, J.S.J., et al., *Reaction mechanisms in the geopolymeric conversion of inorganic waste to useful products*. Journal of Hazardous Materials, 2007. 139(3): p. 506-513.
37. Papias, D., I.P. Giannopoulou, and T. Perraki, *Effect of synthesis parameters on the mechanical properties of fly ash-based geopolymers*. Colloids and Surfaces A: Physicochemical and Engineering Aspects, 2007. 301(1): p. 246-254.
38. Cho, H., et al., *Solution state structure determination of silicate oligomers by ²⁹Si NMR spectroscopy and molecular modeling*. Journal of the American Chemical Society, 2006. 128(7): p. 2324-2335.
39. World, C., *CW.03.08.Concrete.indd*. The Royal Society of Chemistry, March 2008.

40. Ernst Worrell, et al., *CARBON DIOXIDE EMISSIONS FROM THE GLOBAL CEMENT INDUSTRY*. Annual Review of Energy and the Environment, 2001. 26(1): p. 303-329.
41. Wan, Q., et al., *Geopolymerization reaction, microstructure and simulation of metakaolin-based geopolymers at extended Si/Al ratios*. Cement and Concrete Composites, 2017. 79(Supplement C): p. 45-52.
42. Sun, P. and H.-C. Wu, *Chemical and freeze–thaw resistance of fly ash-based inorganic mortars*. Fuel, 2013. 111(Supplement C): p. 740-745.
43. Lior, N., *Sustainable energy development: The present (2009) situation and possible paths to the future*. Energy, 2010. 35(10): p. 3976-3994.
44. Chindaprasirt, P. and S. Rukzon, *Strength, porosity and corrosion resistance of ternary blend Portland cement, rice husk ash and fly ash mortar*. Construction and Building Materials, 2008. 22(8): p. 1601-1606.
45. Malkawi, A.B., et al., *Effects of Alkaline Solution on Properties of the HCFA Geopolymer Mortars*. Procedia Engineering, 2016. 148(Supplement C): p. 710-717.
46. Xie, T. and T. Ozbakkaloglu, *Behavior of low-calcium fly and bottom ash-based geopolymer concrete cured at ambient temperature*. Ceramics International, 2015. 41(4): p. 5945-5958.
47. Duxson, P., et al., *Geopolymer technology: the current state of the art*. Journal of Materials Science, 2007. 42(9): p. 2917-2933.
48. Provis, J.L., *Alkali-activated materials*. Cement and Concrete Research, 2017.
49. Phair, J.W. and J.S.J. van Deventer, *Characterization of Fly-Ash-Based Geopolymeric Binders Activated with Sodium Aluminate*. Industrial & Engineering Chemistry Research, 2002. 41(17): p. 4242-4251.
50. Khale, D. and R. Chaudhary, *Mechanism of geopolymerization and factors influencing its development: a review*. Journal of Materials Science, 2007. 42(3): p. 729-746.
51. Simčič, T., et al., *Chloride ion penetration into fly ash modified concrete during wetting–drying cycles*. Construction and Building Materials, 2015. 93(Supplement C): p. 1216-1223.
52. Shravan Kumar, K.R., *Assessment of Chloride Ion Penetration of Alkali Activated Low Calcium Fly Ash based Geopolymer Concrete* Key Engineering Materials, 2016.

53. Ma, Y., J. Hu, and G. Ye, *The pore structure and permeability of alkali activated fly ash*. Fuel, 2013. 104(Supplement C): p. 771-780.
54. Deb, P.S., *Durability of Fly Ash Based Geopolymer Concrete*, in *Civil Engineering*. June 2013, Curtin University. p. 178.
55. Yunsheng, Z., Wei, *Fly Ash Based Geopolymer Concrete*. Indian Concrete Journal, 2006.
56. Talha Junaid, M., et al., *A mix design procedure for low calcium alkali activated fly ash-based concretes*. Construction and Building Materials, 2015. 79(Supplement C): p. 301-310.
57. Ramujee, K., *Development of Low Calcium Flyash Based Geopolymer Concrete*. Journal of Engineering and Technology, 2014.
58. Nematollahi, B. and J. Sanjayan, *Effect of different superplasticizers and activator combinations on workability and strength of fly ash based geopolymer*. Materials & Design, 2014. 57(Supplement C): p. 667-672.
59. Carabba, L., S. Manzi, and C.M. Bignozzi, *Superplasticizer Addition to Carbon Fly Ash Geopolymers Activated at Room Temperature*. Materials, 2016. 9(7).
60. LI, K.-L., *Study on Abilities of Mineral Admixtures and Geopolymer to Restrain ASR*. Key Engineering Materials, 2006.
61. Brew, D.R.M. and K.J.D. MacKenzie, *Geopolymer synthesis using silica fume and sodium aluminate*. Journal of Materials Science, 2007. 42(11): p. 3990-3993.
62. Güneyisi, E. and M. Gesoğlu, *A study on durability properties of high-performance concretes incorporating high replacement levels of slag*. Materials and Structures, 2008. 41(3): p. 479-493.
63. Cai, L., H. Wang, and Y. Fu, *Freeze–thaw resistance of alkali–slag concrete based on response surface methodology*. Construction and Building Materials, 2013. 49(Supplement C): p. 70-76.
64. Beaudoin, J.J. and C. MacInnis, *The mechanism of frost damage in hardened cement paste*. Cement and Concrete Research, 1974. 4(2): p. 139-147.
65. Shi Yan, Y.H., *Aging Mechanism of Dam Concrete under the action of Freeze-Thaw Damage* Applied Mechanics and Materials 2014.
66. Fan, L., *Research into the concrete freeze-thaw damage mechanism based on the principle of thermodynamics*. Applied Mechanics and Materials 2013.

67. Ben Li, K.W., *STUDY ON THE DAMAGE MECHANISM OF PORE STRUCTURE IN CONCRETE SUBJECTED TO FREEZE-THAW CYCLES*. THE CIVIL ENGINEERING JOURNAL, 2015.
68. Criado, M., et al., *Alkali activated fly ash: effect of admixtures on paste rheology*. Rheologica Acta, 2009. 48(4): p. 447-455.
69. Steven, G. and K. Paul, *Effect of Fly Ash on the Air-Void Stability of Concrete*. Special Publication. 79.
70. Freeman, E., et al., *Interactions of carbon-containing fly ash with commercial air-entraining admixtures for concrete*. Fuel, 1997. 76(8): p. 761-765.
71. Hill, R.L., et al., *An examination of fly ash carbon and its interactions with air entraining agent*. Cement and Concrete Research, 1997. 27(2): p. 193-204.
72. Division, F.H., *Freeze Thaw Resistance of Concrete with Marginal Air Content*. 2006, U.S Department of Transportation.
73. Skvara, F., *Alkali Activated Material - Geopolymer* Department of Glass and Ceramics- Faculty of Chemical Technology, ICT Prague, 2007.
74. Savas, B., S. Ahmad, and D. Fedroff, *Freeze-Thaw Durability of Concrete with Ground Waste Tire Rubber*. Transportation Research Record: Journal of the Transportation Research Board, 1997. 1574: p. 80-88.
75. Richardson, A., et al., *Crumb rubber used in concrete to provide freeze-thaw protection (optimal particle size)*. Journal of Cleaner Production, 2016. 112(Part 1): p. 599-606.
76. Richardson, A.E., K.A. Coventry, and G. Ward, *Freeze/thaw protection of concrete with optimum rubber crumb content*. Journal of Cleaner Production, 2012. 23(1): p. 96-103.
77. Gadkar, S. and P. Rangaraju, *The Effect of Crumb Rubber on Freeze-Thaw Durability of Portland Cement Concrete*. 2013.
78. International, A., *Standard Specification for Coal Fly Ash and Raw or Calcined Natural Pozzolan for Use in Concrete*. ASTM, 2017.
79. International, A., *Standard Specification for Chemical Admixtures for Concrete*. ASTM, 2017.
80. International, A., *Standard Specification for Air-Entraining Admixtures for Concrete*. ASTM, 2016.

81. Officials, A.A.o.S.a.H.T., *Standard Specification for Air-Entraining Admixtures for Concrete (ASTM Designation C260/C260M-10a)*. 2016, AASHTO.
82. Li, W., et al., *Water Absorption and Critical Degree of Saturation Relating to Freeze-Thaw Damage in Concrete Pavement Joints*. *Journal of Materials in Civil Engineering*, 2012. 24(3): p. 299-307.
83. Bentz, D.P., *SORPTIVITY-BASED SERVICE LIFE PREDICTIONS FOR CONCRETE PAVEMENTS*. National Institute of Standards and Technology, 2001. Building and Fire Research Laboratory.
84. International, A., *Standard Test Method for Flow of Hydraulic Cement Mortar*. 2015, ASTM.
85. International, A., *Standard Test Method for Compressive Strength of Hydraulic Cement Mortars (Using 2-in. or [50-mm] Cube Specimens)*, in *ASTM C109 / C109M - 16a*. 2016, ASTM.
86. International, A., *Standard Test Method for Resistance of Concrete to Rapid Freezing and Thawing*, in *ASTM C666 / C666M - 15*. 2015, ASTM.
87. International, A., *Standard Test Method for Air Content of Hydraulic Cement Mortar*, in *ASTM C185 - 15a*. 2015, ASTM.
88. theconstructor.org. *Effect of Air Entrained Concrete on Strength of Concrete*. 2017; Available from: <https://theconstructor.org/concrete/air-entrained-concrete-strength-effects/8427/>.

II. IMPROVING THE FREEZE THAW DURABILITY OF CLASS C FLY ASH-BASED GEOPOLYMER MORTARS USING COMPATIBLE ADDITIVES

Simon Peter Sargon^a, and Mohamed A. ElGawady^b

^aCivil, Architectural and Environmental Engineering, Missouri University of Science and Technology.

^bAssociate Professor and Benavides Faculty Scholar; Civil, Architectural and Environmental Engineering, Missouri University of Science and Technology, corresponding author.

HIGHLIGHTS

- Characteristics of two fly ash sources and rubber were investigated for multiple additives.
- The findings provide the optimum reduction of water with superplasticizers
- Air entrainment was implemented with air entraining admixtures and rubber, successfully inhibiting deterioration in freeze thaw.

ABSTRACT

In light of the ongoing emphasis on sustainability, the last few years have seen a manifest increase in using geopolymer cement as an Eco-friendly replacement of the Portland Cement represent with 80 to 90% less CO₂ emission. However, since the geopolymer relies on using byproducts such as fly ash as a main component of the binder part, a high fluctuation in some of the key characterization such ad durability was reported. Simultaneously, most of the durability improvement admixtures in the market have uncertain behavior with geopolymer since they were prepared to be used with Portland Cement. Based on that, an experimental study was performed to improve the freeze-thaw durability of geopolymer mortar by trying different techniques and selecting the compatible and effective admixtures. Two superplasticizers were tried with two fly ashes to reduce the free water and improve the workability which results in an

improvement in the durability. Two air entraining agents with different chemistry, in addition to the recycled rubber, was used as an additive to improve the durability. In addition to the workability of fresh mortar, the compressive strength of mortar cubes was tested before and after exposing them to 36 cycles of freeze and thaw. The performance of each admixture was varied from fly ash to another and from mix to another with a clear improvement on the durability (from 18% to 36%) based on the chemical composition. All matrixes with the rubber inclusion showed an improvement in strength retention by 40%., from 50% loss in the reference matrix.

Keywords

Geopolymer; Mortar; Class C Fly ash; Curing; Compressive strength; Energy efficiency

1. INTRODUCTION

For every ton of ordinary Portland cement (OPC) produced, one ton of CO₂ is released into the atmosphere which contributes 5 percent of annual anthropogenic global CO₂ production [39]. Combining this high CO₂ emission/ton of cement with the incessant demand of cement production results in a large and growing carbon footprint and raise the need for Eco-friendly methods to reduce this negative impact [40]. One of the solutions to address this issue is using solid waste or by-product powders, and fly ash (FA) is one of the successful options to consider.

Fly ash has been widely used as a partial replacement of OPC to improve the performance in terms of relative strength, anti-corrosive ability, freeze-thaw durability, and fire resistance [7, 41, 42]. From the sustainability aspect, the usage of fly ash helps because of two reasons, the aforementioned reduction in the dependence on OPC, and

reducing the ongoing polluting disposal principles of FA which is connected to the national and statewide increase of using coal power plants as a source for energy [1, 43]. However, the use of fly ash has been limited to up to 30% as a partial replacement of OPC, as it has been found to affect the performance of the matrix beyond this percentage negatively [44].

One of the promising solutions toward sustainable and Eco-friendly replacement options of conventional concrete is geopolymers, where it is introducing a 100% replacement of cement in concrete mixes using a highly alumina-silica cementitious material like fly ash, rice husk, metakaolin, slag, etc. Due to the ongoing fly ash disposal issue, fly ash is at the forefront of this technology with several researchers exploring possible behavior mechanisms of their matrix [7, 41, 42, 45, 46]. They are synthesized by exposing the aluminosilicate compounds present in the replacement cementitious materials to high alkali solutions to form alkali aluminosilicates (NASH) at comparative strengths to cement compounds (CASH) [47, 48].

Most of the previous studies or applications of fly ash based geopolymer were focusing on using low calcium fly ash (fly ash class F). However, as of recently, there has been an increase in the burning of lignite and sub-bituminous coals rather than older anthracite or bituminous coals, increasing the availability high calcium fly ash (fly ash class C) [49]. Using fly ash class C in geopolymer has the potential to lower the curing temperature since the curing conditions for geopolymers with fly ash class F are under scrutiny due to its slow strength gain at ambient conditions and poor cost-effectiveness at elevated temperatures[21, 50].

Fly ash-based geopolymers are facing the issue of erratic behavior due to the uncontrolled source of fly ash as a by-product. As a result, The implementation of this technology is therefore hindered by the variable consensus on their behavior in durability conditions like freeze-thaw [7, 42], sulfate resistance [9], chloride ion penetration [51, 52], water permeability [53], etc. For example, there is a varied consensus on the performance of geopolymers in terms of durability in freeze-thaw resistance [54]. Alkali-activated mortars and concrete have been shown to possess superior freeze thaw-resistance [55]. However, these studies have been conducted on materials such as low calcium fly ash [56-59], metakaolin [60], silica fume[61], and slag [62, 63], which have a different chemical structure and behavior. With an average of 110 days with temperature below 0°C , freeze-thaw durability is a crucial quality sought after in the Missouri climate, as there is considerable degradation of concrete pavements and roads. The mechanism of freeze-thaw resistance is caused due to the unreacted free water molecules that leave voids in the matrix that expand at low temperatures and breaking the cementitious binders[64]. There are two possible solutions to this issue, reducing the free water in the matrix and introducing controlled air voids to dissipate the stress from free water expansion leading to the disintegration of the paste structure [65-67]. To circumvent these issues, admixtures are a possible solution, as they are already implemented in the field to deal with possible durability and workability issues. However, all admixtures are designed specifically for OPC, which may behave considerably different to that of fly ash.

The freeze-thaw durability of two class C fly ashes with diverse calcium content has been investigated in this study. The first step toward improving the freeze-thaw

durability was reducing the water/fly ash ratio and then reducing the amount of free water. However, by reducing the water/fly ash ratio, the workability of the matrix is significantly affected which raise the need to use superplasticizers. To address the varied consensus in the literature regarding the performance and dosages of different types of admixtures [68]. Two different kinds of superplasticizers (SP) were studied in two dosages based on the suggested quantities used with of OPC concrete.

The second step toward improving the freeze-thaw durability was introducing uniform scattered air voids to the geopolymer matrix to reduce the stress on the matrix by dissipating the stress from free water expansion that leads to the disintegration of paste structure. Two different types of air entraining admixtures (AEA) were used at their suggested minimum and maximum dosages. It must be noted that, even with OPC concrete, air entraining admixtures behave erratically when they mixed with fly ash. Some literature suggests to significantly increase the AEA's when there are more organic materials present [69]. There has also been some discussion regarding the effect of carbon content on the behavior of these admixtures [70, 71]. The effects of air entraining admixtures were found to be dependent upon the type of resin used, the percentage of air entraining, and the spacing factor [72, 73].

Using the same methodology that was used with air entraining admixtures, crumb rubber (CR) has been found to introduce the same effect on the matrix by attracting and entrapping air voids [74]. The effect of the CR on freeze-thaw durability has been found to be influenced by the type of CR, the rubber passing and retaining sieve numbers, and percentage replacement of sand [75-77].

The change in the compressive strength and the visual inspection of 50X50X50 mm mortar cubes was used to study the effect of each additive on the freeze-thaw durability after exposing the specimens to 36 cycles of freeze and thaw according to ASTM C666 procedure A. During the course of this study, the compatibility and the effectiveness of each admixture or additive with two types of fly ash with different calcium content were investigated.

2. MATERIAL PROPERTIES

2.1. FLY ASH CHEMICAL COMPOSITION

Fly ash was obtained from two different coal power plants, Labadie, and Sikestone in Missouri, the United States with high variance in calcium content. X-ray fluorescence (XRF) was used to determine the chemical analysis of the fly ash powders and they were determined to be class C according to ASTM C618 [78] (Table 1). Variable vacuums and filters were used to determine each chemical compound present in the fly ash. This helped determine more accurate results and percentages to one another. The loss of ignition is the carbon content of the fly ashes that is burnt off when subjected to 700 °C for two hours.

Table 1. X-Ray Fluorescence Chemical Analysis.

Fly Ash	CaO (%)	Al₂O₃ (%)	SiO₂ (%)	Na₂O (%)	MgO (%)	P₂O₅ (%)	K₂O (%)	TiO₂ (%)	MnO (%)	Fe₂O₃ (%)	LOI (%)
C36	36.9	13.9	36.8	1.62	4.80	0.70	0.62	0.87	0.03	3.52	0.50
C21	21.2	20.1	43.9	2.87	4.29	0.51	0.70	1.36	0.05	4.96	0.40

LOI: Loss on ignition

A ternary phase diagram comparing CaO-SiO₂-Al₂O₃ was prepared to show the base chemical differences in relation to variable sources (Figure 1).

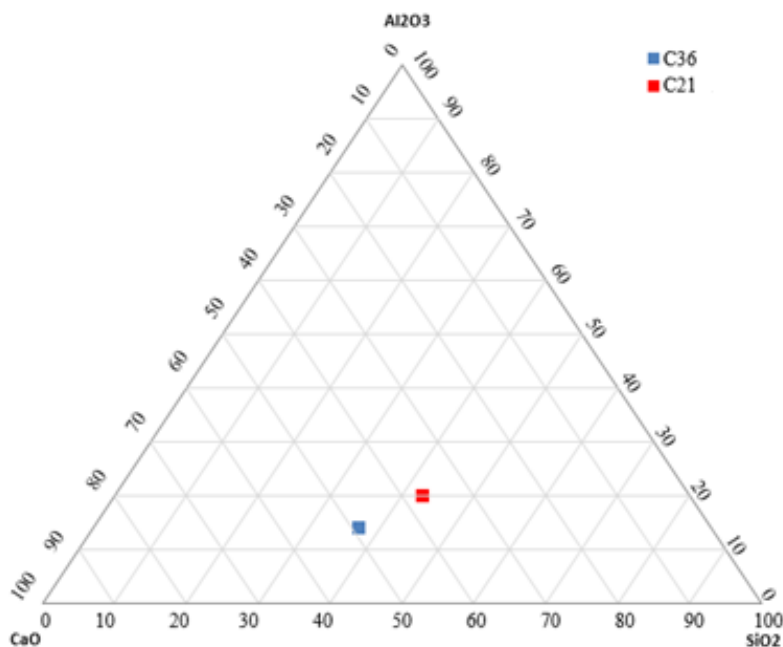


Figure 1. CaO-SiO₂-Al₂O₃ Ternary Phase Diagram.

Based on the calcium content, the fly ashes were named as C 36 and C 21, for Labadie and Sikestone respectively. Mortar samples of these fly ashes that were prepared according to previously conducted studies with a relatively lower alkaline activator/FA ratio, will be referenced as M36 and M21, respectively.

The particle size distribution and surface area of the two fly ashes were determined using a Microtrac S3500 series size analyzer and the Brunauer–Emmett–Teller (BET) method, respectively. It was found that C21 had finer particles with 50% of particles smaller than 12.81 μm and C36 had 50% of particles smaller than 14.75 μm .

The BET method found that C21 had a comparatively larger surface area of 2921 m²/kg than C36, which had a surface area of 2560 m²/kg.

Scanning electron microscopy (SEM) was used to analyze the structure of the particles in the respective fly ashes and examine element analysis using the energy dispersive spectroscopy (EDS) (Figure 2 &3). This mechanism analyzes the base elemental composition of a very minute particular point in the fly ash powders by displacing electrons around the element's atom and recording the emitted displacement energy. The scanning electron microscope captures the area that is run through EDS to identify shape and structure of the recorded elements. As shown in Figure 4, the fly ash particles have a spherical shape as what has been seen in previous literature. This spherical shape is due to the combustion process in the coal-fired power plants, which forms various layers of materials as it is thrown into the air during burning.

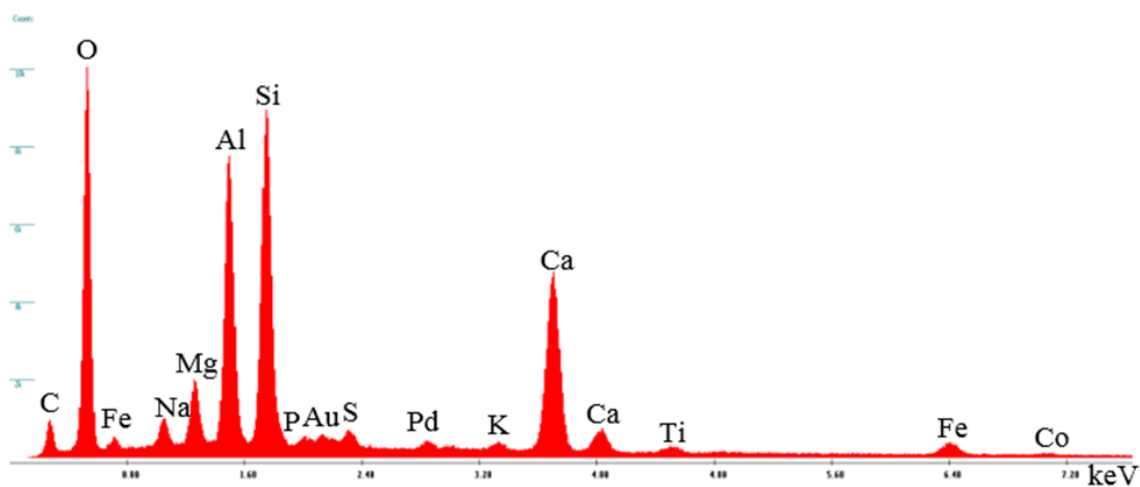


Figure 2. Element analysis using the energy dispersive spectroscopy (EDS) for fly ash C21.

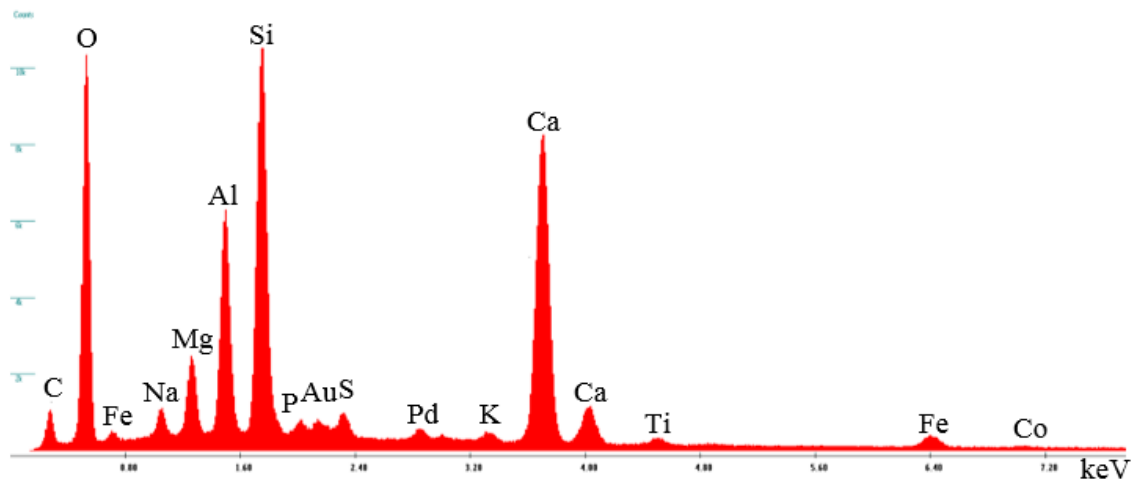


Figure 3. Element analysis using the energy dispersive spectroscopy (EDS) for fly ash C36.

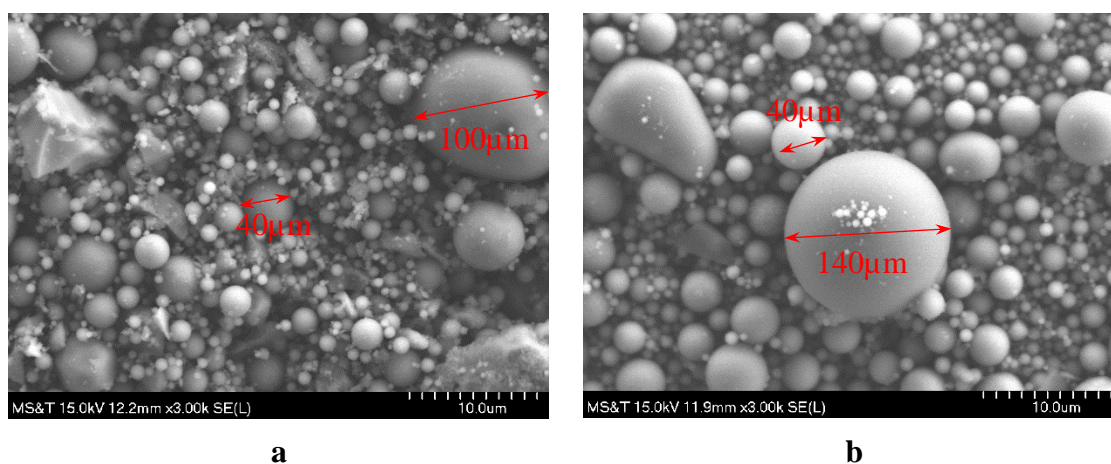


Figure 4. Scanning electron microscopy (SEM) images of fly ash (a) Labadie (C36), and (b) Sikestone (C21).

2.2 ALKALI ACTIVATORS

The alkali activators used in this study were Sodium Hydroxide and Sodium Silicate (Water glass). A 10M molarity of sodium hydroxide was selected as the optimized relativity between gain in strength and the cost analysis in the practical applications of the mortar. There was 77.5% of Sodium and 22.5% of water in the sodium

hydroxide. Type D sodium silicate was used with a sodium content of 14.7%, a silicate content of 29.4%, and a water content of 55.9%.

2.3 FINE AGGREGATE

Missouri River Sand with a specific gravity of 2.6 prepared according to ASTM C778 [28] in Surface Saturated Dry (SSD) condition was used.

2.4 RECYCLED RUBBER

A recycled rubber that came from the scrap tires' processing was used during the course of this study as a replacement of sand from 8 to 16 percent. Two grades of recycled rubber were used during this study. The first grade was for recycled rubber with particles pass sieve No. 50 and retained on sieve No. 100 which leads to a particle size between 0.297 and 0.149 mm. The second grade was for recycled rubber particles pass sieve No. 200 which leads to a particle size smaller than 0.074 mm (74 μm). Figure 5 shows the particle size distribution of both sizes of recycled rubber in addition to two fly ashes using the laser diffraction analyzer.

Table 2. Physical properties of Rubber.

Type of Aggregate	Rubber	
	R<200	50<R<100
Bulk specific gravity	0.87	0.87
Absorption, %	0.1%	0.1%
Coefficient of Uniformity	2.03	2.29
Loose dry unit weight, kg/m^3	625	582
Median particle size, μm	60	225

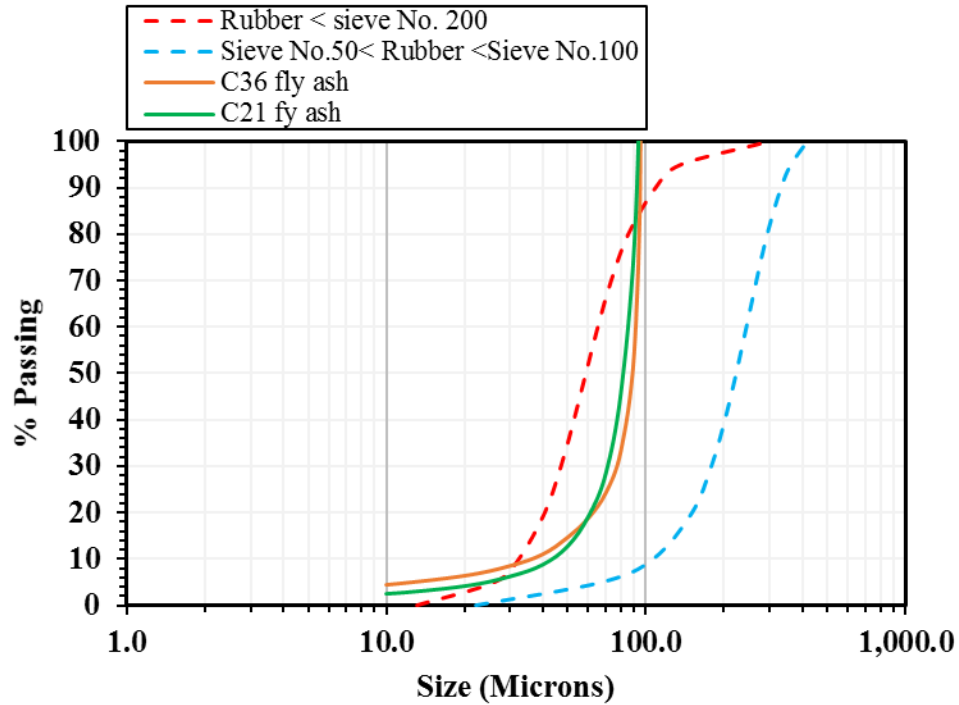


Figure 5. Particle size distribution of C21, C36, Cement, and Rubber.

2.5 ADMIXTURES

The admixtures used were superplasticizers, and air entraining agents.

Superplasticizers Master Glenium 3400 and Master Glenium 7511 were selected.

Glenium 3400 is a high range water reducer based on polycarboxylate chemistry that meets ASTM C494 [79] requirements for Type A and Type F admixtures. Glenium 7511 is a full range water reducer that also meets the requirements of Type A and Type F superplasticizers as per ASTM C494. BASF Master AE200 and BASF Master V10 were used as air entraining agents. Master V10 is a neutralized vinsol resin admixture. Both air entraining admixtures meet the requirements of ASTM C260 [80] and AASHTO M 154 [81].

3. EXPERIMENTAL PROGRAM

3.1. MIX PROPORTIONS

The ratio between alkali activators and fly ash, and the sodium hydroxide to sodium silicate was selected as 1:1, for both ratios to reduce the variables in the study and study the effects of the admixtures alone. The workability of this matrix was determined to have a relatively lower alkaline activator/FA ratio of 0.275 from previous studies, due to its higher workability, to circumvent possible issues encountered with the additives.

Table 3. Mix Designs.

Ratio	Mix Design	Adjusted SP Mix Design
Alkaline/Fly ash	0.275	0.275
Water/Fly ash	0.380	0.360
Silicate/Hydroxide	1.000	1.000

The ratios of admixture to cementitious materials were adjusted according to the suggested quantities in the admixture manuals. These quantities were the maximum and minimum dosages for their respective properties. They were selected to study a large variation of adding the chemical admixtures and to determine its effects on workability, strength, and ability to successfully reduce the water content. Reducing the water in the mixture to its critical degree of saturation, therefore providing only enough water to successfully activate the calcium hydration compounds to induce strength, has been found to help improve freeze-thaw resistance [82, 83].

Table 4. Admixture Mix Designs.

Ratio	Low(mL/Kg)	High(mL/Kg)
Glenium 3400/Fly ash	130	325
Glenium 7500/Fly ash	325	520
AE 200/ Fly ash	32	98
VR10/ Fly ash	32	98

3.2. MIXING PROCEDURE

A three speeds Hobart mixer was used to mix all the mortar specimens. The mixing procedure is as follows,

1. Sand and Fly ash mixed together for 30 seconds at 130 rpm.
2. All batch water added gradually over a 60 second period at 130 rpm.
3. The Sodium hydroxide and Sodium Silicate were mixed together to improve the dissolution of chemicals in the mix.
4. The mixing speed was then increased to 300 rpm and the combination of chemicals was added in 5 equal batches over a 300 second period.
5. After adding the chemicals, the mixer was allowed to continue at 300 rpm for an additional 300 seconds.
6. Increasing the speed beyond 300 rpm was found to be unsatisfactory as there was a loss of material from the bowl.

3.3. WORKABILITY

ASTM C1437 [84] slump flow table was used to record workability of the various mixes and the average of three measurements was recorded.

3.4. CURING PROCEDURE

The specimens were prepared according to ASTM C109 [85] in metal molds of optimum thermal conductivity. These cubes were then placed in their respective curing conditions until the testing periods. The two curing conditions, ambient and elevated temperature (70 °C), were followed for the fly ashes to study the compressive strength effects of temperature with and without additives. Higher calcium class C fly ash, M36,

was cured at ambient conditions due to its higher propensity to obtain significant strength in the formation of CASH compounds. M21 had a relatively lower calcium content and was therefore studied at elevated curing temperatures. Curing the relatively lower fly ash mortar, M21, at ambient conditions was found to be ineffective with highest 7 days strengths of 4400 psi with the same mix design. The elevated curing conditions were controlled and recorded using temperature gauges, a voltmeter, and four thermocouples placed at various locations to ensure uniform distribution of heat in the chamber (Figure 6).

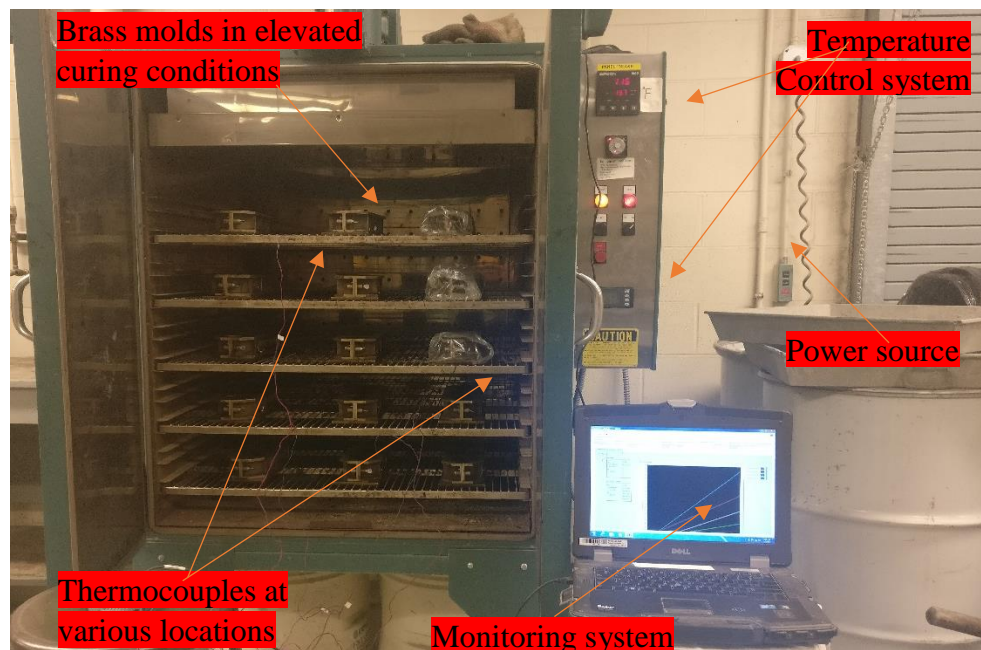


Figure 6. Oven curing procedure.

3.5. FREEZE-THAW CHAMBER

The test for freeze-thaw durability was conducted on 2 inch cubes, breaking reference specimens prior to freeze-thaw and after 36 cycles in the chamber. The loss in strength was considered an indication of the durability of the specimens to retain its

strength after being exposed to extreme climatic conditions. The test cubes were placed in a freeze-thaw chamber according to ASTM C666 [86].

4. RESULTS AND DISCUSSION

4.1. SUPERPLASTICIZER EFFECTS

The first approach to improve the freeze-thaw durability of mortar was to reduce the free water available in the mixture by reducing the mixture water content. However, there is a minimal water content required for wetting the fly ash and facilitates the workability. Figure 7 shows the effects of water content on the workability of two different types of fly ash. As shown in the figure, reducing the water-to-fly ash ratio by 5% reduced the workability by 50%. Reducing the water-to-fly ash ratio by 10% resulted in concrete with approximately no workability.

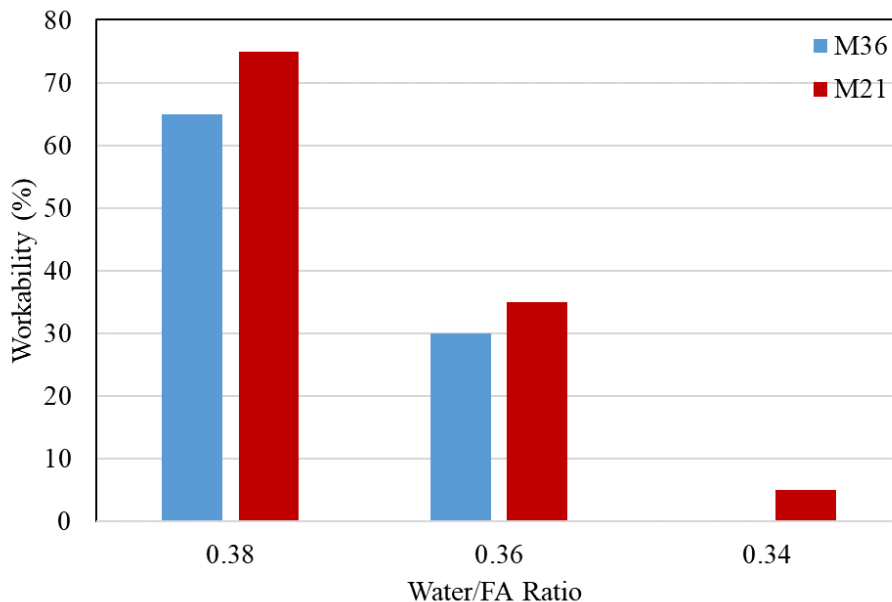


Figure 7. Effect of reducing water on workability

To reduce the water while having a good workability, different types and percentages of SP were investigated (Figure 8). Furthermore, a solid line representing a minimum workability of 30%, which is generally required for mortar, is shown on the figure. As shown in the figure, both types of SP were able to significantly increase the workability. Generally, M21 which has a lower calcium content compared to M36 displayed a higher improvement in the workability with Glenium 3400 in a dosage of 325mL/Kg was the most effective SP.

Glenium 3400 in a dosage of 325mL/Kg was then used in the mixtures while reducing the water-to-fly ash ratio to 0.36 from 0.38. As shown in Figure 8, mixtures Glenium3400-325 (0.36) displayed workability similar to those of the reference specimens without superplasticizer.

Mortar cubes were manufactured using the reference matrix with water-to-fly ash ratio of 0.38 and the new mixture with SP and water-to-fly ash ratio of 0.36. The cubes were subjected to 36 cycles of freeze and thaw and then were tested to determine their compressive strength. The results are shown in Figure 9 for M21, and Figure 10 for M36. As shown in the figure, the initial compressive strength of M21 was improved by almost 10% with an improvement in initial strength from 6600 psi to 7200 psi as the water ratio was reduced from 0.38 to 0.36 and SP was used. Testing the matrix after 36 cycles of freeze-thaw was detrimental to the reference, with a 52% decrease in the strength. Comparatively, by reducing the water ratio to 0.36 with the SP, the loss of strength was only 21% and the compressive strength decreased to 5700 psi.

M36 performed similarly to M21. The initial compressive strength of M63 was improved by approximately 7% with an improvement in initial strength from 5700 psi to

6000 psi as the water ratio was reduced from 0.38 to 0.36 and SP was used. Testing M36 after 36 cycles of freeze-thaw resulted in 36% decrease in the compressive strength. Comparatively, by reducing the water ratio to 0.36 with the SP, the loss of strength was only 16% and the compressive strength decreased to 5000 psi.

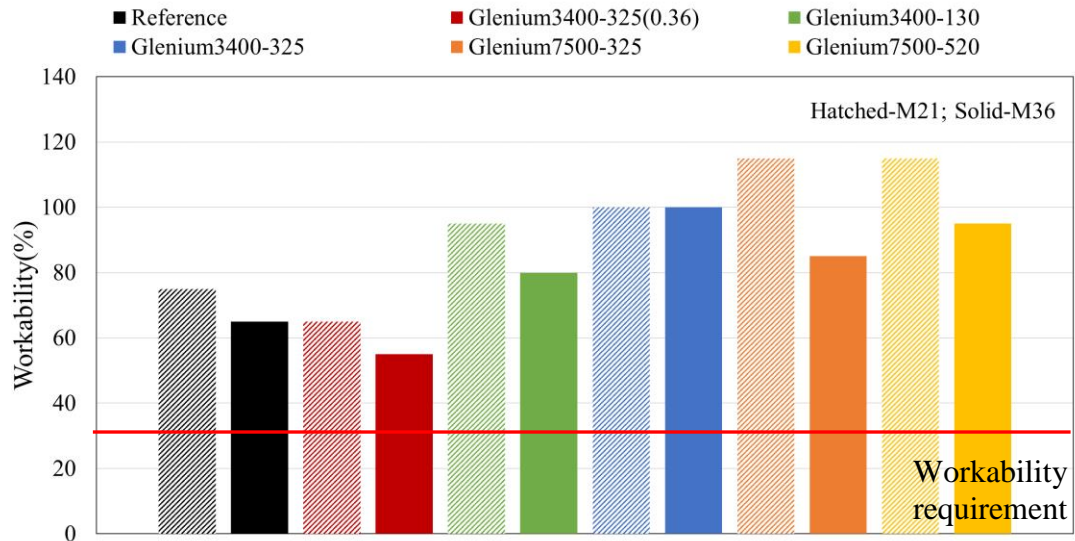


Figure 8. Effects of SP on workability.

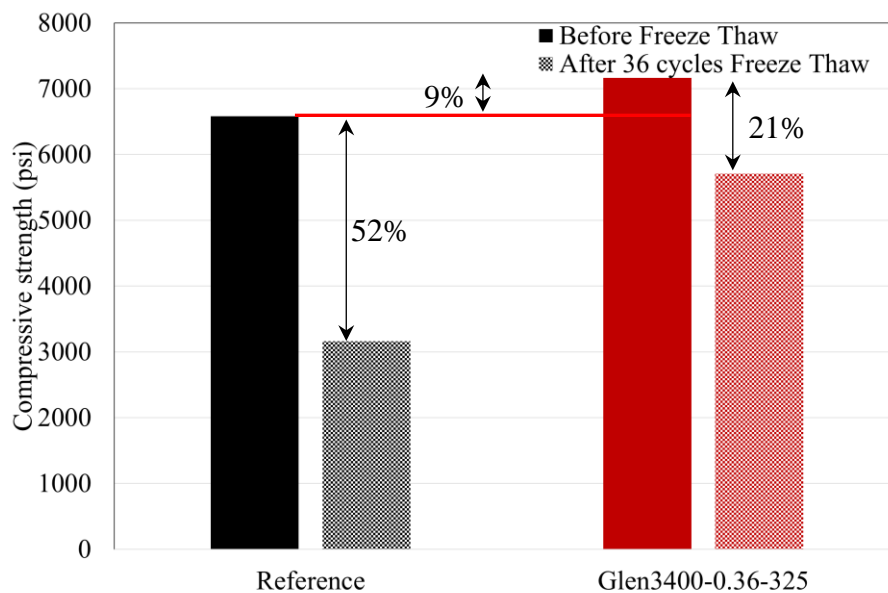


Figure 9. Effects of freeze-thaw on compressive strength of M21 mixture with and without using SP.

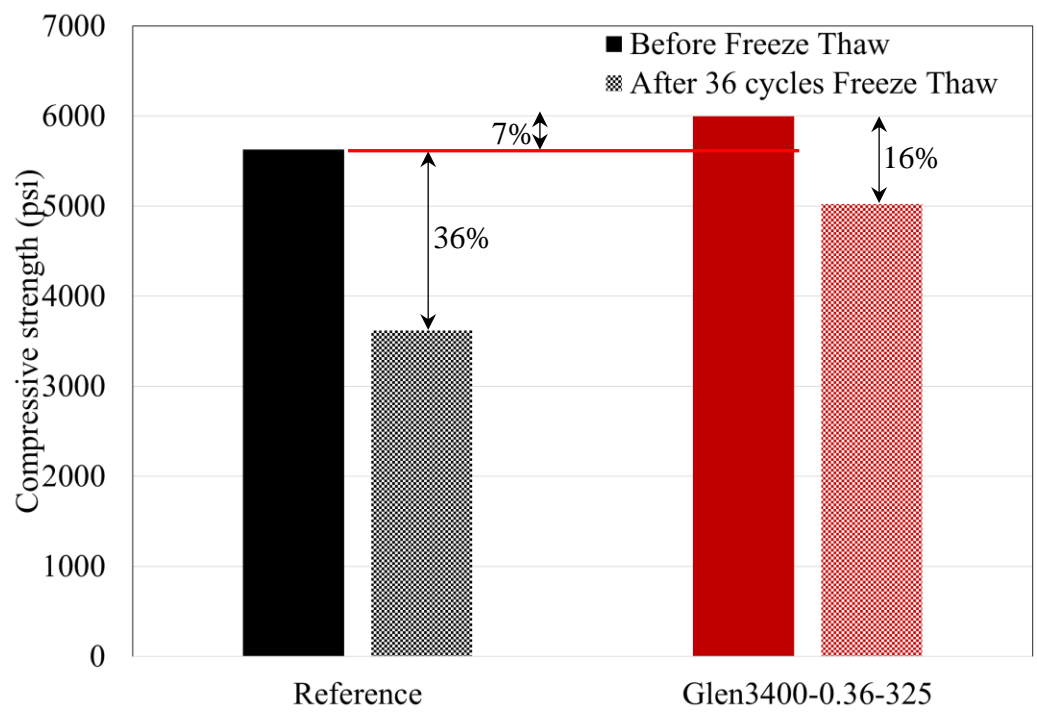


Figure 10. Effects of freeze and thaw cycles on M36 with and without SP.

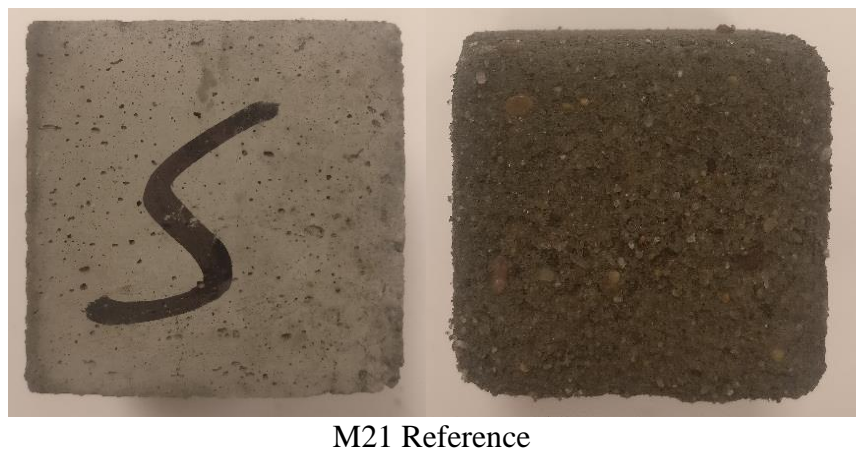
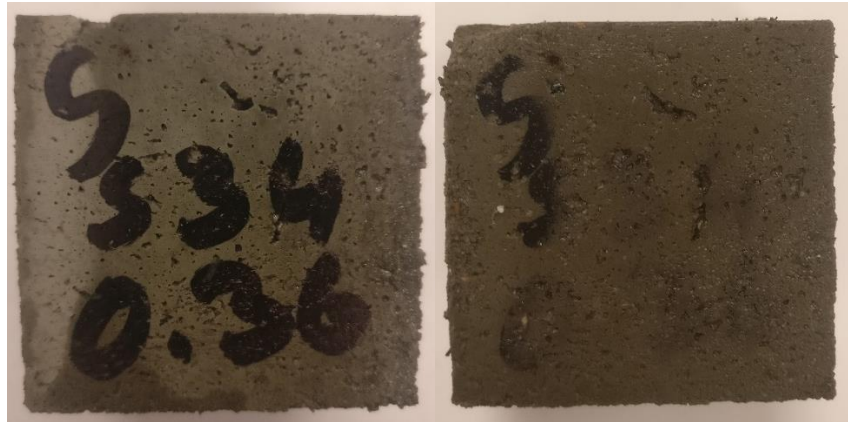


Figure 11. Visual representation of specimens, Before Freeze thaw (left), After 26 Cycles Freeze Thaw (right).



M36 Reference



M21-Glen3400(325)-0.36



M21-Glen3400(325)-0.36

Figure 11. Visual representation of SP specimens, Before Freeze thaw (left), After 26 Cycles Freeze Thaw (right). (Cont.)

4.2. AIR ENTRAINMENT

4.2.1. Air Entraining Admixtures. Introducing a controlled structure of air voids in the matrix decreases the cracking in the mortar due to the stresses of freezing and thawing. Different air-entraining admixtures were introduced at a different percentage. The best air entrained type and percentage were then used for durability studies. Expectedly, increasing the air-entrained content improves the workability as shown in Figure 12.

The actual air entrained in each mixture was determined using ASTM C185–15a [87]. The density of a known volume was calculated using its weight and the air entrainment of the mortars was then calculated and shown in Figure 13. The reference mixture was considered as zero air entrained.

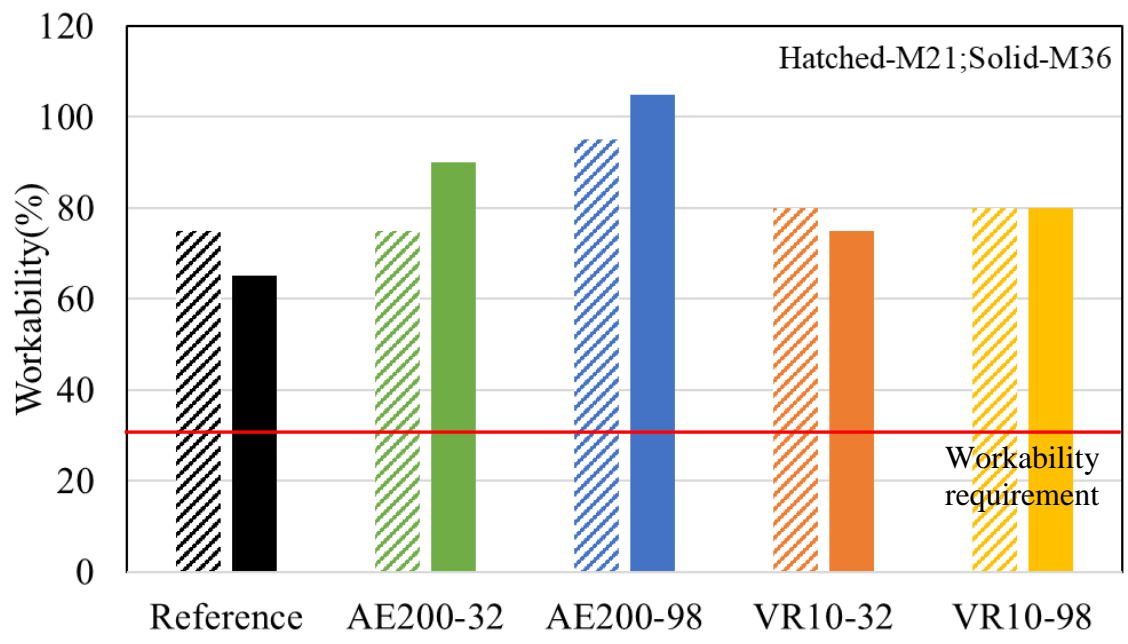


Figure 12. Air Entrainment Workability.

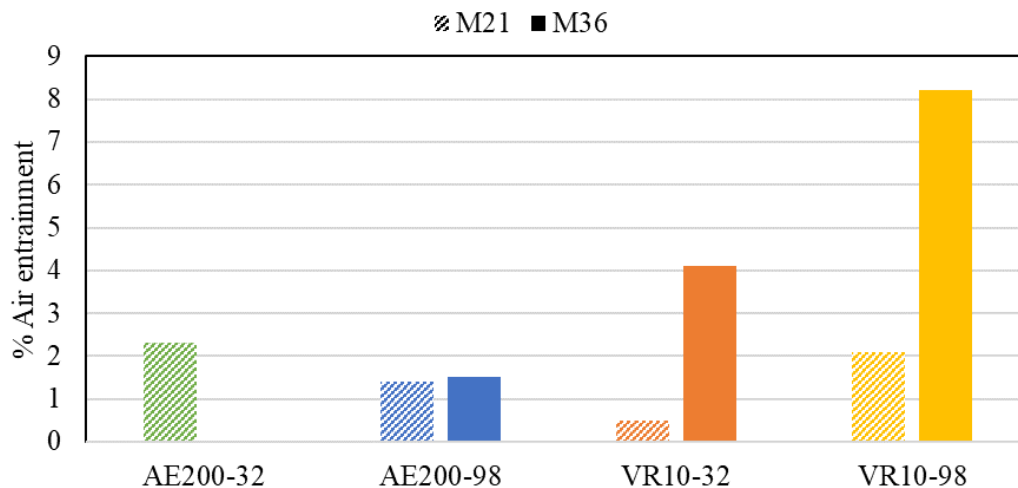


Figure 13. % Air entrainment of AEA.

Overall, M36 entrained more air compared to M21. For M21, it is observed that AE200 in a dosage of 32 mL/Kg was most effective in introducing the target air content into the matrix. However, at this same dosage, there was no observed improvement in air entrainment for M36. The higher dosage of VR 10 resulted in an air entrained of about 8% for M36 while it was 2% for the M21 mixture.

All air entrained mortar mixes were then tested for their initial compressive strength and freeze-thaw durability. Air-entraining admixtures are known to decrease the compressive strength of a matrix by 3 to 7%. Generally, there is 5% loss of strength for every 1% by volume air that is entrained in an OPC matrix [88]. This was the case observed in both M21 and M36, comparing its minimum and maximum dosages. It was observed that heat curing the M21 specimens resulted in acceptable strengths ranging from 6% higher to 18% lower than the compressive strength of the reference mixture. For M35, the reduction in the strength ranged from 22% to 62%. Overall, VR10 at 32mL/Kg or up to 4% air entrained, gave an acceptable initial strength.

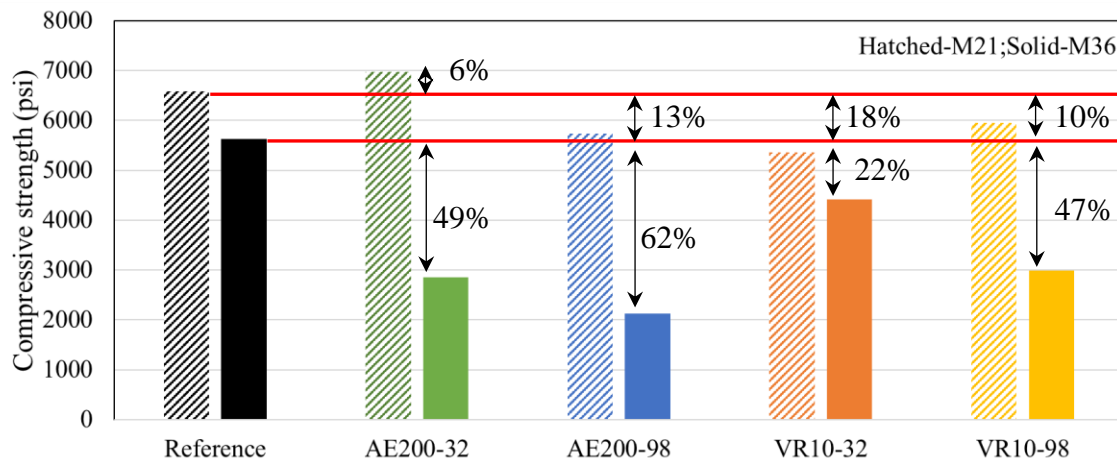


Figure 14. Initial compressive strength-AEA Additive.

As mentioned, the reference specimens displayed a reduction of 52% in the compressive strength after being subjected to 36 cycles of freeze and thaw. In the case of relatively lower calcium fly ash, M21, lower dosages of AE200 improved the overall durability of the mixtures. The air entrained agent reduced the drop in the strength from 52% in the reference specimens to 26%. The retained strength was 5200 psi, which is adequate for most civil engineering applications. Overall, adding any air entrainment in any suggested dosage improved the durability to an extent at elevated curing temperatures. For a higher calcium fly ash, M36, lower dosages of VR10 improved the durability. The air entrained agent reduced the drop-ins strength from 52% in the reference specimen to 6% with the retained strength being 4200 psi.

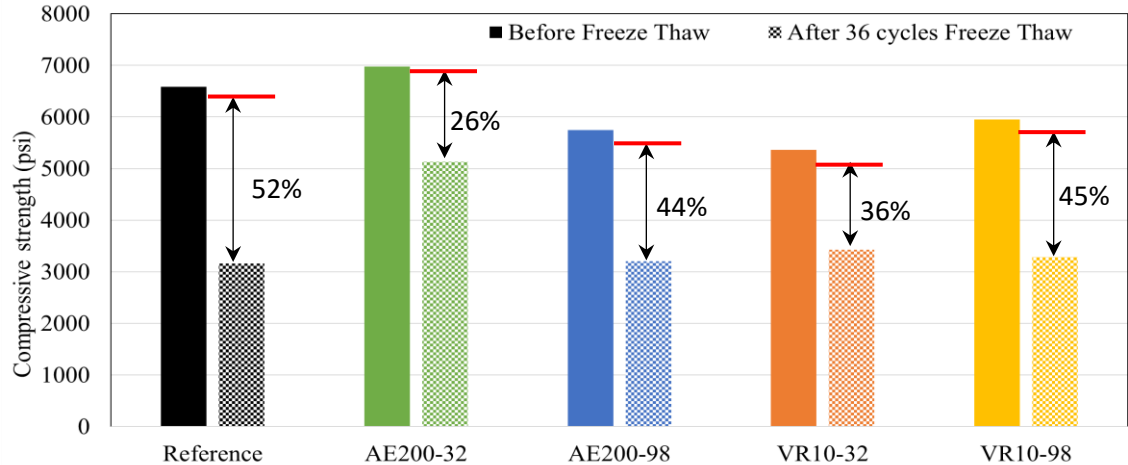


Figure 15. M21 AEA Freeze Thaw Compressive Strength.

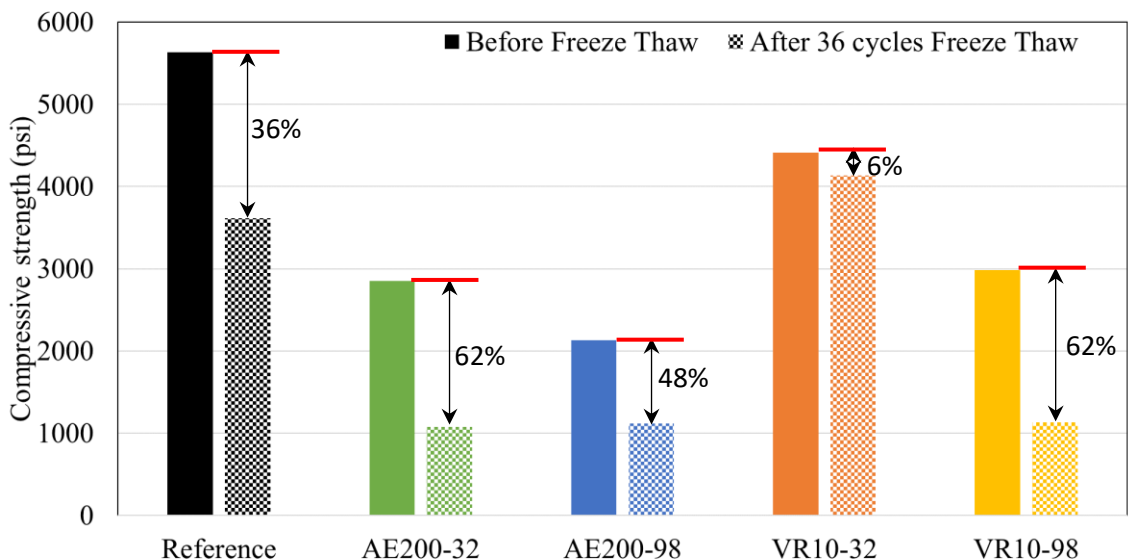


Figure 16. M36 AEA Freeze Thaw Compressive Strength.

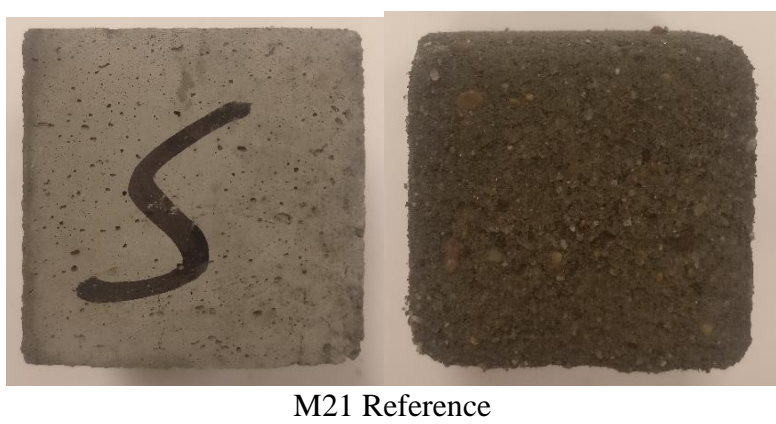
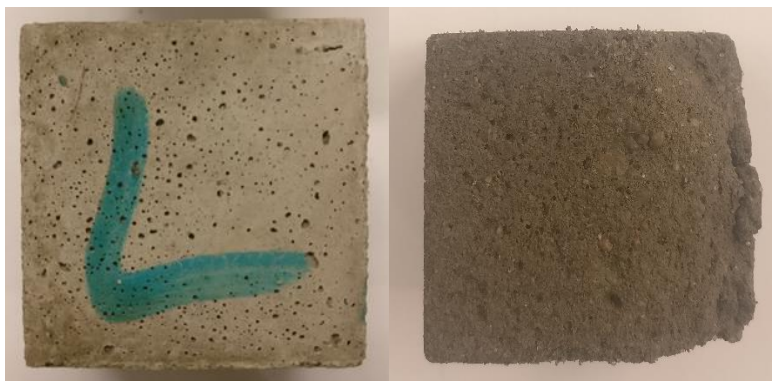


Figure 17. Visual representation of AEA specimens, Before Freeze thaw (left), After 26 Cycles Freeze Thaw (right).



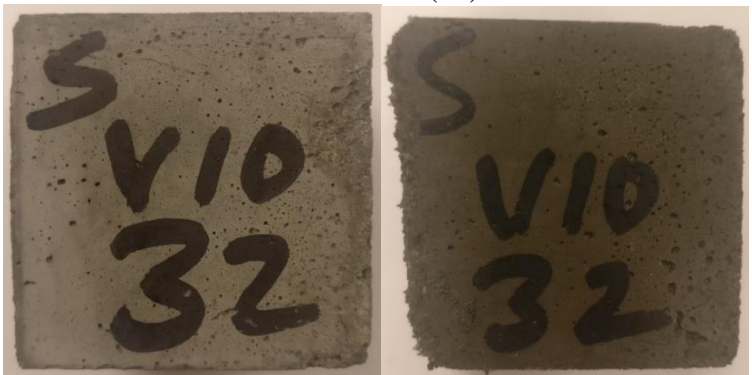
M36 Reference



C21-AE200(32)



C21-AE200(98)



C21-VR10(32)

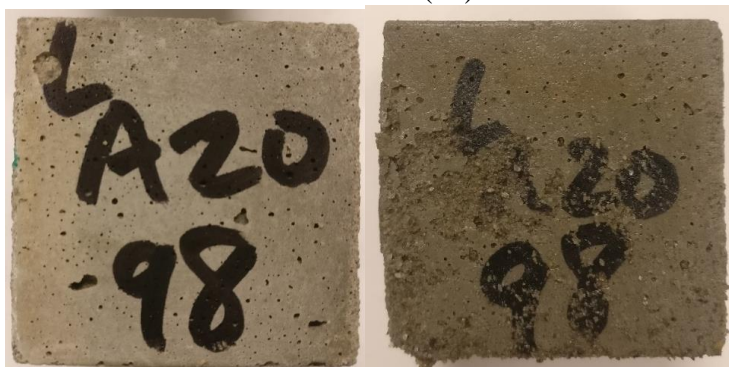
Figure 17. Visual representation of AEA specimens, Before Freeze thaw (left), After 26 Cycles Freeze Thaw (right). (Cont.)



C21-VR10(98)



C36-AE200(32)



C36-AE200(98)



C36-VR10(32)

Figure 17. Visual representation of AEA specimens, Before Freeze thaw (left), After 26 Cycles Freeze Thaw (right). (Cont.)



C36-VR10(98)

Figure 17. Visual representation of AEA specimens, Before Freeze thaw (left), After 26 Cycles Freeze Thaw (right). (Cont.)

4.2.2. Rubber. Another technique that was explored to improve sustainability and durability was the replacement of rubber with sand. The workability, initial compressive strengths, and freeze-thaw strength were then studied.

Increasing the rubber particle size reduced the workability of both fly ashes. Replacing the sand content in a higher percentage from 8% to 16% with rubber had a more detrimental effect on the mixtures workability. This is due to the tendency of the crumb rubber to entrapped water particles and effectively entrap whatever is added to the mixture. Increasing the rubber content and the surface area of the rubber used significantly affected the workability of the mortars. A workability of 30 to 80% was found to be workable and ease the placement. C36, which had a relatively higher calcium content had a lower workability than C21 for all mixes including the references. Overall, rubber particles that passed sieve 50 and retained on sieve 100 satisfied the workability constraints for both fly ashes.

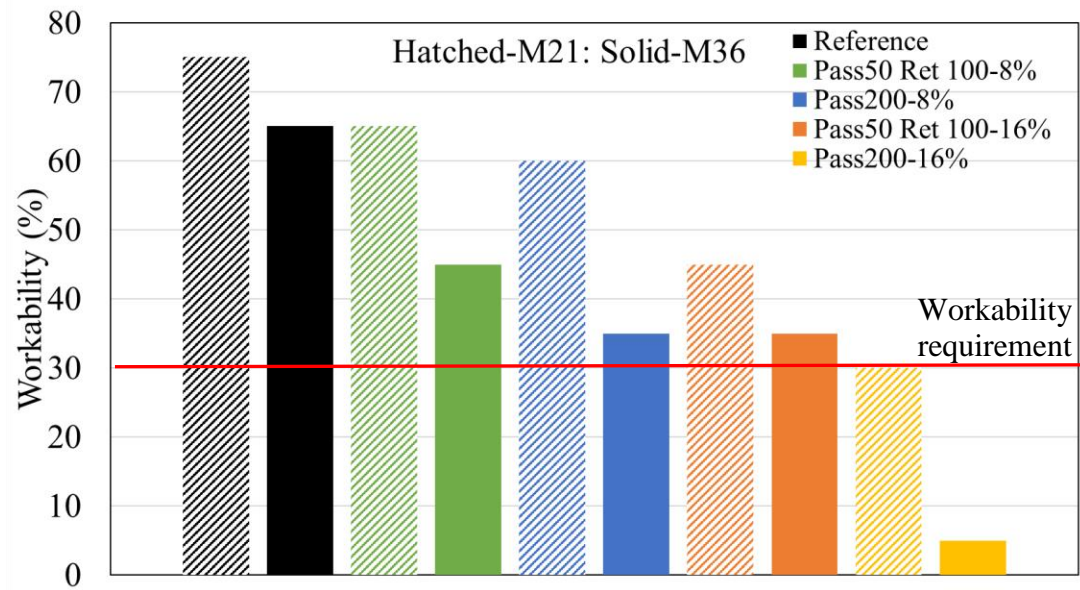


Figure 18. Rubber Replacement Workability.

It was also observed that increasing the rubber replacement percentage, reduced the initial compressive strength of both fly ashes in both sieves. In the case of M21, the zero replacement of rubber had a strength of 6600 psi in an elevated curing temperature, whereas M36 had a comparable strength of 5700 psi, cured in ambient conditions. The observed loss in initial strength in M21 with the replacement of rubber was 1400 psi, using an 8% replacement of rubber passing sieve 50 and retaining on sieve 100. This was a 21% decrease when compared with the reference mixture. In the case of M36, implementing a rubber replacement of 8% with a smaller sieve passing reduced the overall strength by 30%.

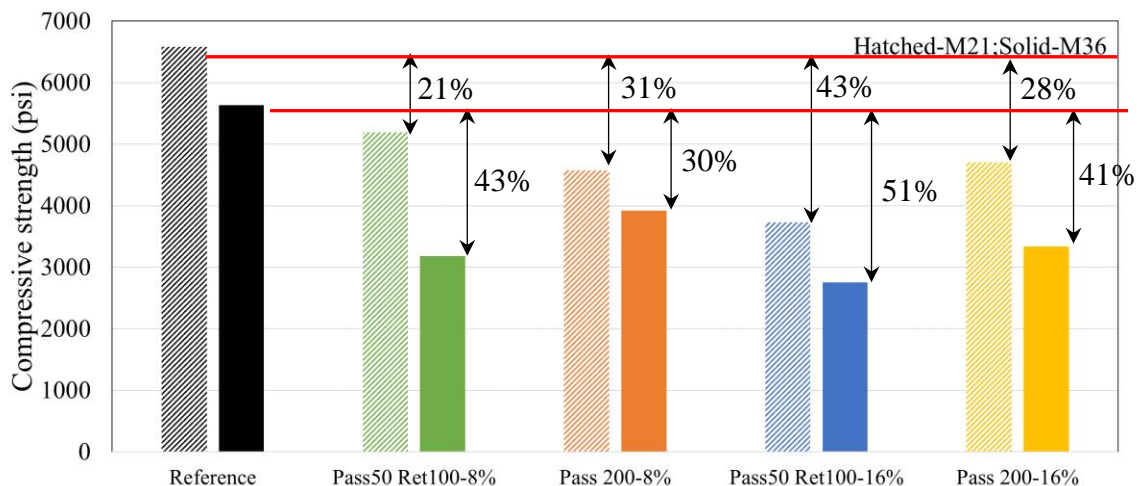


Figure 19. Effect of using rubber on the compressive strength before and after freeze-thaw cycles.

The freeze-thaw durability was significantly improved with the introduction of any rubber additive in any replacement percentage. In the case of M21, after testing the reference mixes for one day in an elevated curing temperature, the cubes were then placed in a freeze-thaw chamber for 36 cycles of freezing and thawing for one week. Immediately after this period, the cubes were dried and tested for its compressive strength. The results indicate that the rubber consistently reduced the damage due to freeze-thaw on average from 36% and 52% to between 8% and 17%. This was the case in both M21 in elevated curing conditions and M36 at ambient conditions. Therefore, even though the initial compressive strength is reduced by 20% to 40%, the freeze-thaw durability was found to significantly improve due to the rubbers air entrapment.

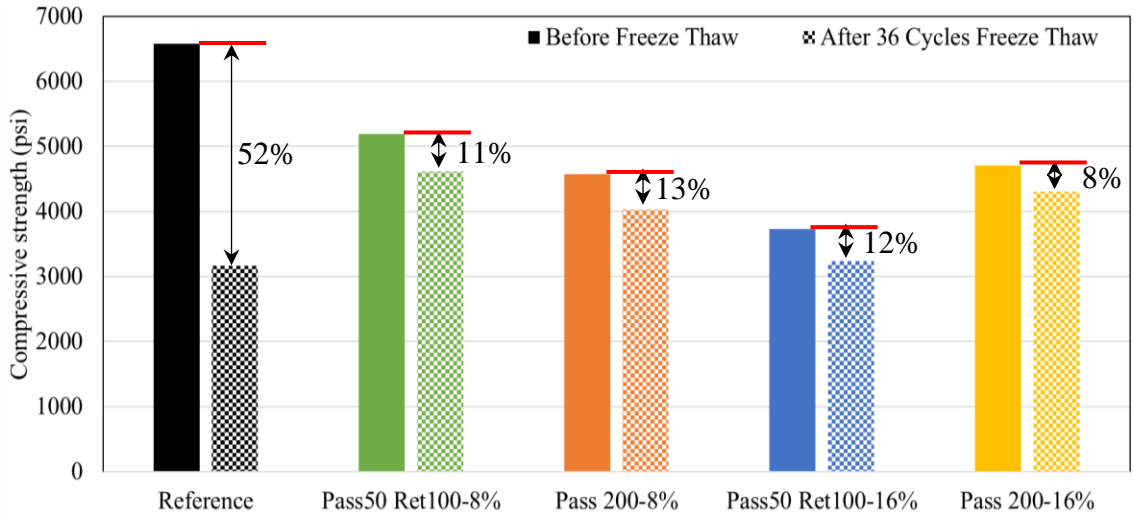


Figure 20. M21 Rubber Freeze Thaw Compressive strength.

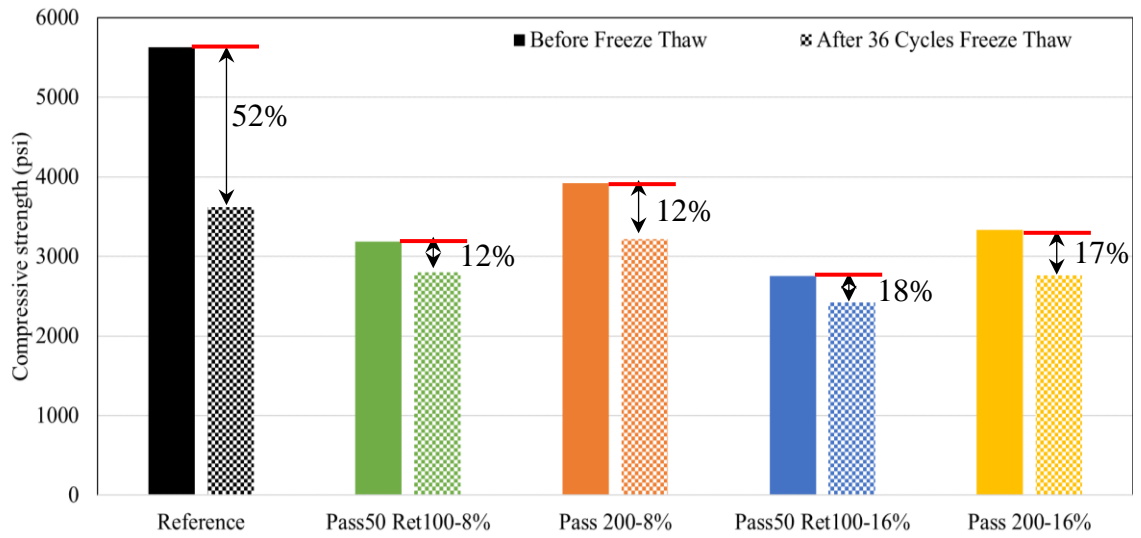
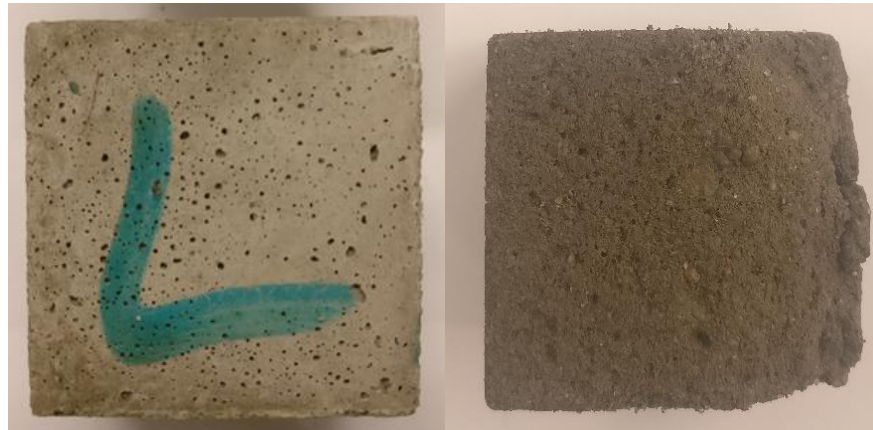


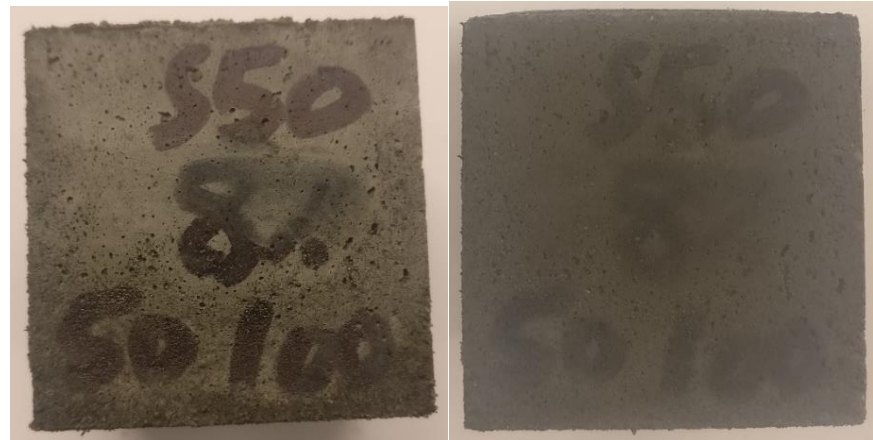
Figure 21. M36 Rubber Freeze Thaw Compressive strength.



C21 Reference

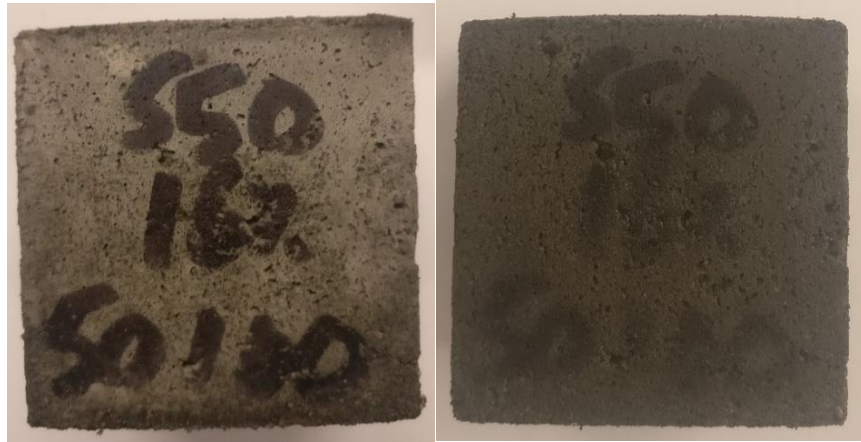


C36 Reference



C21-50/100(8%)

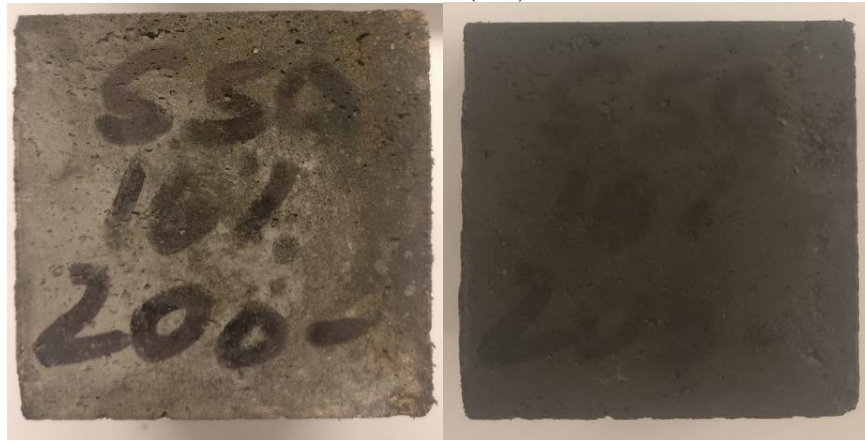
Figure 22. Visual representation of Rubber specimens, Before Freeze thaw (left), After 26 Cycles Freeze Thaw (right).



C21-50/100(16%)



C21-200(8%)



C21-200(16%)

Figure 22. Visual representation of Rubber specimens, Before Freeze thaw (left), After 26 Cycles Freeze Thaw (right). (Cont.)

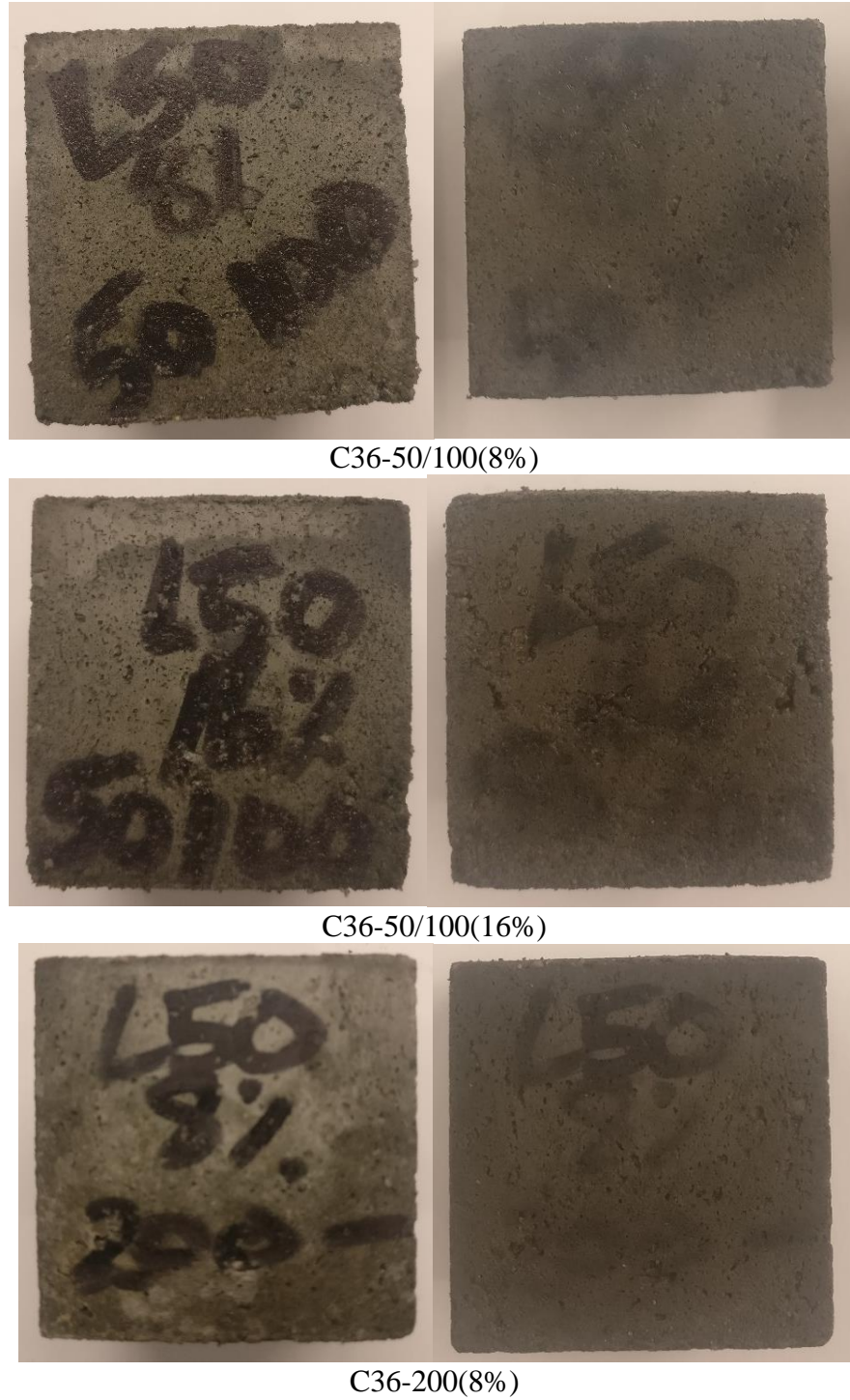


Figure 22. Visual representation of Rubber specimens, Before Freeze thaw (left), After 26 Cycles Freeze Thaw (right). (Cont.)

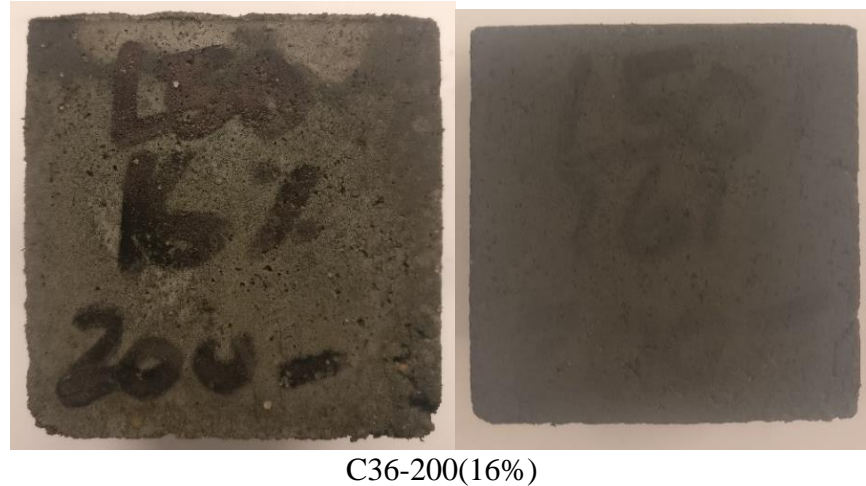


Figure 22. Visual representation of AEA specimens, Before Freeze thaw (left), After 26 Cycles Freeze Thaw (right). (Cont.)

5. CONCLUSION

Mortar cubes prepared and tested for air entrainment, workability, initial compressive strength, and freeze-thaw durability to study the effects of rubber replacements superplasticizers, and air entraining admixtures.

- Testing two types of superplasticizers indicated that Glenium 3400 in a lower dosage gave a preferable balance between workability, compressive strength, and durability. Reducing the water from 0.38 to 0.36 with a 32 mL/Kg Glenium 3400 improved the initial strength, as well as the durability. SP reduced the drop in strength from 52% to 21% in M21 and 36% to 16% in M36.
- The two air entraining admixtures were found to be most effective at lower dosages. AE200 showed preferable air entrainment of 2.3% and improving its initial strength retention by 7% for M21. M36 performed similarly well using VR10, increasing the air entrainment by 0.5% while showing the loss in strength of 22%. However, its durability was improved by 26% from 3500 psi to 4200 psi.

- All matrixes with the rubber showed an improvement in strength retention by 40%.
- It was found that rubber particles retained on sieve 50 to 100 in 8% replacement were most effective to circumvent freeze-thaw issues, showing a 10% loss in strength, even though it reduced its initial strength by 1400 psi from 6600 psi to 5200 psi for M21.
- M36 was also found to have a preferable performance with rubber replacement, improving its durability from 36% to 18% with a sieve passing of 200 with an 8% replacement of sand.

REFERENCES

1. Association, A.R.T.B., *Production and Use of Coal Combustion Products in the United States*. American Coal Ash Association, June 2015.
2. Chindaprasirt, P., T. Chareerat, and V. Sirivivatnanon, *Workability and strength of coarse high calcium fly ash geopolymer*. *Cement and Concrete Composites*, 2007. 29(3): p. 224-229.
3. Administration, U.S.E.I. *Missouri State Profile and Energy Estimates*. 2015.
4. Agency, U.S.E.P. *National Primary Drinking Water Regulations*. 2017.
5. Blissett, R.S. and N.A. Rowson, *A review of the multi-component utilisation of coal fly ash*. *Fuel*, 2012. 97(Supplement C): p. 1-23.
6. Hardjito, D., *On the Development of Fly Ash-Based Geopolymer Concrete*. ACI Materials, 2004.
7. Kong, D.L.Y. and J.G. Sanjayan, *Effect of elevated temperatures on geopolymer paste, mortar and concrete*. *Cement and Concrete Research*, 2010. 40(2): p. 334-339.
8. Wallah, S.E., *Creep Behaviour of Fly Ash-Based Geopolymer Concrete*. *Civil Engineering Dimension*, September 2010.
9. Thokchom, S., *Resistance of Fly Ash Based Geopolymer Mortars in Sulphuric Acid*. *ARNP Journal of Engineering and Applied Sciences* February 2009.
10. Somna, K., et al., *NaOH-activated ground fly ash geopolymer cured at ambient temperature*. *Fuel*, 2011. 90(6): p. 2118-2124.
11. Jian Ping Zhu, Q.L.G., Dong Xu Li, Cun Jun Li, *Influence of Particle Size Distribution of Fly Ash on Compressive Strength and Durability of Portland Cement Concrete*. *Materials Science Forum*, June 2011.
12. Vassilev, S.V., *Methods for Characterization of Composition of Fly Ashes from Coal-Fired Power Stations: A Critical Overview*. Central Laboratory of Mineralogy and Crystallography, March 9, 2005.
13. Chindaprasirt, P., et al., *Effect of SiO₂ and Al₂O₃ on the setting and hardening of high calcium fly ash-based geopolymer systems*. *Journal of Materials Science*, 2012. 47(12): p. 4876-4883.

14. Silva, P.D., K. Sagoe-Crenstil, and V. Sirivivatnanon, *Kinetics of geopolymerization: Role of Al₂O₃ and SiO₂*. Cement and Concrete Research, 2007. 37(4): p. 512-518.
15. van Jaarsveld, J.G.S. and J.S.J. van Deventer, *Effect of the Alkali Metal Activator on the Properties of Fly Ash-Based Geopolymers*. Industrial & Engineering Chemistry Research, 1999. 38(10): p. 3932-3941.
16. Rattanasak, U. and P. Chindaprasirt, *Influence of NaOH solution on the synthesis of fly ash geopolymer*. Minerals Engineering, 2009. 22(12): p. 1073-1078.
17. Dimitrios Panias, I.P.G., Theodora Perraki, *Effect of synthesis parameters on the mechanical properties of fly ash-based geopolymers*. Metallurgy and Materials Technology, December 2006.
18. Criado, M., A. Palomo, and A. Fernández-Jiménez, *Alkali activation of fly ashes. Part 1: Effect of curing conditions on the carbonation of the reaction products*. Fuel, 2005. 84(16): p. 2048-2054.
19. Guo, X., H. Shi, and W.A. Dick, *Compressive strength and microstructural characteristics of class C fly ash geopolymer*. Cement and Concrete Composites, 2010. 32(2): p. 142-147.
20. Abdullah, M.M.A., et al., *The Relationship of NaOH Molarity, Na₂SiO₃/NaOH Ratio, Fly Ash/Alkaline Activator Ratio, and Curing Temperature to the Strength of Fly Ash-Based Geopolymer*. Advanced Materials Research, 2011. 328-330: p. 1475-1482.
21. Pan, Z., J.G. Sanjayan, and B.V. Rangan, *An investigation of the mechanisms for strength gain or loss of geopolymer mortar after exposure to elevated temperature*. Journal of Materials Science, 2009. 44(7): p. 1873-1880.
22. Chindaprasirt, P., P. De Silva, and S. Hanjitsuwan, *Effect of High-Speed Mixing on Properties of High Calcium Fly Ash Geopolymer Paste*. Arabian Journal for Science and Engineering, 2014. 39(8): p. 6001-6007.
23. Gomaa, E., et al., *Fresh properties and compressive strength of high calcium alkali activated fly ash mortar*. Journal of King Saud University - Engineering Sciences, 2017. 29(4): p. 356-364.
24. Lowke, D., *Effect of Mixing Energy on Fresh Properties of SCC*. March 2005.
25. Conrad, K.L., *Geochemical Database of Feed Coal and Coal Combustion Products (CCPs) from Five Power Plants in the United States*. United States Geological Survey, November, 2011.

26. Manual, X.A., *X-Ray Radiation Safety-Manual for Operator Training*. 2010.
27. ASTM, *Standard Specification for Coal Fly Ash and Raw or Calcined Natural Pozzolan for Use in Concrete*. 2015, ASTM International.
28. International, A., *C778 - 17 Standard Specification for Standard Sand*. ASTM, 2017.
29. Hammer, G.R., *Climate of Missouri*. National Oceanic and Atmosphere Administration, 01/31/2006.
30. C191-13, A.S., *Standard Test Methods for Time of Setting of Hydraulic Cement by Vicat Needle*. ASTM International, 2013.
31. 15, A.S.C., *Standard Test Method for Flow of Hydraulic Cement Mortar*. ASTM International, 2015.
32. C109/C109M-16a, A.S., *Standard Test Method for Compressive Strength of Hydraulic Cement Mortars (Using 2-in. or [50-mm] Cube Specimens)*. ASTM International, 2016.
33. Provis, J.L. and S.A. Bernal, *Geopolymers and Related Alkali-Activated Materials*. Annual Review of Materials Research, 2014. 44: p. 299-327.
34. Siyal, A.A., et al., *Effects of Parameters on the Setting Time of Fly Ash Based Geopolymers Using Taguchi Method*. Procedia Engineering, 2016. 148: p. 302-307.
35. Yip, C.K., et al., *Effect of calcium silicate sources on geopolymerisation*. Cement and Concrete Research, 2008. 38(4): p. 554-564.
36. van Deventer, J.S.J., et al., *Reaction mechanisms in the geopolymeric conversion of inorganic waste to useful products*. Journal of Hazardous Materials, 2007. 139(3): p. 506-513.
37. Pantias, D., I.P. Giannopoulou, and T. Perraki, *Effect of synthesis parameters on the mechanical properties of fly ash-based geopolymers*. Colloids and Surfaces A: Physicochemical and Engineering Aspects, 2007. 301(1): p. 246-254.
38. Cho, H., et al., *Solution state structure determination of silicate oligomers by ²⁹Si NMR spectroscopy and molecular modeling*. Journal of the American Chemical Society, 2006. 128(7): p. 2324-2335.
39. World, C., *CW.03.08.Concrete.indd*. The Royal Society of Chemistry, March 2008.

40. Ernst Worrell, et al., *CARBON DIOXIDE EMISSIONS FROM THE GLOBAL CEMENT INDUSTRY*. Annual Review of Energy and the Environment, 2001. 26(1): p. 303-329.
41. Wan, Q., et al., *Geopolymerization reaction, microstructure and simulation of metakaolin-based geopolymers at extended Si/Al ratios*. Cement and Concrete Composites, 2017. 79(Supplement C): p. 45-52.
42. Sun, P. and H.-C. Wu, *Chemical and freeze–thaw resistance of fly ash-based inorganic mortars*. Fuel, 2013. 111(Supplement C): p. 740-745.
43. Lior, N., *Sustainable energy development: The present (2009) situation and possible paths to the future*. Energy, 2010. 35(10): p. 3976-3994.
44. Chindaprasirt, P. and S. Rukzon, *Strength, porosity and corrosion resistance of ternary blend Portland cement, rice husk ash and fly ash mortar*. Construction and Building Materials, 2008. 22(8): p. 1601-1606.
45. Malkawi, A.B., et al., *Effects of Alkaline Solution on Properties of the HCFA Geopolymer Mortars*. Procedia Engineering, 2016. 148(Supplement C): p. 710-717.
46. Xie, T. and T. Ozbakkaloglu, *Behavior of low-calcium fly and bottom ash-based geopolymer concrete cured at ambient temperature*. Ceramics International, 2015. 41(4): p. 5945-5958.
47. Duxson, P., et al., *Geopolymer technology: the current state of the art*. Journal of Materials Science, 2007. 42(9): p. 2917-2933.
48. Provis, J.L., *Alkali-activated materials*. Cement and Concrete Research, 2017.
49. Phair, J.W. and J.S.J. van Deventer, *Characterization of Fly-Ash-Based Geopolymeric Binders Activated with Sodium Aluminate*. Industrial & Engineering Chemistry Research, 2002. 41(17): p. 4242-4251.
50. Khale, D. and R. Chaudhary, *Mechanism of geopolymerization and factors influencing its development: a review*. Journal of Materials Science, 2007. 42(3): p. 729-746.
51. Simčič, T., et al., *Chloride ion penetration into fly ash modified concrete during wetting–drying cycles*. Construction and Building Materials, 2015. 93(Supplement C): p. 1216-1223.
52. Shravan Kumar, K.R., *Assessment of Chloride Ion Penetration of Alkali Activated Low Calcium Fly Ash based Geopolymer Concrete* Key Engineering Materials, 2016.

53. Ma, Y., J. Hu, and G. Ye, *The pore structure and permeability of alkali activated fly ash*. Fuel, 2013. 104(Supplement C): p. 771-780.
54. Deb, P.S., *Durability of Fly Ash Based Geopolymer Concrete*, in *Civil Engineering*. June 2013, Curtin University. p. 178.
55. Yunsheng, Z., Wei, *Fly Ash Based Geopolymer Concrete*. Indian Concrete Journal, 2006.
56. Talha Junaid, M., et al., *A mix design procedure for low calcium alkali activated fly ash-based concretes*. Construction and Building Materials, 2015. 79(Supplement C): p. 301-310.
57. Ramujee, K., *Development of Low Calcium Flyash Based Geopolymer Concrete*. Journal of Engineering and Technology, 2014.
58. Nematollahi, B. and J. Sanjayan, *Effect of different superplasticizers and activator combinations on workability and strength of fly ash based geopolymer*. Materials & Design, 2014. 57(Supplement C): p. 667-672.
59. Carabba, L., S. Manzi, and C.M. Bignozzi, *Superplasticizer Addition to Carbon Fly Ash Geopolymers Activated at Room Temperature*. Materials, 2016. 9(7).
60. LI, K.-L., *Study on Abilities of Mineral Admixtures and Geopolymer to Restrain ASR*. Key Engineering Materials, 2006.
61. Brew, D.R.M. and K.J.D. MacKenzie, *Geopolymer synthesis using silica fume and sodium aluminate*. Journal of Materials Science, 2007. 42(11): p. 3990-3993.
62. Güneysi, E. and M. Gesoğlu, *A study on durability properties of high-performance concretes incorporating high replacement levels of slag*. Materials and Structures, 2008. 41(3): p. 479-493.
63. Cai, L., H. Wang, and Y. Fu, *Freeze–thaw resistance of alkali–slag concrete based on response surface methodology*. Construction and Building Materials, 2013. 49(Supplement C): p. 70-76.
64. Beaudoin, J.J. and C. MacInnis, *The mechanism of frost damage in hardened cement paste*. Cement and Concrete Research, 1974. 4(2): p. 139-147.
65. Shi Yan, Y.H., *Aging Mechanism of Dam Concrete under the action of Freeze-Thaw Damage* Applied Mechanics and Materials 2014.
66. Fan, L., *Research into the concrete freeze-thaw damage mechanism based on the principle of thermodynamics*. Applied Mechanics and Materials 2013.

67. Ben Li, K.W., *STUDY ON THE DAMAGE MECHANISM OF PORE STRUCTURE IN CONCRETE SUBJECTED TO FREEZE-THAW CYCLES*. THE CIVIL ENGINEERING JOURNAL, 2015.
68. Criado, M., et al., *Alkali activated fly ash: effect of admixtures on paste rheology*. Rheologica Acta, 2009. 48(4): p. 447-455.
69. Steven, G. and K. Paul, *Effect of Fly Ash on the Air-Void Stability of Concrete*. Special Publication. 79.
70. Freeman, E., et al., *Interactions of carbon-containing fly ash with commercial air-entraining admixtures for concrete*. Fuel, 1997. 76(8): p. 761-765.
71. Hill, R.L., et al., *An examination of fly ash carbon and its interactions with air entraining agent*. Cement and Concrete Research, 1997. 27(2): p. 193-204.
72. Division, F.H., *Freeze Thaw Resistance of Concrete with Marginal Air Content*. 2006, U.S Department of Transportation.
73. Skvara, F., *Alkali Activated Material - Geopolymer* Department of Glass and Ceramics- Faculty of Chemical Technology, ICT Prague, 2007.
74. Savas, B., S. Ahmad, and D. Fedroff, *Freeze-Thaw Durability of Concrete with Ground Waste Tire Rubber*. Transportation Research Record: Journal of the Transportation Research Board, 1997. 1574: p. 80-88.
75. Richardson, A., et al., *Crumb rubber used in concrete to provide freeze-thaw protection (optimal particle size)*. Journal of Cleaner Production, 2016. 112(Part 1): p. 599-606.
76. Richardson, A.E., K.A. Coventry, and G. Ward, *Freeze/thaw protection of concrete with optimum rubber crumb content*. Journal of Cleaner Production, 2012. 23(1): p. 96-103.
77. Gadkar, S. and P. Rangaraju, *The Effect of Crumb Rubber on Freeze-Thaw Durability of Portland Cement Concrete*. 2013.
78. International, A., *Standard Specification for Coal Fly Ash and Raw or Calcined Natural Pozzolan for Use in Concrete*. ASTM, 2017.
79. International, A., *Standard Specification for Chemical Admixtures for Concrete*. ASTM, 2017.
80. International, A., *Standard Specification for Air-Entraining Admixtures for Concrete*. ASTM, 2016.

81. Officials, A.A.o.S.a.H.T., *Standard Specification for Air-Entraining Admixtures for Concrete (ASTM Designation C260/C260M-10a)*. 2016, AASHTO.
82. Li, W., et al., *Water Absorption and Critical Degree of Saturation Relating to Freeze-Thaw Damage in Concrete Pavement Joints*. Journal of Materials in Civil Engineering, 2012. 24(3): p. 299-307.
83. Bentz, D.P., *SORPTIVITY-BASED SERVICE LIFE PREDICTIONS FOR CONCRETE PAVEMENTS*. National Institute of Standards and Technology, 2001. Building and Fire Research Laboratory.
84. International, A., *Standard Test Method for Flow of Hydraulic Cement Mortar*. 2015, ASTM.
85. International, A., *Standard Test Method for Compressive Strength of Hydraulic Cement Mortars (Using 2-in. or [50-mm] Cube Specimens)*, in *ASTM C109 / C109M - 16a*. 2016, ASTM.
86. International, A., *Standard Test Method for Resistance of Concrete to Rapid Freezing and Thawing*, in *ASTM C666 / C666M - 15*. 2015, ASTM.
87. International, A., *Standard Test Method for Air Content of Hydraulic Cement Mortar*, in *ASTM C185 - 15a*. 2015, ASTM.
88. theconstructor.org. *Effect of Air Entrained Concrete on Strength of Concrete*. 2017; Available from: <https://theconstructor.org/concrete/air-entrained-concrete-strength-effects/8427/>.

ACKNOWLEDGEMENTS

The authors gratefully acknowledge Missouri Department of Transportation (MODOT), Missouri Department of Natural Resources (MODNR), and Ameren Corporation for their contributions and support during this study. Appreciation is also extended to PQ Corporation, Malvern, PA for donating type DTM sodium silicate liquid.

However, the conclusions and the opinions expressed in this paper are those of the authors and do not necessarily reflect the official views or policies of the aforementioned corporations.

SECTION

3. SUMMARY, CONCLUSIONS AND RECOMMENDATIONS

3.1. SUMMARY OF RESEARCH WORK

Testing fly ashes from different sources at various time intervals and temperatures helped determine the optimum ratios of chemicals, curing times, and curing temperatures for a particular chemical composition. This optimization can be attributed to energy efficiency or time necessary to achieve strength based on the particular needs in practical implementations. Five fly ashes were sourced from five different coal power plants in Missouri and studied at five different curing temperatures at five intervals of time. This will optimize chemical ratios and curing conditions for different fly ash chemical contents, and save time and money. The fly ashes were tested for X-ray Fluorescence (XRF), SEM-EDS, and X-ray Diffraction (XRD) to understand the various elements and subsequent compounds formed in the respective hydration and geopolymerization mechanisms. Setting time was determined to be governed by the calcium content of the fly ash and workability was governed by the amount of viscous silicate and water added. Mortar cubes were prepared and tested for air entrainment, workability, initial compressive strength, and freeze-thaw durability to study the effects of rubber replacements superplasticizers, and air entraining admixtures.

3.2. CONCLUSIONS

The following section summarizes the conclusions from the experimental studies

- Preliminary strength results found a negligible difference in strength between consistently exposing the specimens in a controlled environment of 30 °C and an imitated regime of elevated curing of a typical Missouri summer week. Therefore,

results of 30 °C can be relied upon to imitate a Missouri summer. There was considerable strength gain over lower temperatures for all the fly ashes. Fly ash M36-2.65 and M28-2.20, which had higher calcium contents, showed improved performances at lower temperatures indicating prominent hydration mechanisms, similar to cement.

- Fly ash M24-2.30 had a favorable Si/Al ratio but was still consistently outperformed in strength due to its lower calcium content at ambient conditions and higher calcium content at elevated conditions. The optimized mixing procedure was found to be at an elevated temperature of 70 Celsius for 24 hours.
- Fly ash M25-2.35, and M21-2.20 were found to be closely relatable in performance at the various curing regimes and chemical conditions. M21-2.20 outperformed all the other fly ashes at higher temperatures due to its lower Si/Al ratio and preferable calcium content to be unhindered at these elevated conditions.
- Testing two types of superplasticizers indicated that Glenium 3400 in a lower dosage gave a preferable balance between workability, compressive strength, and durability. Reducing the water from 0.38 to 0.36 with a 32 mL/Kg Glenium 3400 improved the initial strength, as well as the durability. SP reduced the drop in strength from 52% to 21% in M21 and 36% to 16% in M36.
- The two air entraining admixtures were found to be most effective at lower dosages. AE200 showed preferable air entrainment of 2.3% and improving its initial strength retention by 7% for M21. M36 performed similarly well using VR10, increasing the air entrainment by 0.5% while showing the loss in strength

of 22%. However, its durability was improved by 700 psi from 3500 psi to 4200 psi.

- All matrixes with the rubber showed an improvement in strength retention by 40%.
- It was found that rubber particles retained on sieve 50 to 100 in 8% replacement were most effective to circumvent freeze-thaw issues, showing a 10% loss in strength, even though it reduced its initial strength by 1400 psi from 6600 psi to 5200 psi for M21.
- M36 was also found to have a preferable performance with rubber replacement, improving its durability from 36% to 18% with a sieve passing of 200 with an 8% replacement of sand.

3.3. RECOMMENDATIONS

- Study the chemical analysis, surface area, and particle size distribution of the fly ashes using cone and quartering to obtain homogeneous results for the materials.
- Set ratio between alkali activators as 1:1, alkali to fly ash ratios can be increased for relatively lower calcium fly ashes
- Use mixing speeds up to 300 rpm to improve workability, setting times and obtain complete dissolution of chemicals for improved strength characteristics.
- Use oven bags to reduce cracking of the mortars by reducing moisture loss in elevated curing conditions.
- Cure relatively higher calcium fly ashes at ambient temperatures.
- Cure relatively lower calcium fly ashes at 70°C for 8-16 hours or 55°C for 48 hours.

- Implement lower dosages of Superplasticizers and reduce water/fly ash ratio to improve durability
- Use lower dosages of air entraining admixtures to improve durability without compromising compressive strength.
- Introduce a higher sieve of rubber of passing 50 and retaining 100, in dosages of up to 8% to significantly improve durability without compromising workability.

BIBLIOGRAPHY

1. Association, A.R.T.B., *Production and Use of Coal Combustion Products in the United States*. American Coal Ash Association, June 2015.
2. Chindaprasirt, P., T. Chareerat, and V. Sirivivatnanon, *Workability and strength of coarse high calcium fly ash geopolymer*. *Cement and Concrete Composites*, 2007. 29(3): p. 224-229.
3. Administration, U.S.E.I. *Missouri State Profile and Energy Estimates*. 2015.
4. Agency, U.S.E.P. *National Primary Drinking Water Regulations*. 2017.
5. Blissett, R.S. and N.A. Rowson, *A review of the multi-component utilisation of coal fly ash*. *Fuel*, 2012. 97(Supplement C): p. 1-23.
6. Hardjito, D., *On the Development of Fly Ash-Based Geopolymer Concrete*. ACI Materials, 2004.
7. Kong, D.L.Y. and J.G. Sanjayan, *Effect of elevated temperatures on geopolymer paste, mortar and concrete*. *Cement and Concrete Research*, 2010. 40(2): p. 334-339.
8. Wallah, S.E., *Creep Behaviour of Fly Ash-Based Geopolymer Concrete*. *Civil Engineering Dimension*, September 2010.
9. Thokchom, S., *Resistance of Fly Ash Based Geopolymer Mortars in Sulphuric Acid*. *ARNP Journal of Engineering and Applied Sciences* February 2009.
10. Somna, K., et al., *NaOH-activated ground fly ash geopolymer cured at ambient temperature*. *Fuel*, 2011. 90(6): p. 2118-2124.
11. Jian Ping Zhu, Q.L.G., Dong Xu Li, Cun Jun Li, *Influence of Particle Size Distribution of Fly Ash on Compressive Strength and Durability of Portland Cement Concrete*. *Materials Science Forum*, June 2011.
12. Vassilev, S.V., *Methods for Characterization of Composition of Fly Ashes from Coal-Fired Power Stations: A Critical Overview*. Central Laboratory of Mineralogy and Crystallography, March 9, 2005.
13. Chindaprasirt, P., et al., *Effect of SiO₂ and Al₂O₃ on the setting and hardening of high calcium fly ash-based geopolymer systems*. *Journal of Materials Science*, 2012. 47(12): p. 4876-4883.

14. Silva, P.D., K. Sagoe-Crenstil, and V. Sirivivatnanon, *Kinetics of geopolymerization: Role of Al₂O₃ and SiO₂*. Cement and Concrete Research, 2007. 37(4): p. 512-518.
15. van Jaarsveld, J.G.S. and J.S.J. van Deventer, *Effect of the Alkali Metal Activator on the Properties of Fly Ash-Based Geopolymers*. Industrial & Engineering Chemistry Research, 1999. 38(10): p. 3932-3941.
16. Rattanasak, U. and P. Chindaprasirt, *Influence of NaOH solution on the synthesis of fly ash geopolymer*. Minerals Engineering, 2009. 22(12): p. 1073-1078.
17. Dimitrios Panias, I.P.G., Theodora Perraki, *Effect of synthesis parameters on the mechanical properties of fly ash-based geopolymers*. Metallurgy and Materials Technology, December 2006.
18. Criado, M., A. Palomo, and A. Fernández-Jiménez, *Alkali activation of fly ashes. Part I: Effect of curing conditions on the carbonation of the reaction products*. Fuel, 2005. 84(16): p. 2048-2054.
19. Guo, X., H. Shi, and W.A. Dick, *Compressive strength and microstructural characteristics of class C fly ash geopolymer*. Cement and Concrete Composites, 2010. 32(2): p. 142-147.
20. Abdullah, M.M.A., et al., *The Relationship of NaOH Molarity, Na₂SiO₃/NaOH Ratio, Fly Ash/Alkaline Activator Ratio, and Curing Temperature to the Strength of Fly Ash-Based Geopolymer*. Advanced Materials Research, 2011. 328-330: p. 1475-1482.
21. Pan, Z., J.G. Sanjayan, and B.V. Rangan, *An investigation of the mechanisms for strength gain or loss of geopolymer mortar after exposure to elevated temperature*. Journal of Materials Science, 2009. 44(7): p. 1873-1880.
22. Chindaprasirt, P., P. De Silva, and S. Hanjitsuwan, *Effect of High-Speed Mixing on Properties of High Calcium Fly Ash Geopolymer Paste*. Arabian Journal for Science and Engineering, 2014. 39(8): p. 6001-6007.
23. Gomaa, E., et al., *Fresh properties and compressive strength of high calcium alkali activated fly ash mortar*. Journal of King Saud University - Engineering Sciences, 2017. 29(4): p. 356-364.
24. Lowke, D., *Effect of Mixing Energy on Fresh Properties of SCC*. March 2005.
25. Conrad, K.L., *Geochemical Database of Feed Coal and Coal Combustion Products (CCPs) from Five Power Plants in the United States*. United States Geological Survey, November, 2011.

26. Manual, X.A., *X-Ray Radiation Safety-Manual for Operator Training*. 2010.
27. ASTM, *Standard Specification for Coal Fly Ash and Raw or Calcined Natural Pozzolan for Use in Concrete*. 2015, ASTM International.
28. International, A., *C778 - 17 Standard Specification for Standard Sand*. ASTM, 2017.
29. Hammer, G.R., *Climate of Missouri*. National Oceanic and Atmosphere Administration, 01/31/2006.
30. C191-13, A.S., *Standard Test Methods for Time of Setting of Hydraulic Cement by Vicat Needle*. ASTM International, 2013.
31. 15, A.S.C., *Standard Test Method for Flow of Hydraulic Cement Mortar*. ASTM International, 2015.
32. C109/C109M-16a, A.S., *Standard Test Method for Compressive Strength of Hydraulic Cement Mortars (Using 2-in. or [50-mm] Cube Specimens)*. ASTM International, 2016.
33. Provis, J.L. and S.A. Bernal, *Geopolymers and Related Alkali-Activated Materials*. Annual Review of Materials Research, 2014. 44: p. 299-327.
34. Siyal, A.A., et al., *Effects of Parameters on the Setting Time of Fly Ash Based Geopolymers Using Taguchi Method*. Procedia Engineering, 2016. 148: p. 302-307.
35. Yip, C.K., et al., *Effect of calcium silicate sources on geopolymerisation*. Cement and Concrete Research, 2008. 38(4): p. 554-564.
36. van Deventer, J.S.J., et al., *Reaction mechanisms in the geopolymeric conversion of inorganic waste to useful products*. Journal of Hazardous Materials, 2007. 139(3): p. 506-513.
37. Pantias, D., I.P. Giannopoulou, and T. Perraki, *Effect of synthesis parameters on the mechanical properties of fly ash-based geopolymers*. Colloids and Surfaces A: Physicochemical and Engineering Aspects, 2007. 301(1): p. 246-254.
38. Cho, H., et al., *Solution state structure determination of silicate oligomers by ²⁹Si NMR spectroscopy and molecular modeling*. Journal of the American Chemical Society, 2006. 128(7): p. 2324-2335.
39. World, C., *CW.03.08.Concrete.indd*. The Royal Society of Chemistry, March 2008.

40. Ernst Worrell, et al., *CARBON DIOXIDE EMISSIONS FROM THE GLOBAL CEMENT INDUSTRY*. Annual Review of Energy and the Environment, 2001. 26(1): p. 303-329.
41. Wan, Q., et al., *Geopolymerization reaction, microstructure and simulation of metakaolin-based geopolymers at extended Si/Al ratios*. Cement and Concrete Composites, 2017. 79(Supplement C): p. 45-52.
42. Sun, P. and H.-C. Wu, *Chemical and freeze–thaw resistance of fly ash-based inorganic mortars*. Fuel, 2013. 111(Supplement C): p. 740-745.
43. Lior, N., *Sustainable energy development: The present (2009) situation and possible paths to the future*. Energy, 2010. 35(10): p. 3976-3994.
44. Chindaprasirt, P. and S. Rukzon, *Strength, porosity and corrosion resistance of ternary blend Portland cement, rice husk ash and fly ash mortar*. Construction and Building Materials, 2008. 22(8): p. 1601-1606.
45. Malkawi, A.B., et al., *Effects of Alkaline Solution on Properties of the HCFA Geopolymer Mortars*. Procedia Engineering, 2016. 148(Supplement C): p. 710-717.
46. Xie, T. and T. Ozbakkaloglu, *Behavior of low-calcium fly and bottom ash-based geopolymer concrete cured at ambient temperature*. Ceramics International, 2015. 41(4): p. 5945-5958.
47. Duxson, P., et al., *Geopolymer technology: the current state of the art*. Journal of Materials Science, 2007. 42(9): p. 2917-2933.
48. Provis, J.L., *Alkali-activated materials*. Cement and Concrete Research, 2017.
49. Phair, J.W. and J.S.J. van Deventer, *Characterization of Fly-Ash-Based Geopolymeric Binders Activated with Sodium Aluminate*. Industrial & Engineering Chemistry Research, 2002. 41(17): p. 4242-4251.
50. Khale, D. and R. Chaudhary, *Mechanism of geopolymerization and factors influencing its development: a review*. Journal of Materials Science, 2007. 42(3): p. 729-746.
51. Simčič, T., et al., *Chloride ion penetration into fly ash modified concrete during wetting–drying cycles*. Construction and Building Materials, 2015. 93(Supplement C): p. 1216-1223.
52. Shravan Kumar, K.R., *Assessment of Chloride Ion Penetration of Alkali Activated Low Calcium Fly Ash based Geopolymer Concrete* Key Engineering Materials, 2016.

53. Ma, Y., J. Hu, and G. Ye, *The pore structure and permeability of alkali activated fly ash*. Fuel, 2013. 104(Supplement C): p. 771-780.
54. Deb, P.S., *Durability of Fly Ash Based Geopolymer Concrete*, in *Civil Engineering*. June 2013, Curtin University. p. 178.
55. Yunsheng, Z., Wei, *Fly Ash Based Geopolymer Concrete*. Indian Concrete Journal, 2006.
56. Talha Junaid, M., et al., *A mix design procedure for low calcium alkali activated fly ash-based concretes*. Construction and Building Materials, 2015. 79(Supplement C): p. 301-310.
57. Ramujee, K., *Development of Low Calcium Flyash Based Geopolymer Concrete*. Journal of Engineering and Technology, 2014.
58. Nematollahi, B. and J. Sanjayan, *Effect of different superplasticizers and activator combinations on workability and strength of fly ash based geopolymer*. Materials & Design, 2014. 57(Supplement C): p. 667-672.
59. Carabba, L., S. Manzi, and C.M. Bignozzi, *Superplasticizer Addition to Carbon Fly Ash Geopolymers Activated at Room Temperature*. Materials, 2016. 9(7).
60. LI, K.-L., *Study on Abilities of Mineral Admixtures and Geopolymer to Restrain ASR*. Key Engineering Materials, 2006.
61. Brew, D.R.M. and K.J.D. MacKenzie, *Geopolymer synthesis using silica fume and sodium aluminate*. Journal of Materials Science, 2007. 42(11): p. 3990-3993.
62. Güneyisi, E. and M. Gesoğlu, *A study on durability properties of high-performance concretes incorporating high replacement levels of slag*. Materials and Structures, 2008. 41(3): p. 479-493.
63. Cai, L., H. Wang, and Y. Fu, *Freeze–thaw resistance of alkali–slag concrete based on response surface methodology*. Construction and Building Materials, 2013. 49(Supplement C): p. 70-76.
64. Beaudoin, J.J. and C. MacInnis, *The mechanism of frost damage in hardened cement paste*. Cement and Concrete Research, 1974. 4(2): p. 139-147.
65. Shi Yan, Y.H., *Aging Mechanism of Dam Concrete under the action of Freeze-Thaw Damage* Applied Mechanics and Materials 2014.
66. Fan, L., *Research into the concrete freeze-thaw damage mechanism based on the principle of thermodynamics*. Applied Mechanics and Materials 2013.

67. Ben Li, K.W., *STUDY ON THE DAMAGE MECHANISM OF PORE STRUCTURE IN CONCRETE SUBJECTED TO FREEZE-THAW CYCLES*. THE CIVIL ENGINEERING JOURNAL, 2015.
68. Criado, M., et al., *Alkali activated fly ash: effect of admixtures on paste rheology*. Rheologica Acta, 2009. 48(4): p. 447-455.
69. Steven, G. and K. Paul, *Effect of Fly Ash on the Air-Void Stability of Concrete*. Special Publication. 79.
70. Freeman, E., et al., *Interactions of carbon-containing fly ash with commercial air-entraining admixtures for concrete*. Fuel, 1997. 76(8): p. 761-765.
71. Hill, R.L., et al., *An examination of fly ash carbon and its interactions with air entraining agent*. Cement and Concrete Research, 1997. 27(2): p. 193-204.
72. Division, F.H., *Freeze Thaw Resistance of Concrete with Marginal Air Content*. 2006, U.S Department of Transportation.
73. Skvara, F., *Alkali Activated Material - Geopolymer* Department of Glass and Ceramics- Faculty of Chemical Technology, ICT Prague, 2007.
74. Savas, B., S. Ahmad, and D. Fedroff, *Freeze-Thaw Durability of Concrete with Ground Waste Tire Rubber*. Transportation Research Record: Journal of the Transportation Research Board, 1997. 1574: p. 80-88.
75. Richardson, A., et al., *Crumb rubber used in concrete to provide freeze-thaw protection (optimal particle size)*. Journal of Cleaner Production, 2016. 112(Part 1): p. 599-606.
76. Richardson, A.E., K.A. Coventry, and G. Ward, *Freeze/thaw protection of concrete with optimum rubber crumb content*. Journal of Cleaner Production, 2012. 23(1): p. 96-103.
77. Gadkar, S. and P. Rangaraju, *The Effect of Crumb Rubber on Freeze-Thaw Durability of Portland Cement Concrete*. 2013.
78. International, A., *Standard Specification for Coal Fly Ash and Raw or Calcined Natural Pozzolan for Use in Concrete*. ASTM, 2017.
79. International, A., *Standard Specification for Chemical Admixtures for Concrete*. ASTM, 2017.
80. International, A., *Standard Specification for Air-Entraining Admixtures for Concrete*. ASTM, 2016.

81. Officials, A.A.o.S.a.H.T., *Standard Specification for Air-Entraining Admixtures for Concrete (ASTM Designation C260/C260M-10a)*. 2016, AASHTO.
82. Li, W., et al., *Water Absorption and Critical Degree of Saturation Relating to Freeze-Thaw Damage in Concrete Pavement Joints*. *Journal of Materials in Civil Engineering*, 2012. 24(3): p. 299-307.
83. Bentz, D.P., *SORPTIVITY-BASED SERVICE LIFE PREDICTIONS FOR CONCRETE PAVEMENTS*. National Institute of Standards and Technology, 2001. Building and Fire Research Laboratory.
84. International, A., *Standard Test Method for Flow of Hydraulic Cement Mortar*. 2015, ASTM.
85. International, A., *Standard Test Method for Compressive Strength of Hydraulic Cement Mortars (Using 2-in. or [50-mm] Cube Specimens)*, in *ASTM C109 / C109M - 16a*. 2016, ASTM.
86. International, A., *Standard Test Method for Resistance of Concrete to Rapid Freezing and Thawing*, in *ASTM C666 / C666M - 15*. 2015, ASTM.
87. International, A., *Standard Test Method for Air Content of Hydraulic Cement Mortar*, in *ASTM C185 - 15a*. 2015, ASTM.
88. theconstructor.org. *Effect of Air Entrained Concrete on Strength of Concrete*. 2017; Available from: <https://theconstructor.org/concrete/air-entrained-concrete-strength-effects/8427/>.

VITA

Simon Peter Sargon was born in Mumbai, India in 1994. He received his Bachelor degree of Civil Engineering in 2015 from Panimalar Engineering College (Chennai, India). He began his Master Degree, as an on campus student, in Spring 2016.

In the last year of his Bachelor studies, he participated in several projects and internships, working on designing floating production storage and offloading (FPSO) ship platforms, self-healing concretes by bacterial mineral precipitation, Inbuilt Grey Water Treatment System, and Waste Management and Green Solutions. In May 2018, he received his Master's degree in Civil Engineering from Missouri University of Science and Technology.